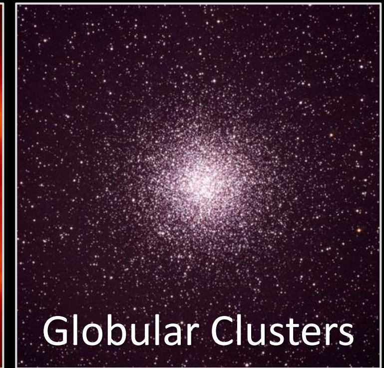

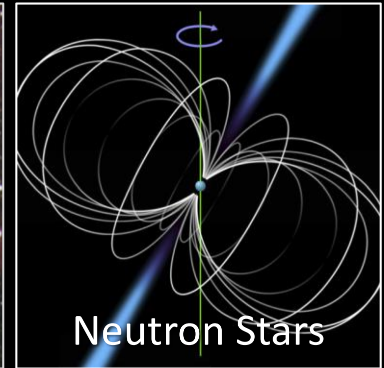

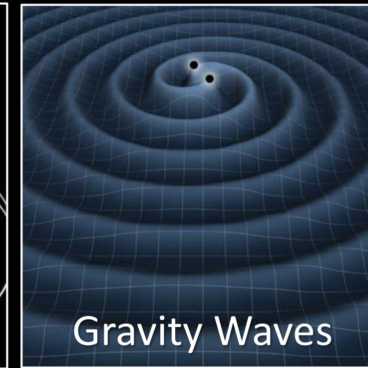

Particle-Physics Constraints from Stars

MAX-PLANCK-GESELLSCHAFT

Max-Planck-Institut für Physik
(Werner-Heisenberg-Institut)

SFB 1258 | Neutrinos Dark Matter Messengers

Georg G. Raffelt, Max-Planck-Institut für Physik, München

Particle-Physics Constraints from Stars

Low-mass particles (neutrinos, axions and friends, hidden photons, low-mass carriers of new forces, ...) can be probed by stars.

- Particles from the Sun and their detection
- Impact of new energy-loss channels on low-mass stars
- Supernova 1987A
- Neutron-star cooling
- Axion conversion in pulsar magnetospheres
- Superradiance of ultra-light bosons from black holes

In this lecture focus on the astrophysics of these arguments (often not so clear to particle physicists) and not so much on the latest results for all types of particles

EVOLUTION OF STARS

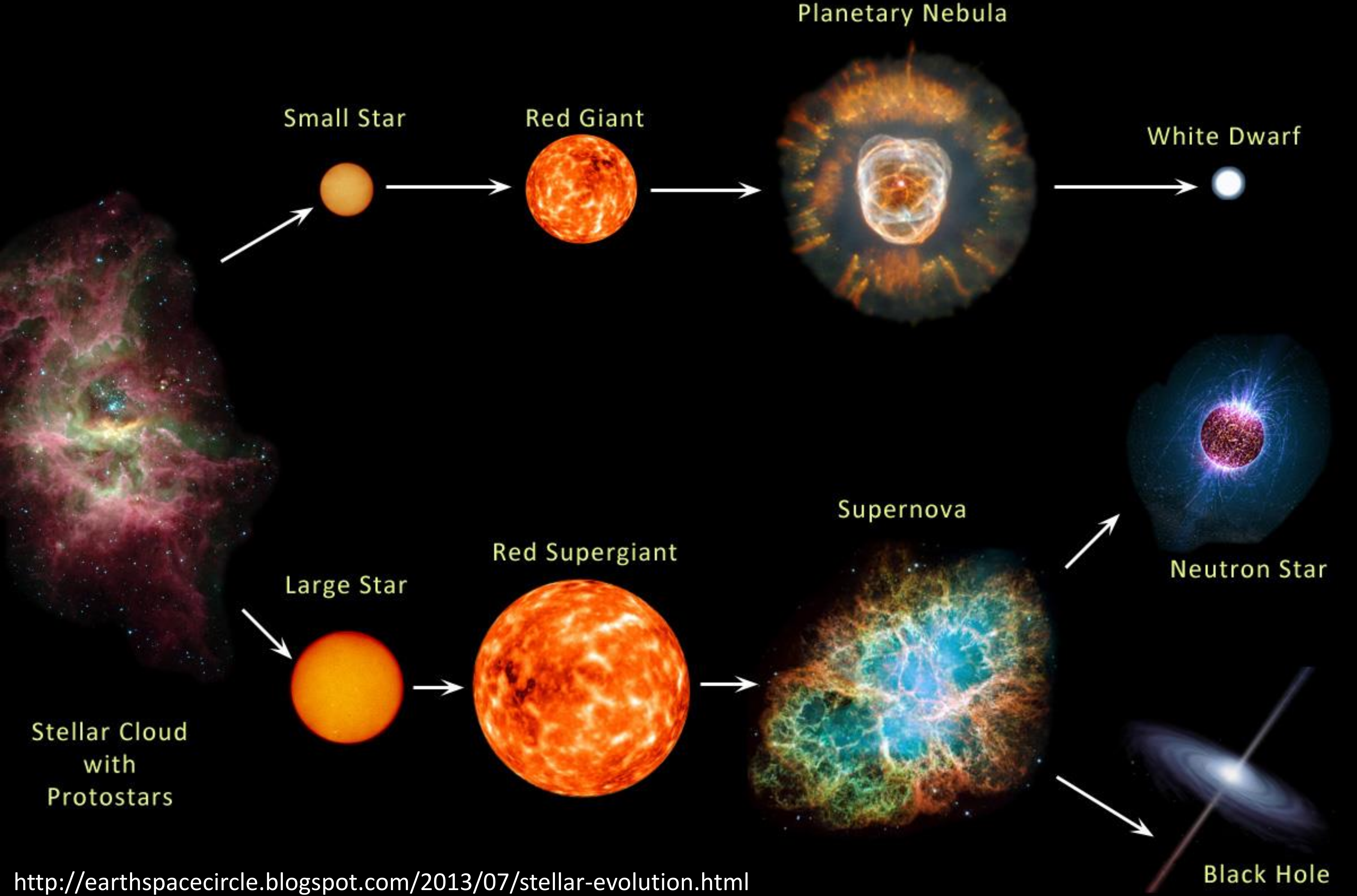

http://earthspacecircle.blogspot.com/2013/07/stellar-evolution.html

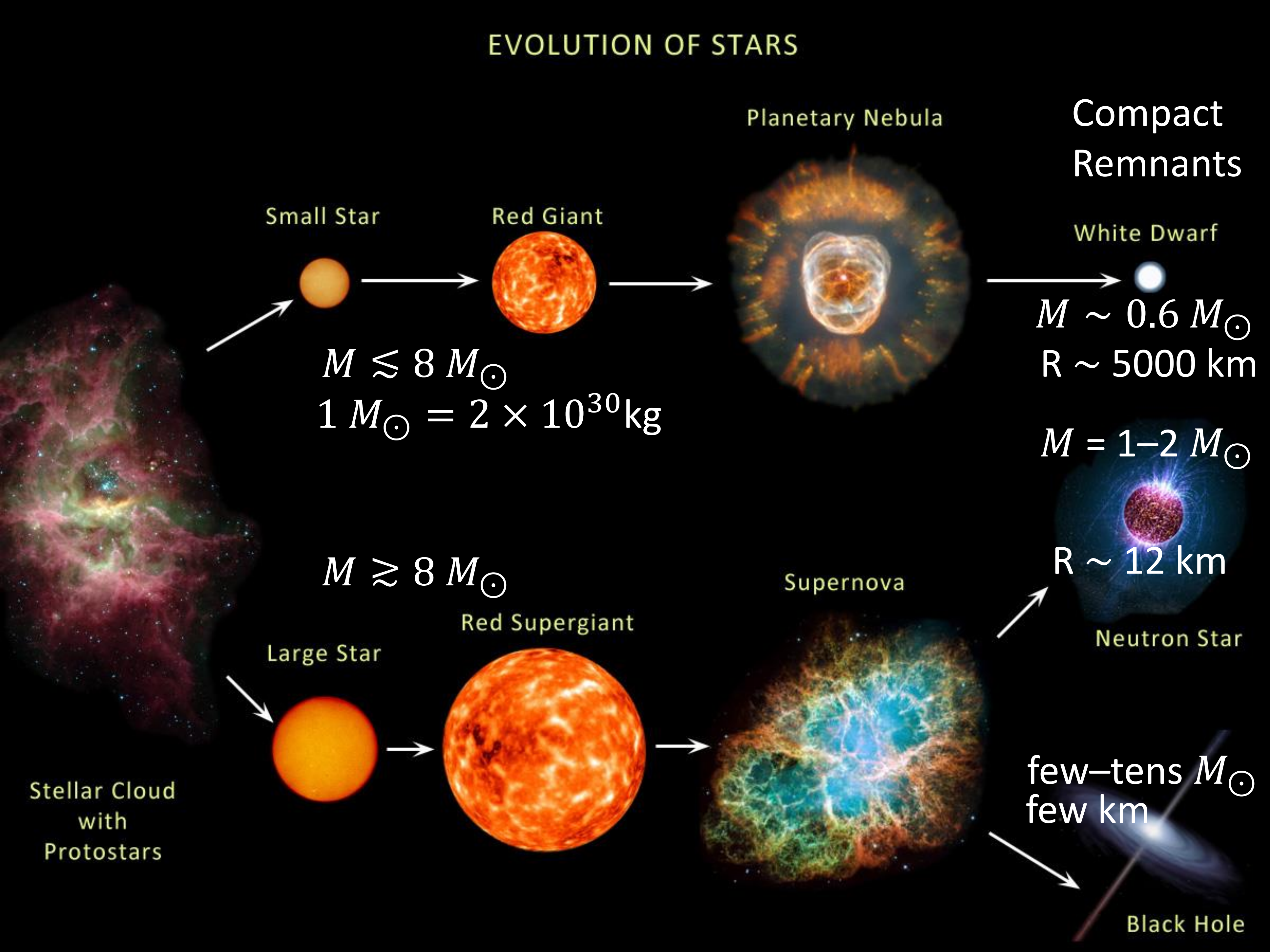
EVOLUTION OF STARS
Planetary Nebula
Compact Remnants
Small Star
Red Giant
White Dwarf
$M \sim 0.6\ M_\odot$
R ~ 5000 km
$M \lesssim 8\ M_\odot$
$1\ M_\odot = 2 \times 10^{30}$kg
$M = 1\text{–}2\ M_\odot$
R ~ 12 km
$M \gtrsim 8\ M_\odot$
Supernova
Red Supergiant
Neutron Star
Large Star
Stellar Cloud with Protostars
few–tens $M_\odot$
few km
Black Hole

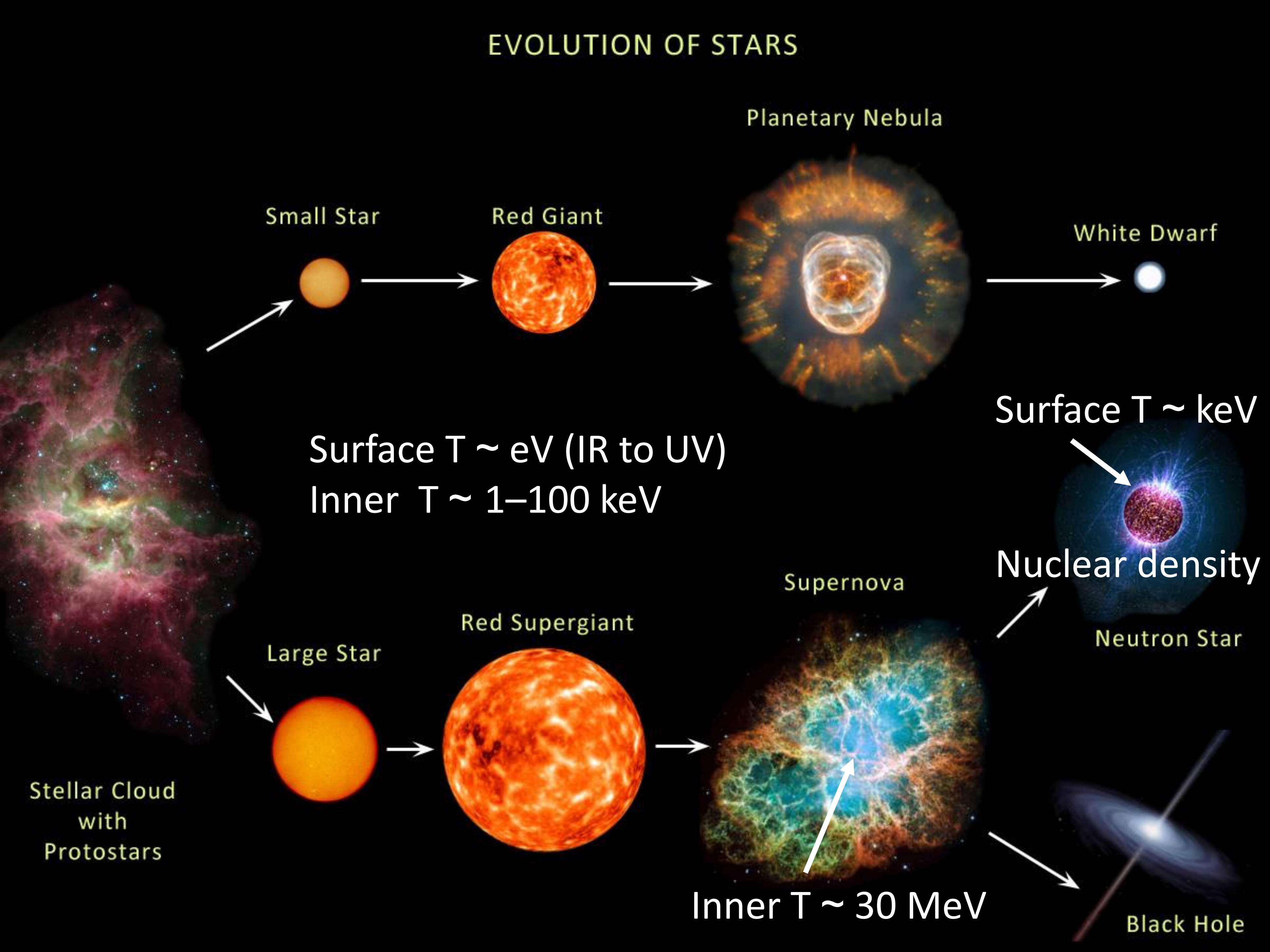

EVOLUTION OF STARS
Planetary Nebula
Small Star
Red Giant
White Dwarf
Surface T ~ keV
Surface T ~ eV (IR to UV)
Inner T ~ 1–100 keV
Nuclear density
Supernova
Neutron Star
Red Supergiant
Large Star
Stellar Cloud
with
Protostars
Inner T ~ 30 MeV
Black Hole

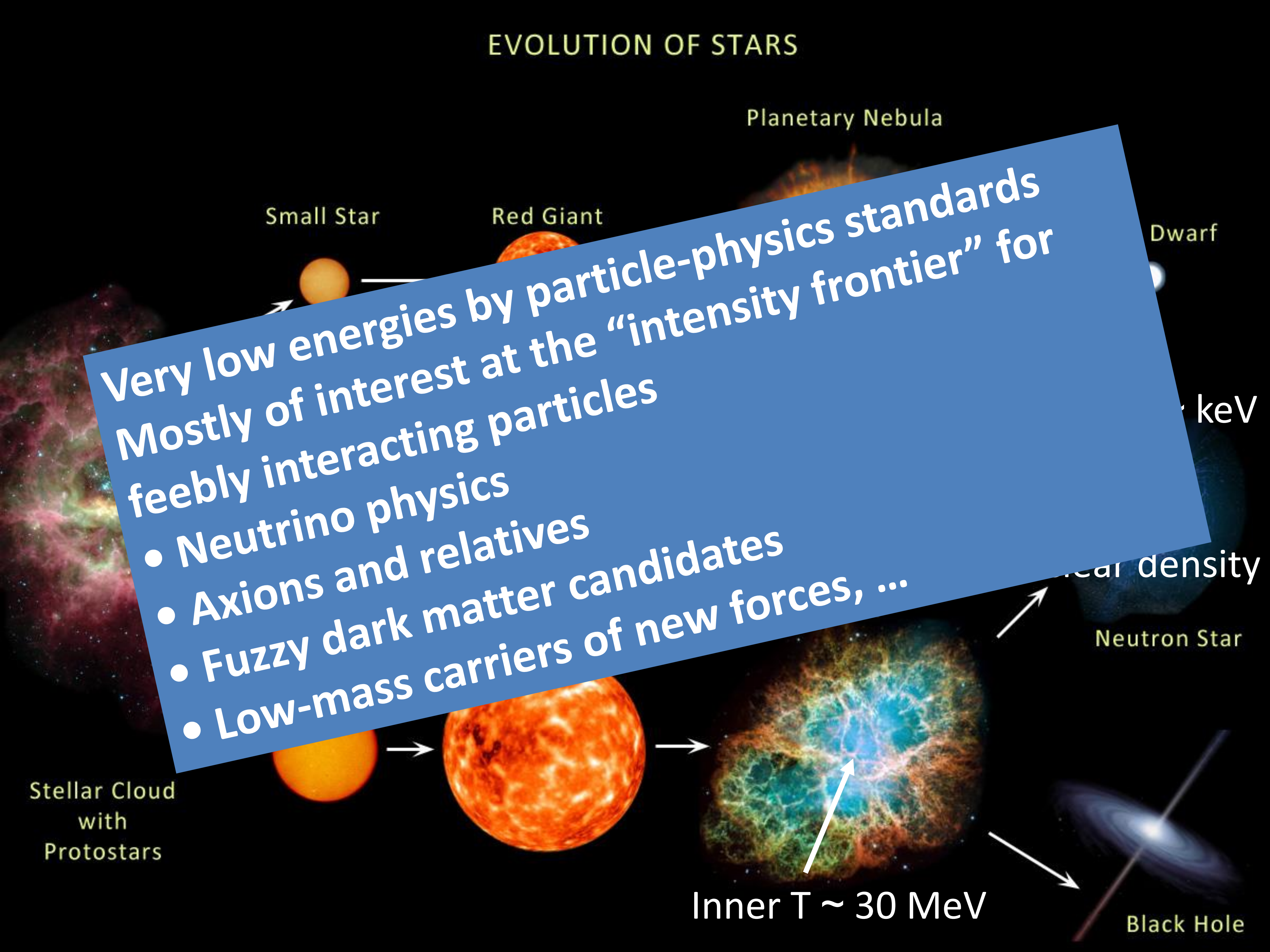

EVOLUTION OF STARS
Planetary Nebula
Small Star
Red Giant
Dwarf
keV
density
Neutron Star
Stellar Cloud with Protostars
Inner T ~ 30 MeV
Black Hole
Very low energies by particle-physics standards
Mostly of interest at the “intensity frontier” for feebly interacting particles
• Neutrino physics
• Axions and relatives
• Fuzzy dark matter candidates
• Low-mass carriers of new forces, …

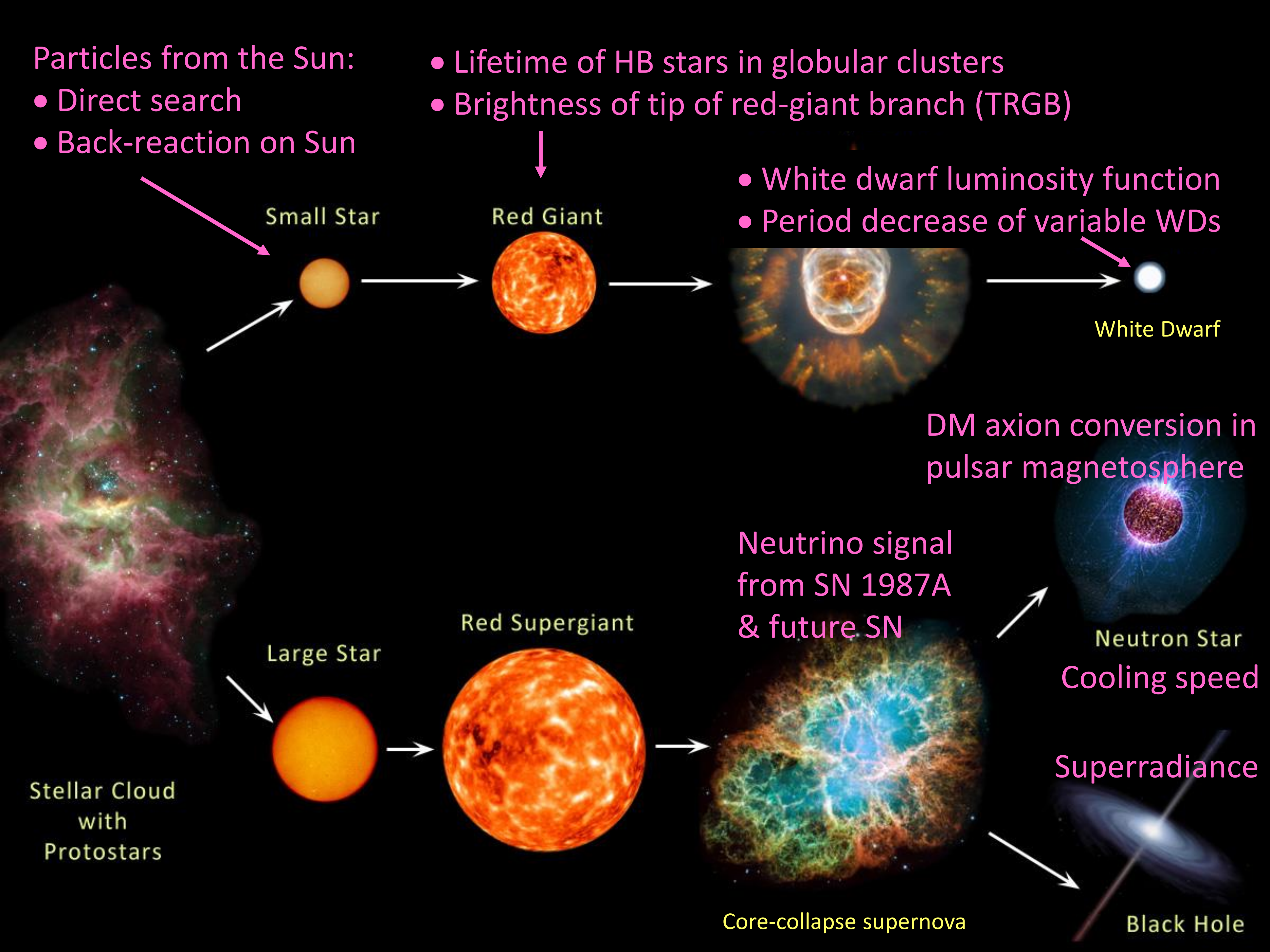
Particles from the Sun:
• Direct search
• Back-reaction on Sun
• Lifetime of HB stars in globular clusters
• Brightness of tip of red-giant branch (TRGB)
• White dwarf luminosity function
• Period decrease of variable WDs
Small Star
Red Giant
White Dwarf
DM axion conversion in pulsar magnetosphere
Neutrino signal from SN 1987A & future SN
Neutron Star
Cooling speed
Red Supergiant
Large Star
Superradiance
Stellar Cloud with Protostars
Core-collapse supernova
Black Hole

Particles from the Sun

2002 Solar Neutrinos (R.Davis, M.Koshiba)

2015 Solar Nu Oscillations (A.McDonald)

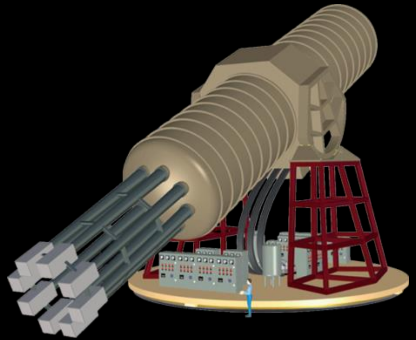

Search for solar axions with CAST and future IAXO

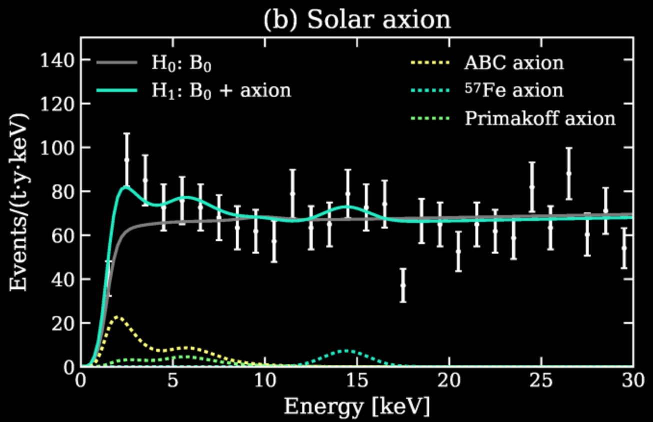

Excess events in XENON1T DM search. Solar axions? arXiv:2006.09721

Neutrinos from the Sun

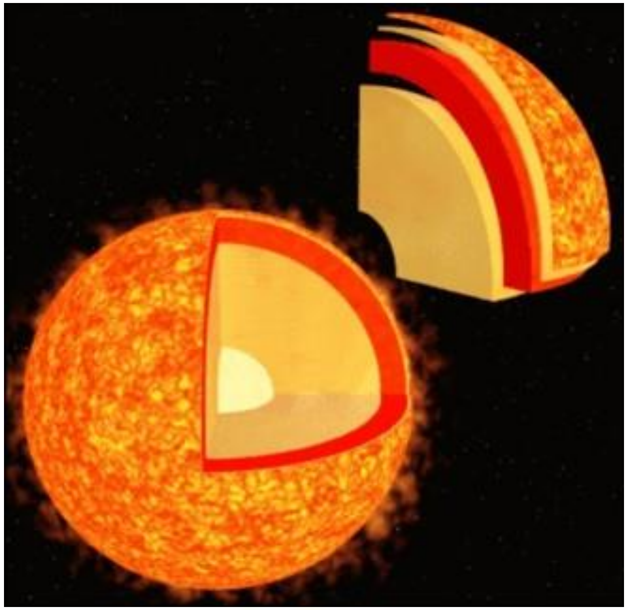

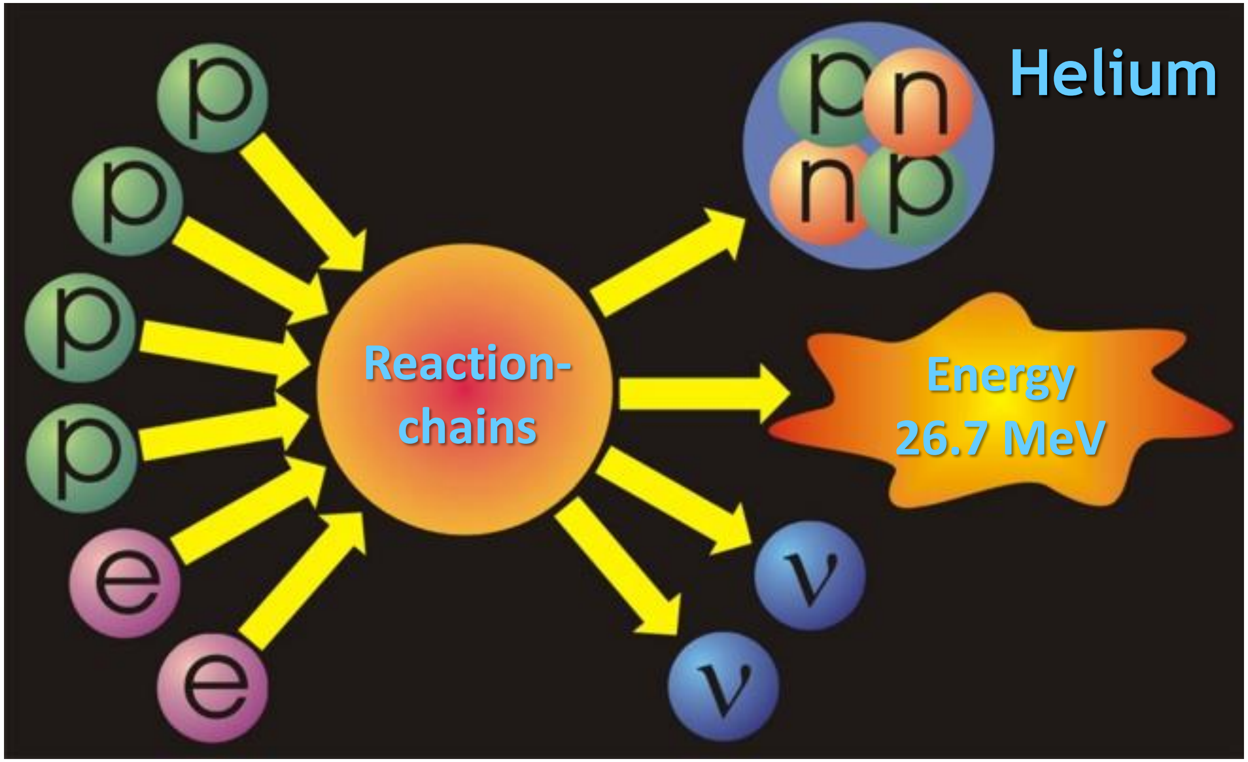

Solar radiation: 98 % light (photons)
2 % neutrinos
At Earth 66 billion neutrinos/cm^2 sec

Hans Bethe (1906–2005, Nobel prize 1967)
Thermonuclear reaction chains (1938)

Hydrogen Burning

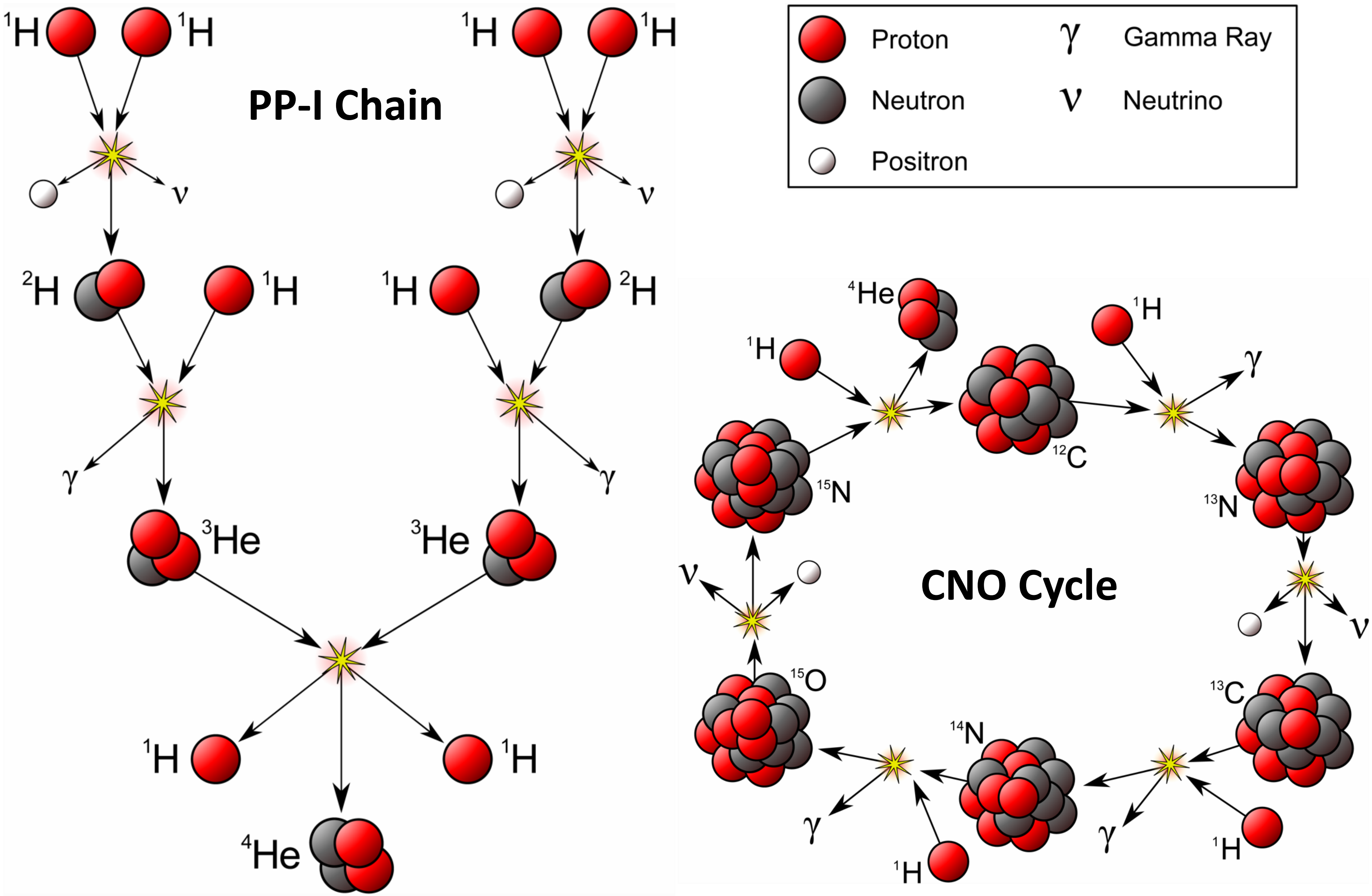

Solar Neutrinos from Nuclear Reactions

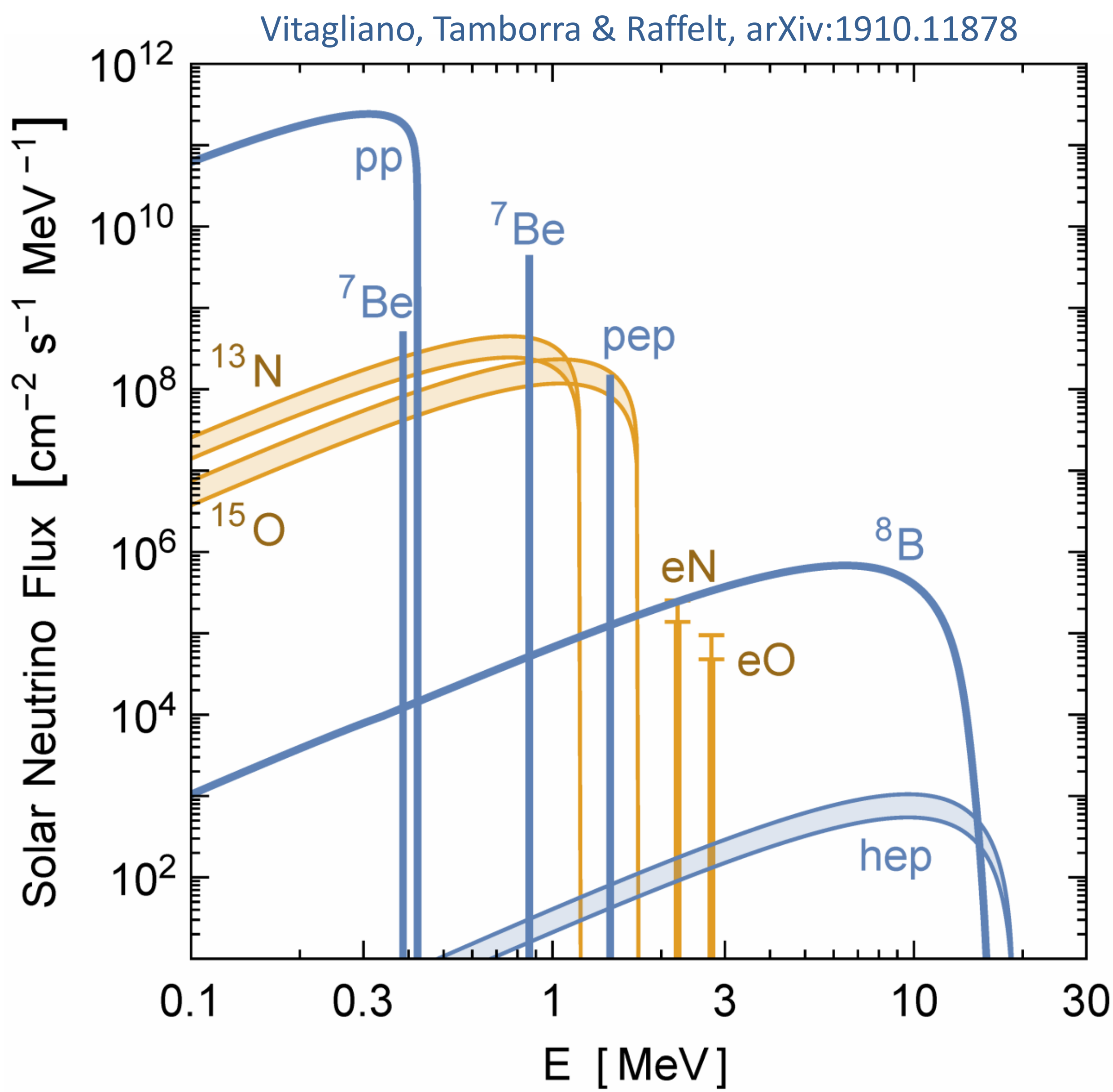

All components of pp chains (blue) have been measured

Very recently direct experimental evidence for CNO fluxes (orange) in Borexino
arXiv:2006.15115 (06/2020)
Nature 587 (2020) 577

Favors higher flux, but cannot decide between “high” and “low” CNO abundance

Solar Neutrino Spectroscopy with Borexino

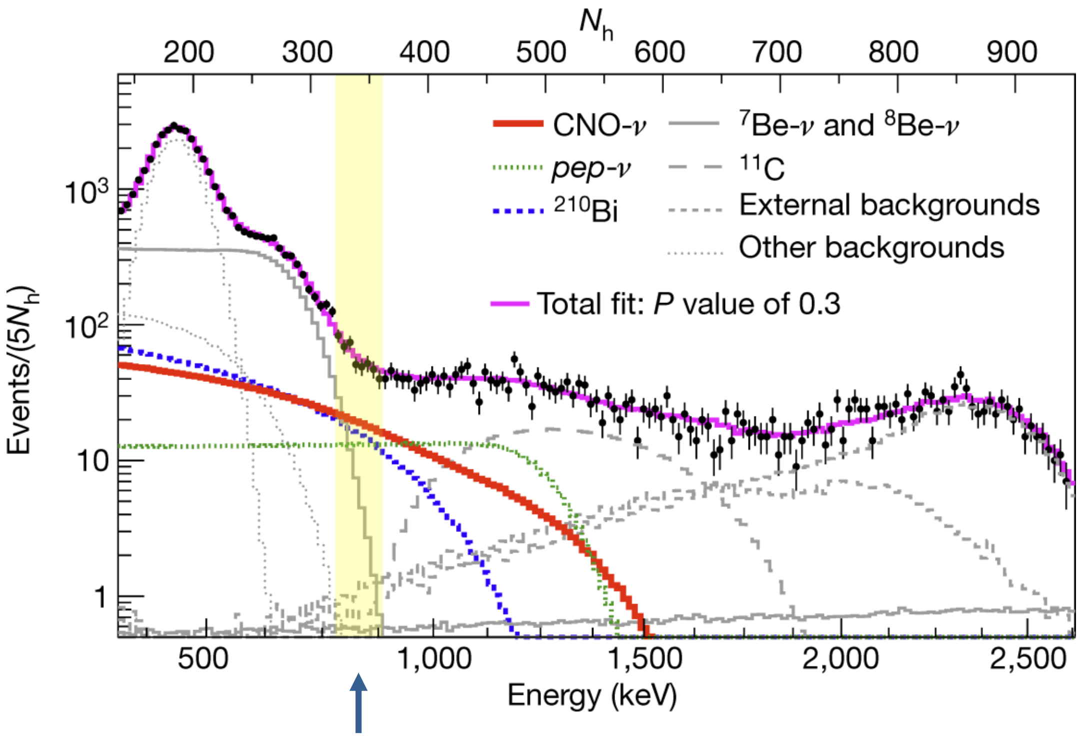

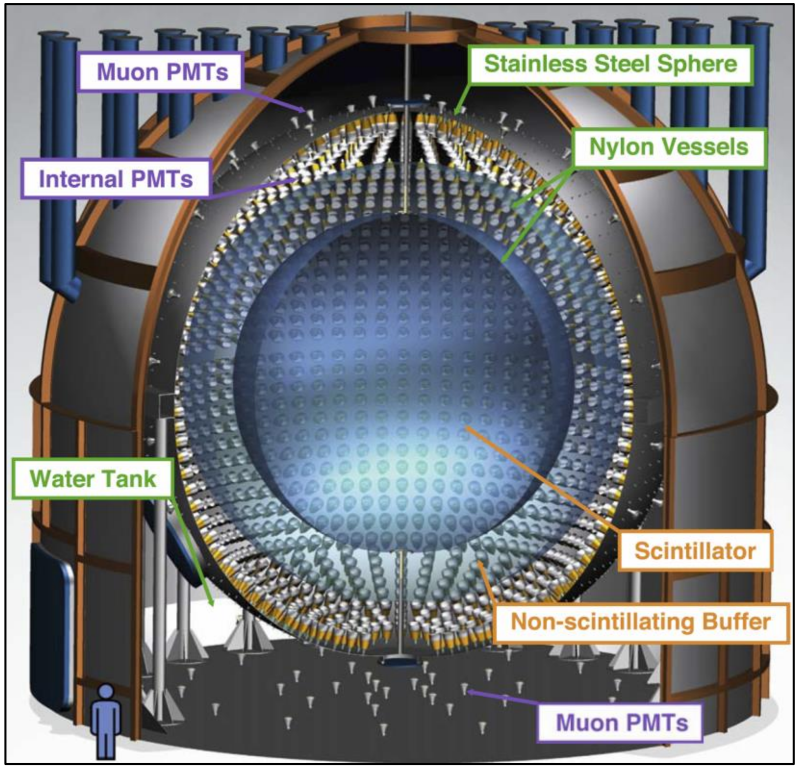

Region of interest:
Crucial background beta decay of ^{210}Bi

$$^{210}\mathrm{Pb} \xrightarrow[22.3\,\mathrm{yr}]{\beta^-} {}^{210}\mathrm{Bi} \xrightarrow[5\,\mathrm{d}]{\beta^-} {}^{210}\mathrm{Po} \xrightarrow[138.4\,\mathrm{d}]{\alpha} {}^{206}\mathrm{Pb}$$

Reduction and stabilization by controlling convective flows in scintillator

Borexino Collaboration:
Experimental evidence of neutrinos produced in the CNO fusion cycle in the Sun
Nature 587 (2020) 577

Thermal Neutrinos: Production Processes

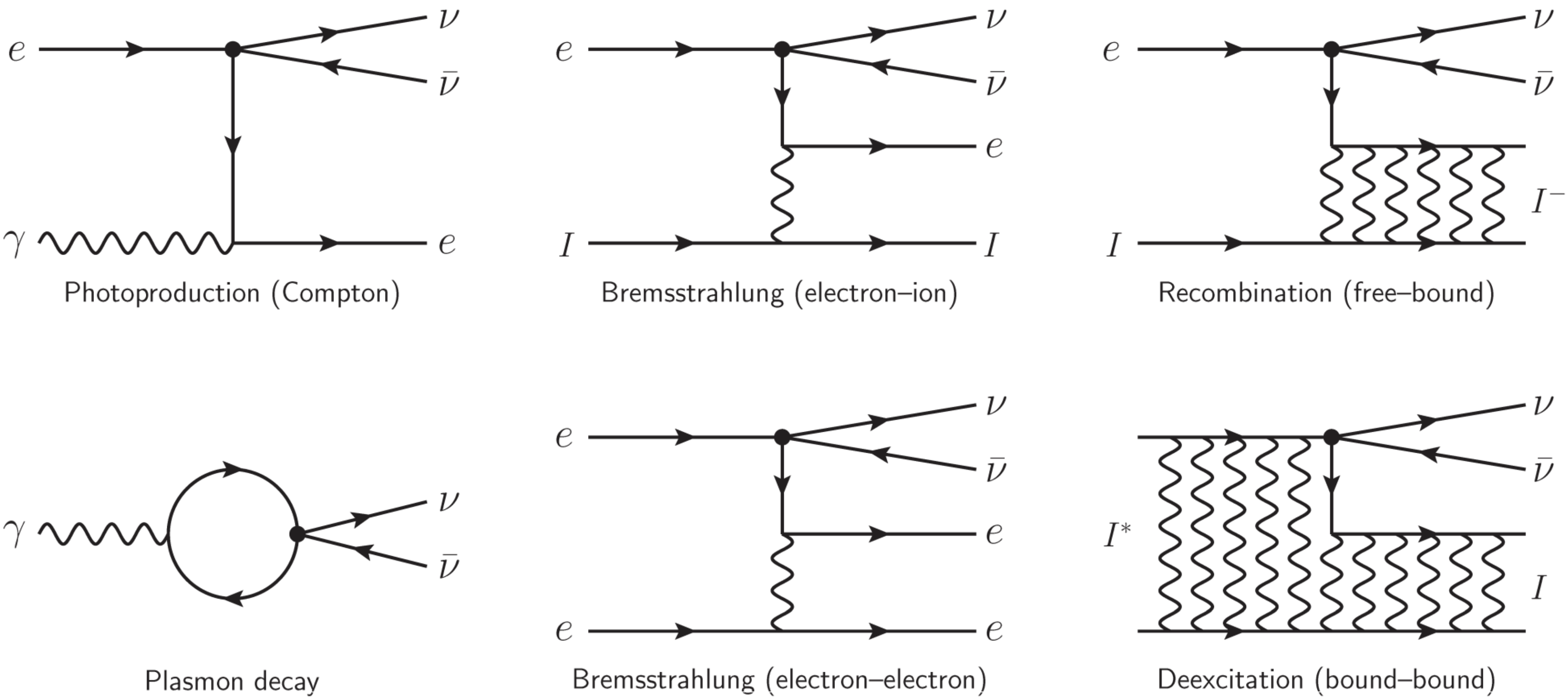

Figure 1. Processes for thermal neutrino pair production in the Sun.

Vitagliano, Redondo & Raffelt, arXiv:1708.02248

Solar neutrino flux at keV energies

- Thermally produced neutrinos and antineutrinos dominate at keV energies
- Future detection opportunities?

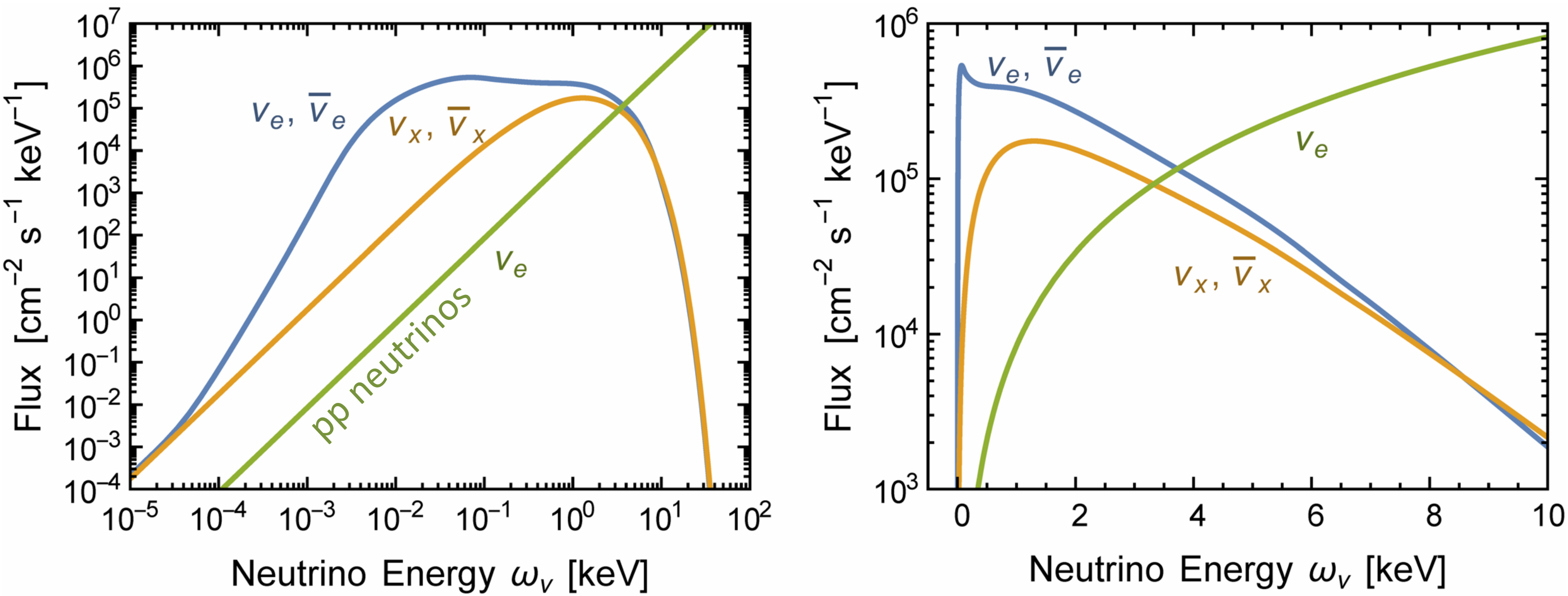

Vitagliano, Raffelt & Redondo, *JCAP 1712 (2017) 010* [arXiv:1708.02248]

Grand Unified Neutrino Spectrum (GUNS) at Earth

Vitagliano, Tamborra & Raffelt, arXiv:1910.11878

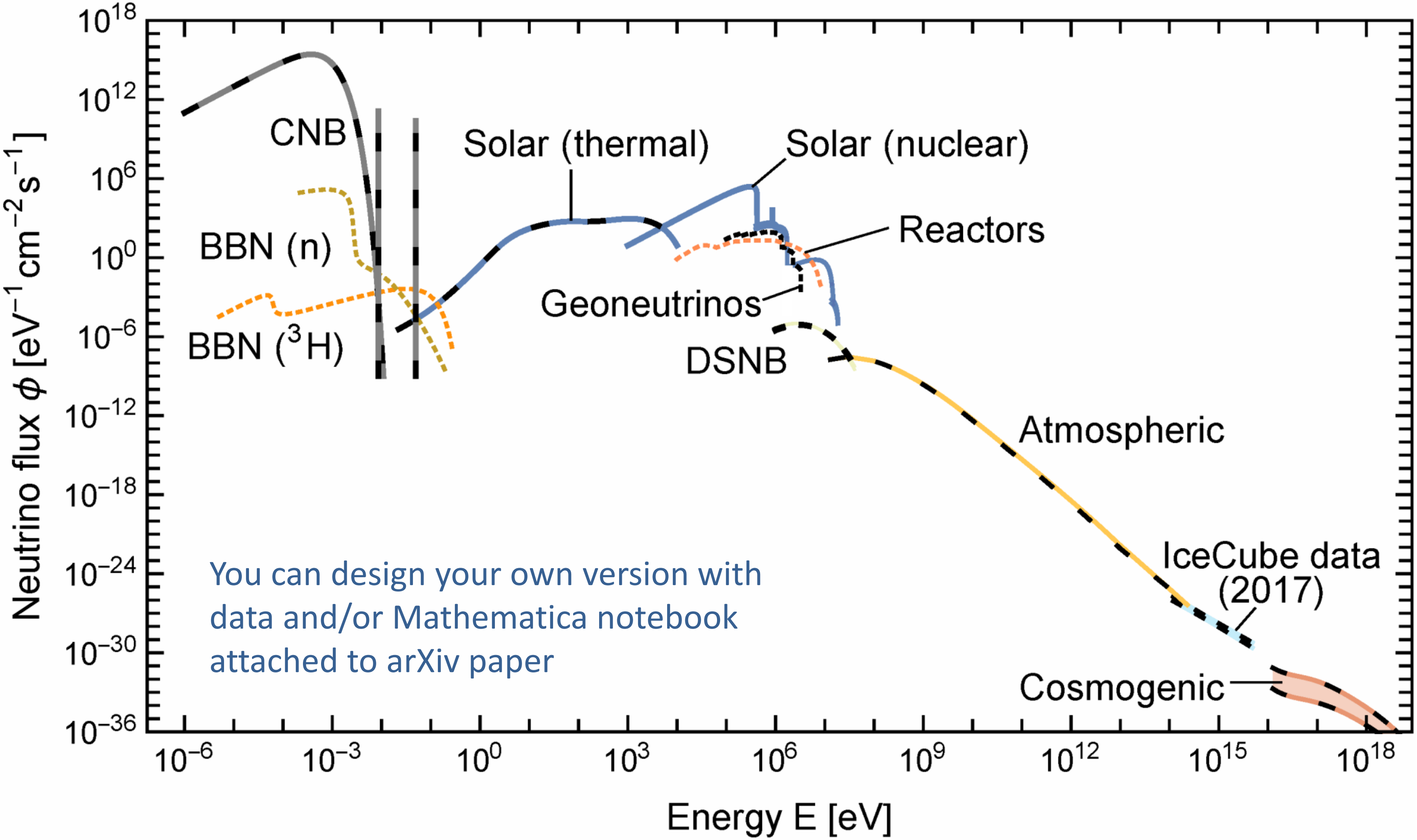

You can design your own version with data and/or Mathematica notebook attached to arXiv paper

Grand Unified Neutrino Spectrum (GUNS) at Earth

Ch. Spiering, arXiv:1207.4952

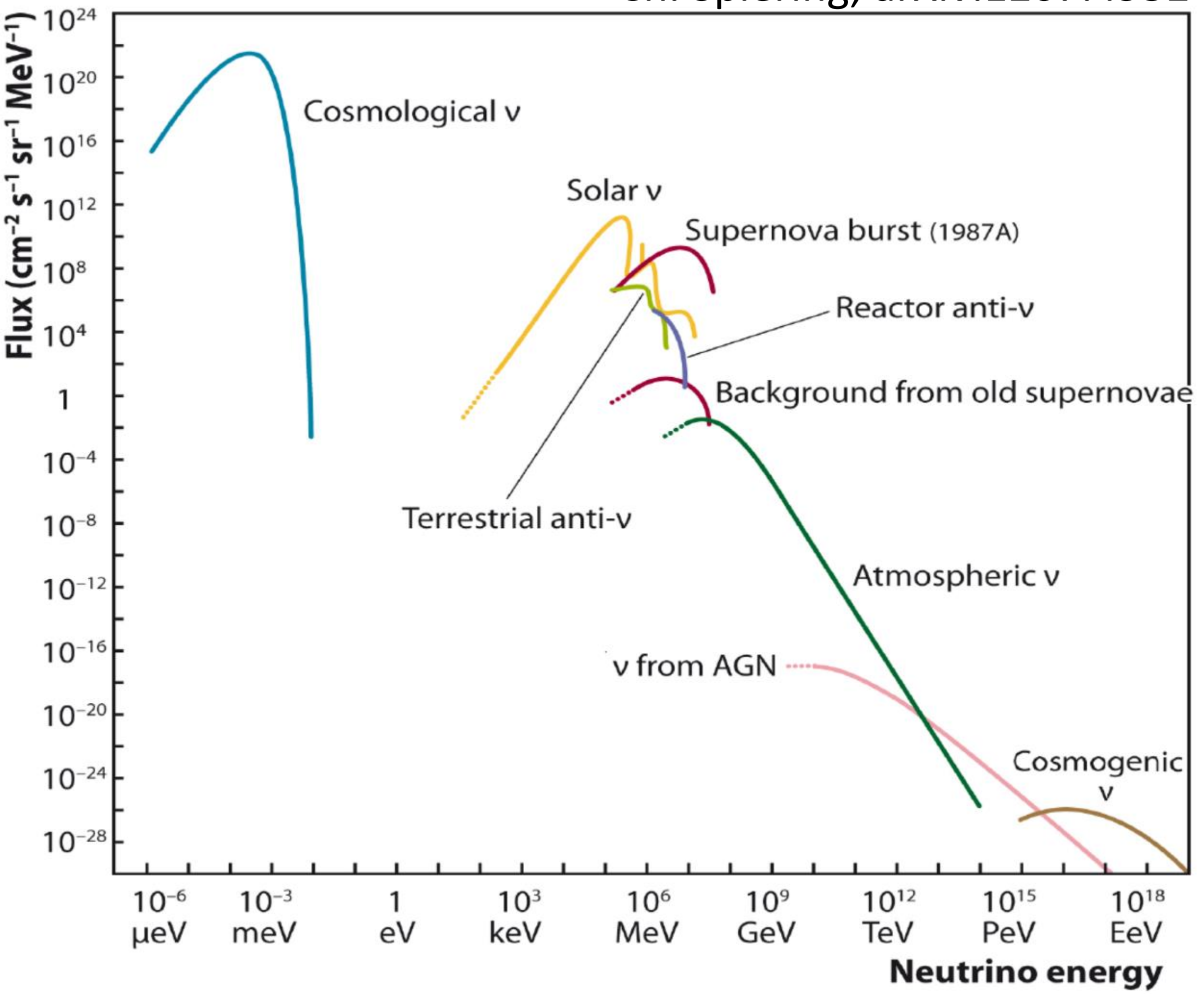

Often shown GUNS plot, but has many issues
Probably should be retired

VOLUME 51, NUMBER 16 PHYSICAL REVIEW LETTERS 17 OCTOBER 1983

Experimental Tests of the "Invisible" Axion

P. Sikivie
Physics Department, University of Florida, Gainesville, Florida 32611
(Received 13 July 1983)

Experiments are proposed which address the question of the existence of the "invisible" axion for the whole allowed range of the axion decay constant. These experiments exploit the coupling of the axion to the electromagnetic field, axion emission by the sun, and/or the cosmological abundance and presumed clustering of axions in the halo of our galaxy.

Primakoff effect:

Axion-photon transition in external static E or B field
(Originally discussed for π^0 by Henri Primakoff 1951)

Pierre Sikivie:

Macroscopic B-field can provide a large coherent transition rate over a big volume (low-mass axions)

- Axion helioscope:
  Look at the Sun through a dipole magnet
- Axion haloscope:
  Look for dark-matter axions with
  A microwave resonant cavity

Let's point a magnet at the sun…

…and look for X-Rays!

By CAST student Sebastian Baum

LHC Magnet Mounted as a Telescope to Follow the Sun

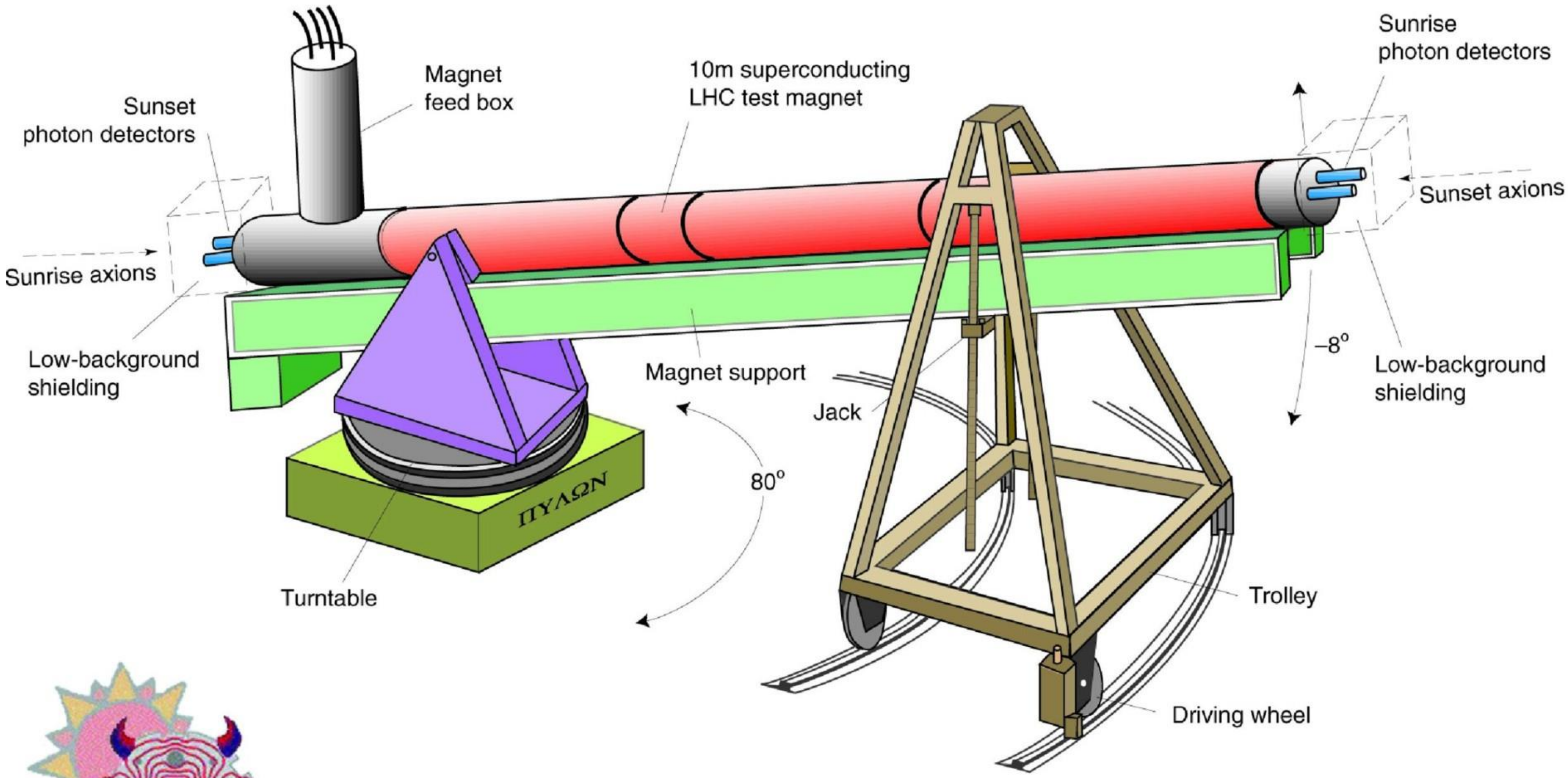

Cern **A**xion **S**olar **T**elescope

→ CAST Movie on YouTube

Searching for Solar Axions with CAST

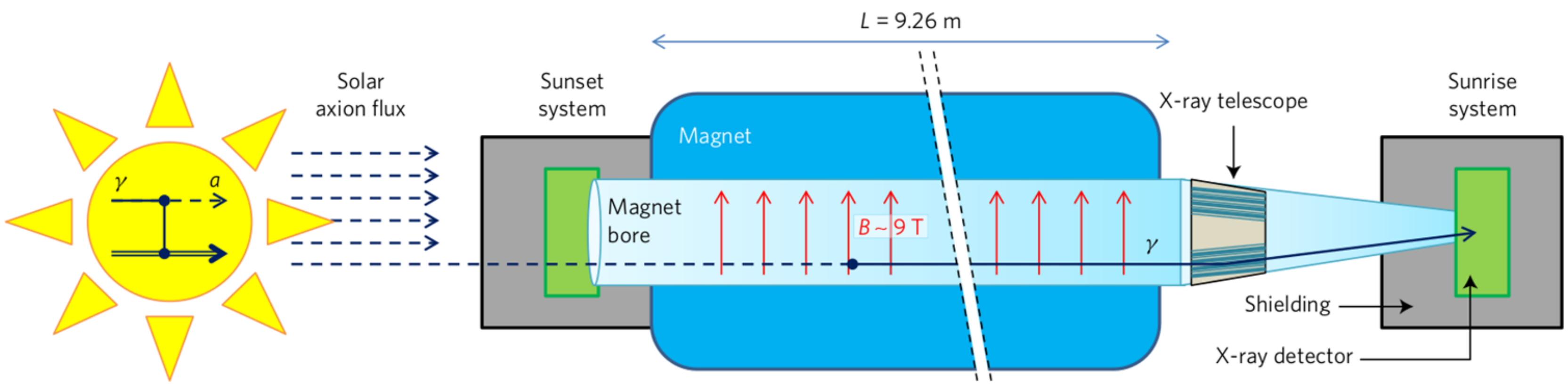

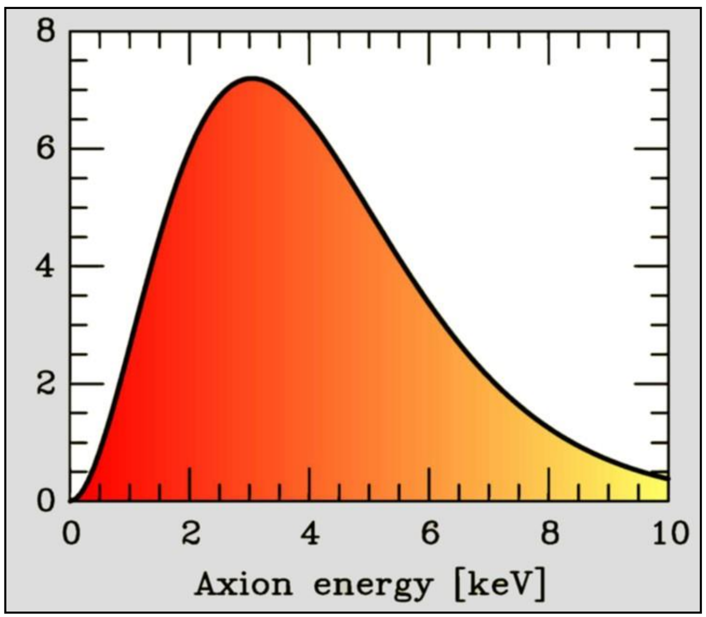

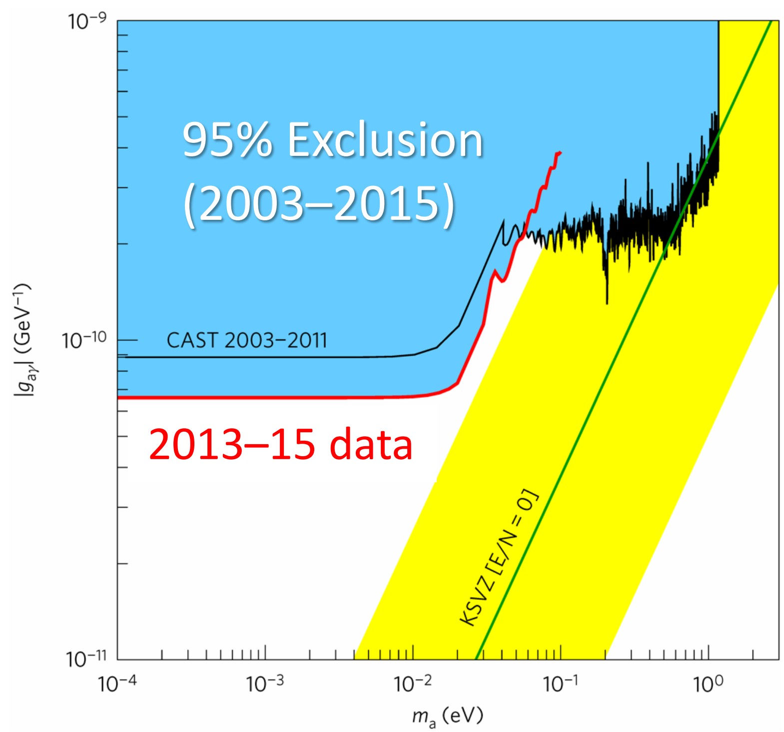

Flux: $g_{10}^2\ 3.7 \times 10^{11}\ \mathrm{cm^{-2}s^{-1}}$

New CAST limit on the axion-photon interaction, Nature Physics 13 (2017) 584 [1705.02290]

Next Generation Axion Helioscope (IAXO)

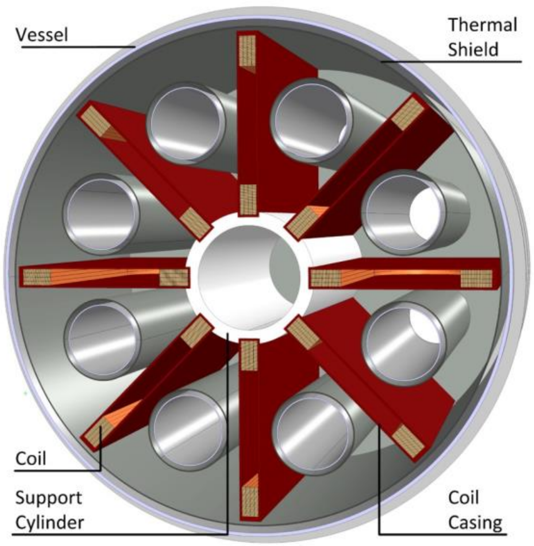

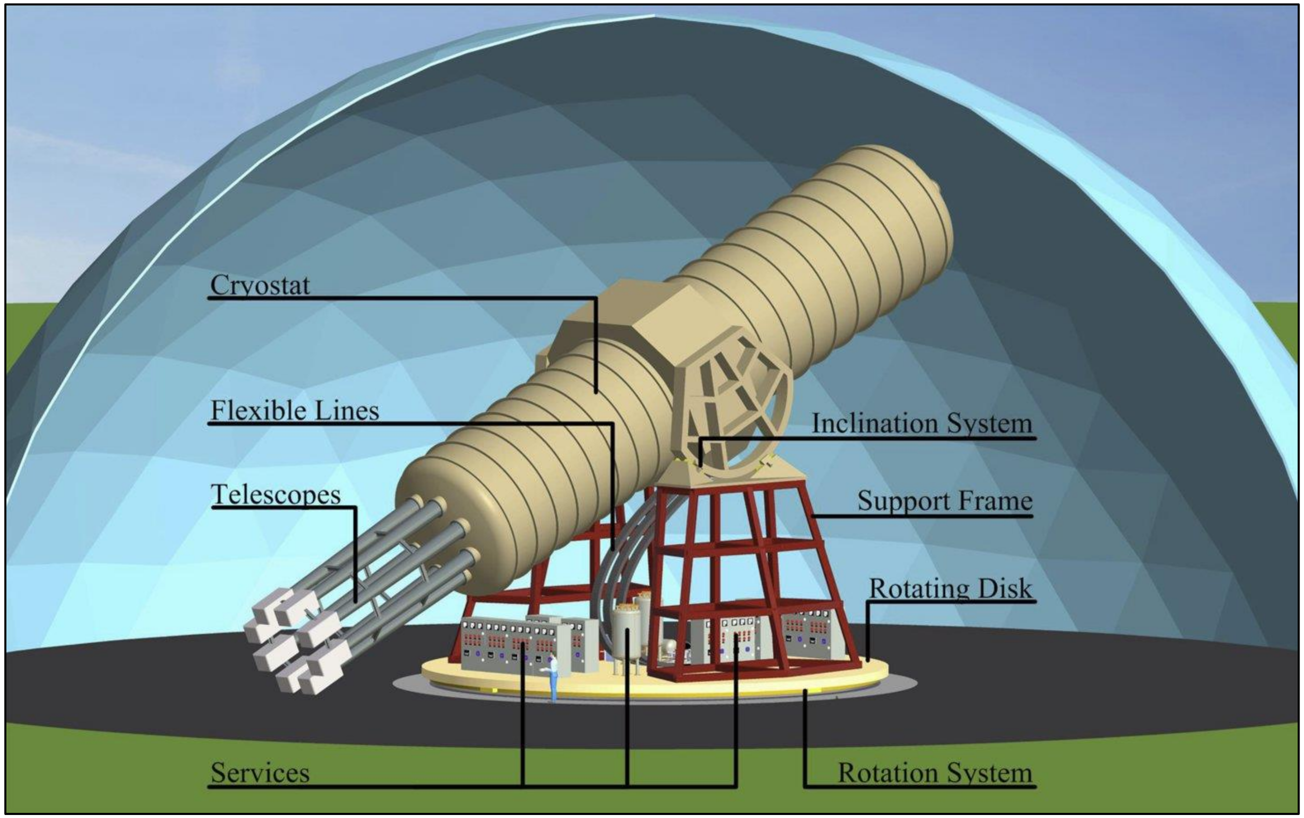

Need new magnet w/
– Much bigger aperture: $\sim 1\ \mathrm{m}^2$ per bore
– Lighter (no iron yoke)
– Bores at T_{room}

- Irastorza et al.: Towards a new generation axion helioscope, arXiv:1103.5334
- Armengaud et al.: Conceptual Design of the International Axion Observatory (IAXO), arXiv:1401.3233

(Baby) IAXO Sensitivty Forecast

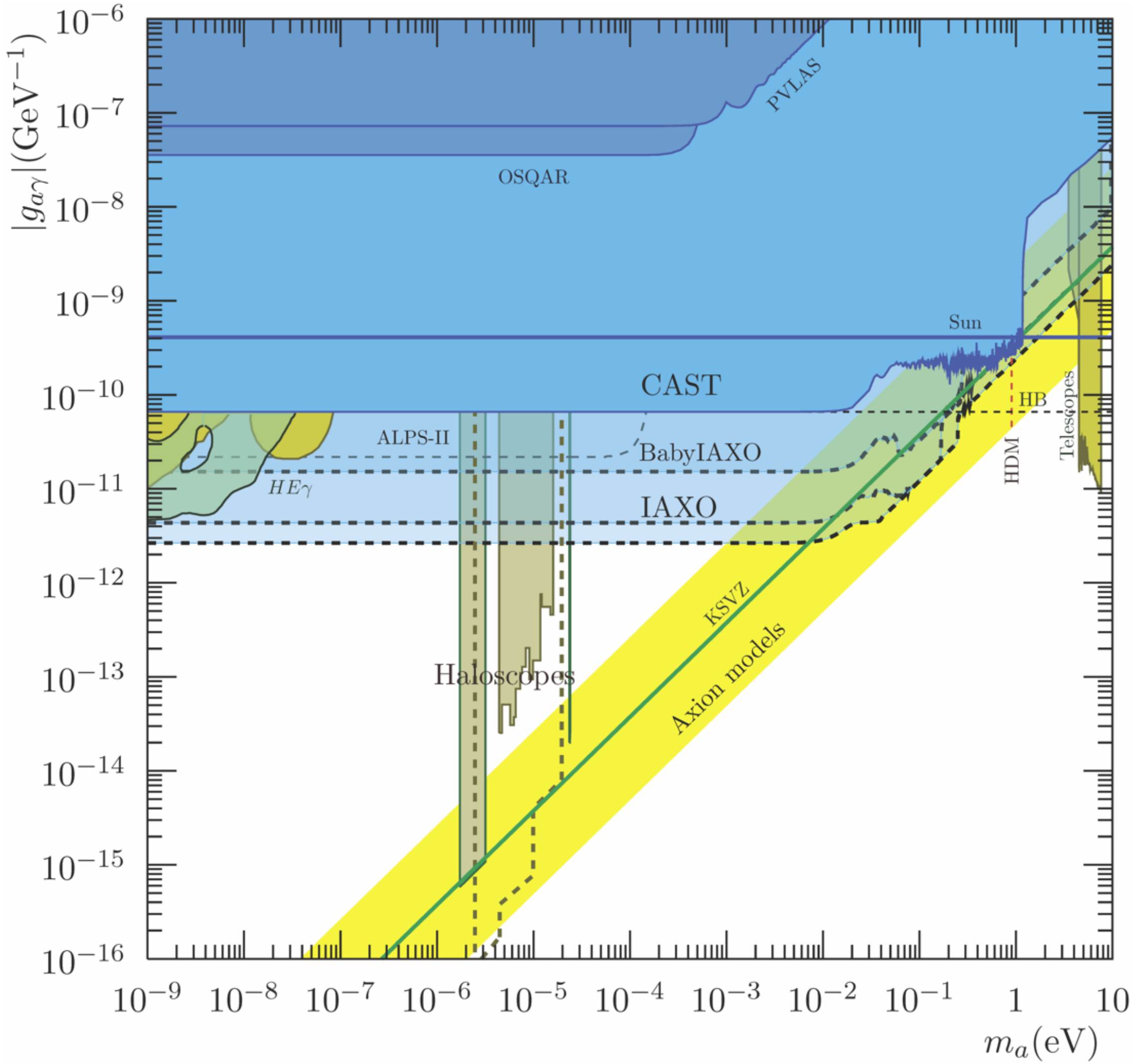

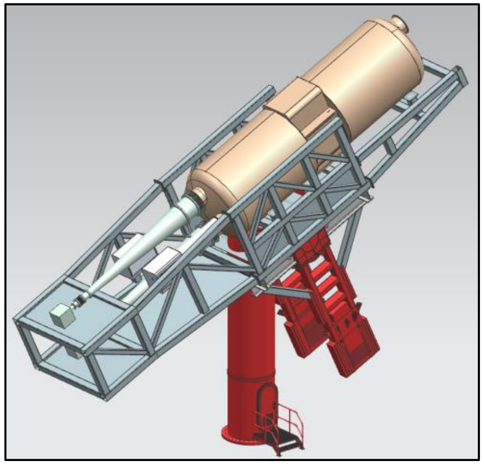

Baby IAXO @ DESY
Operation 2024+

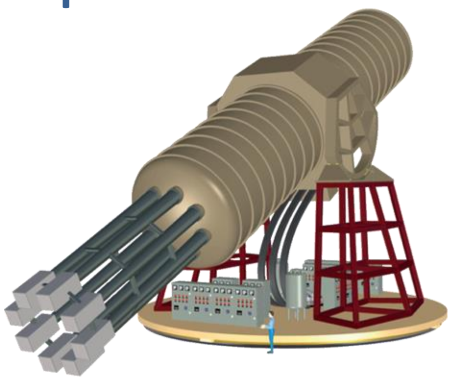

Physics potential of the International Axion Observatory (IAXO)
JCAP 1906 (2019) 047, arXiv:1904.09155

Observation of Excess Electronic Recoil Events in XENON1T

arXiv:2006.09721 (17 June 2020)
~ 150 citations

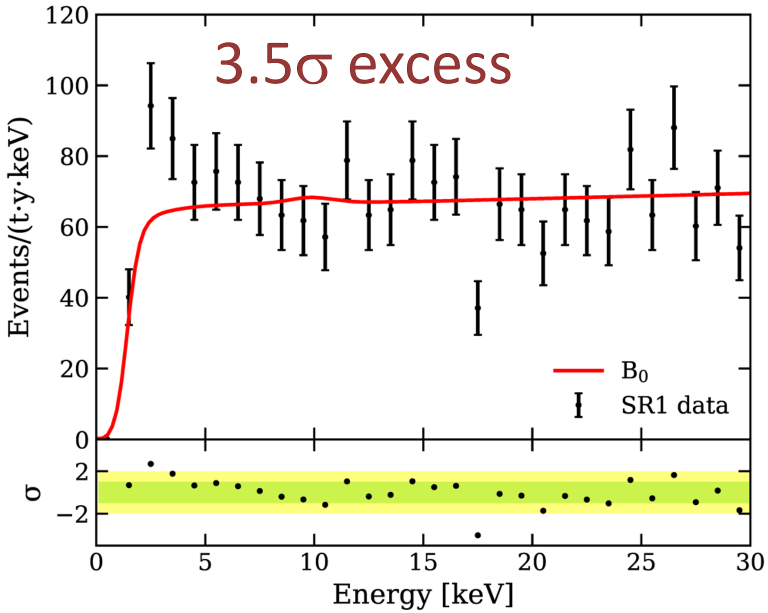

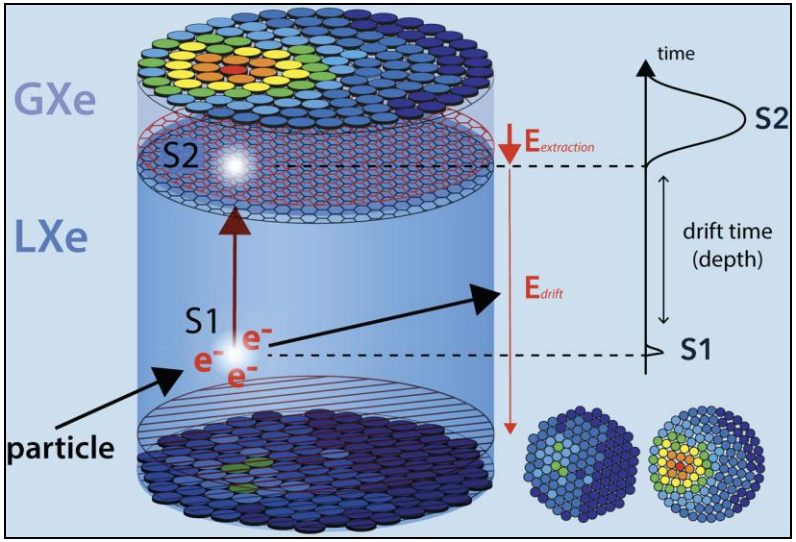

Caused by solar axions or other particles from the Sun?

keV-Range Energy Depositions

Nuclear recoil

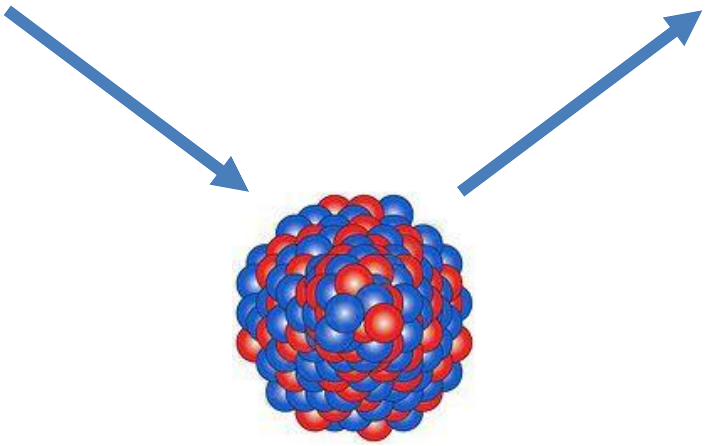

Dark-matter WIMPs

Coherent scattering of
10 MeV solar neutrinos

Electronic recoil (ER)

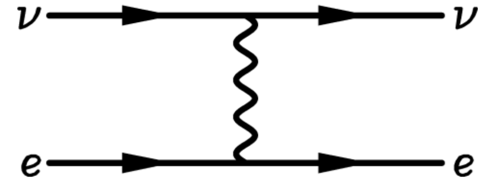

Solar neutrinos with large dipole moments

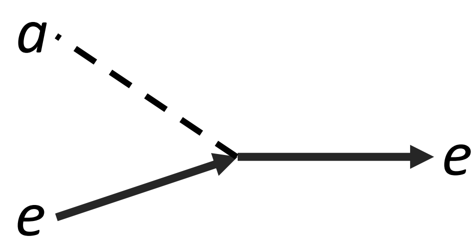

Solar axions (keV energies)

keV-mass bosonic DM particles
(ALP-like, hidden photons, …)

Observation of Excess Electronic Recoil Events in XENON1T

arXiv:2006.09721 (17 June 2020), accepted in PRD

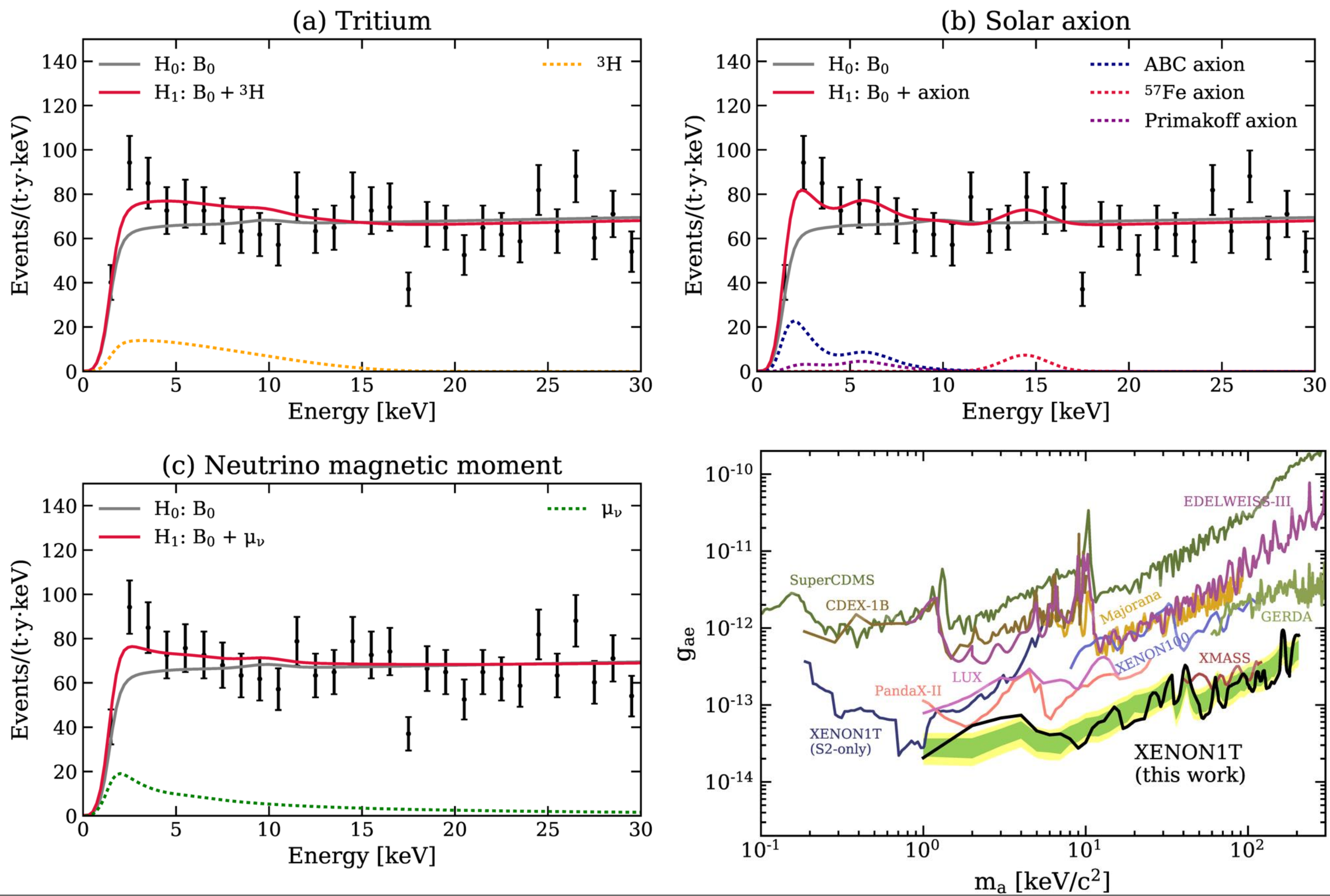

Solar Axions/ALPs

Redondo, arXiv:1310.0823

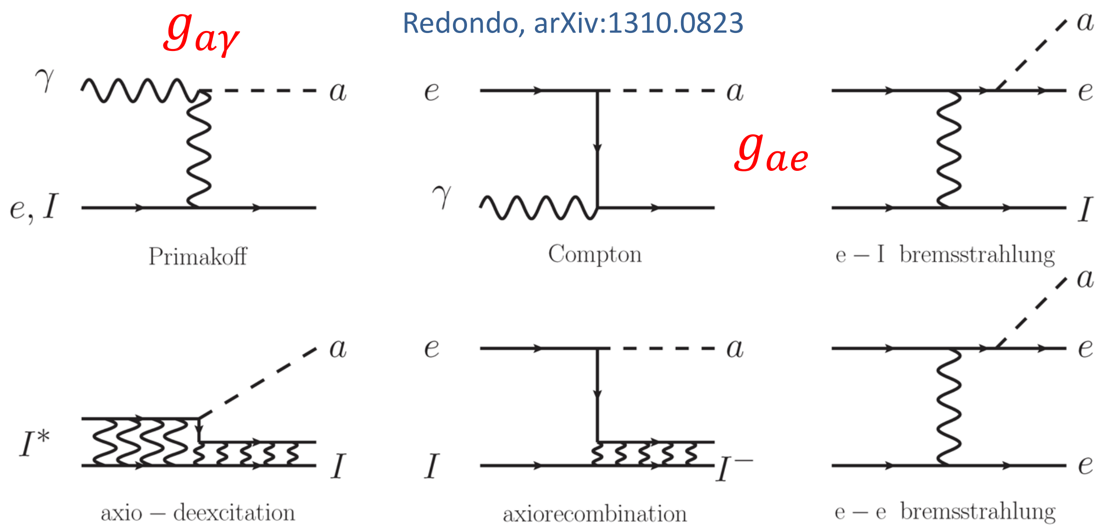

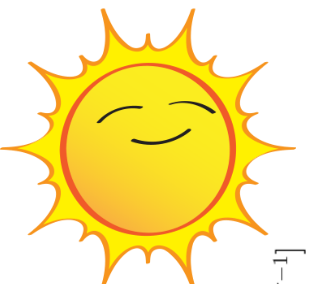

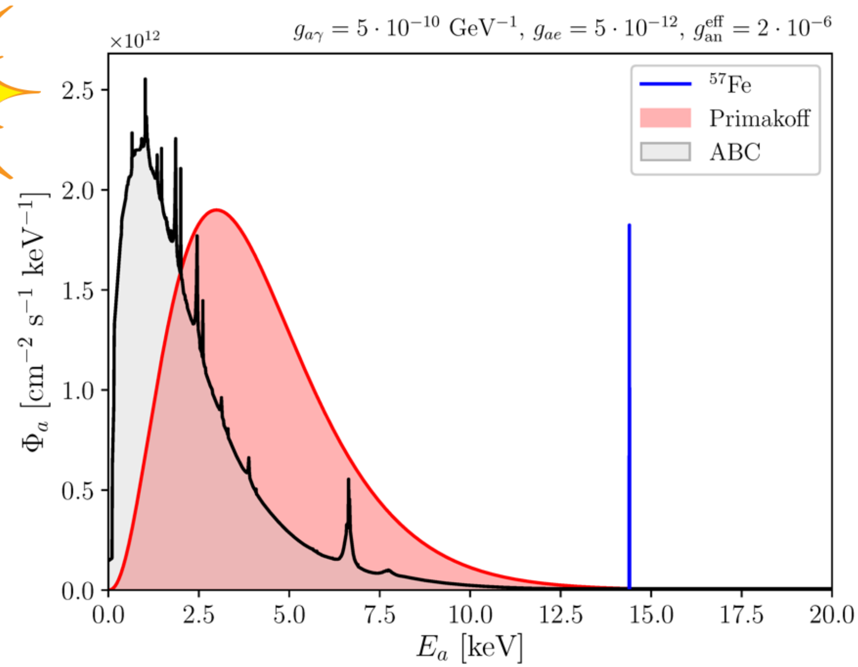

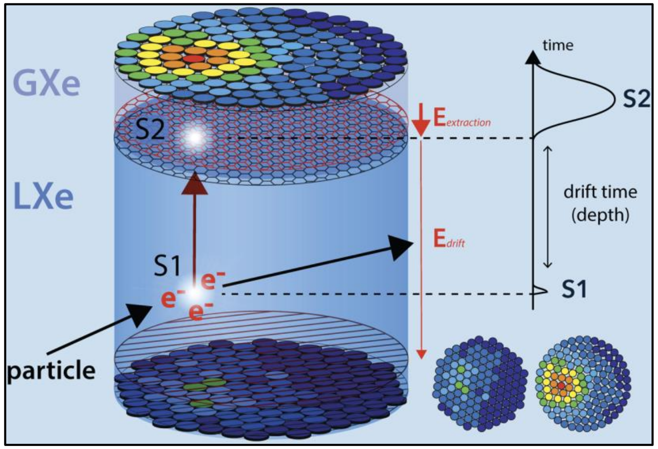

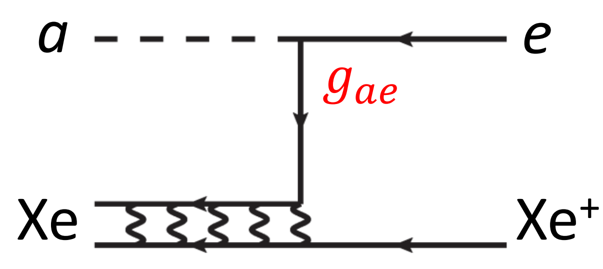

XENON Collab. 2006.09721

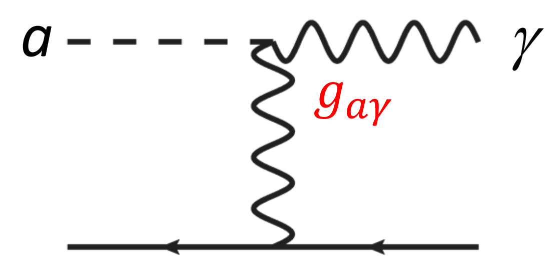

Dent+ 2006.15118, Gao+ 2006.14598

XENON1T Results for Solar Axions/ALPs

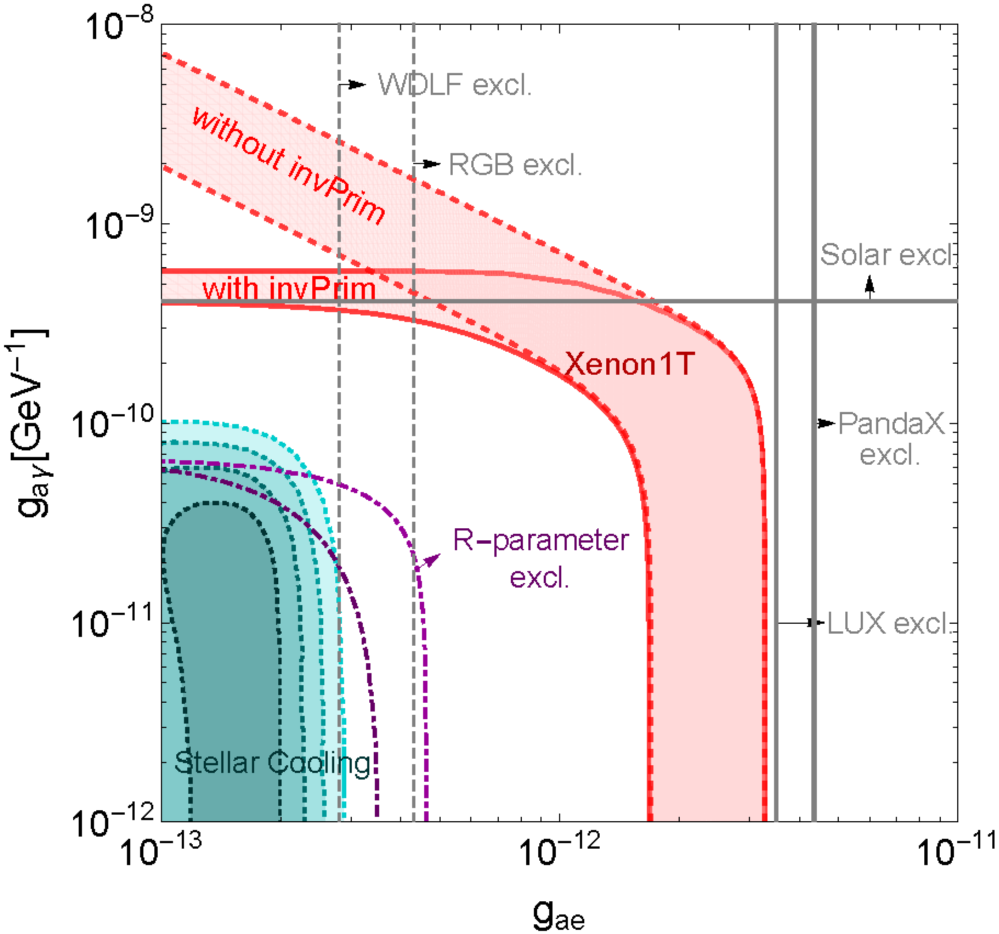

Gao+ 2006.14598v4
(includes xenon form factor of arXiv:2012.02508)

See also Dent+ 2006.15118

According to limits from stellar energy losses, XENON1T excess cannot be caused by solar axions/ALPs

EVOLUTION OF STARS

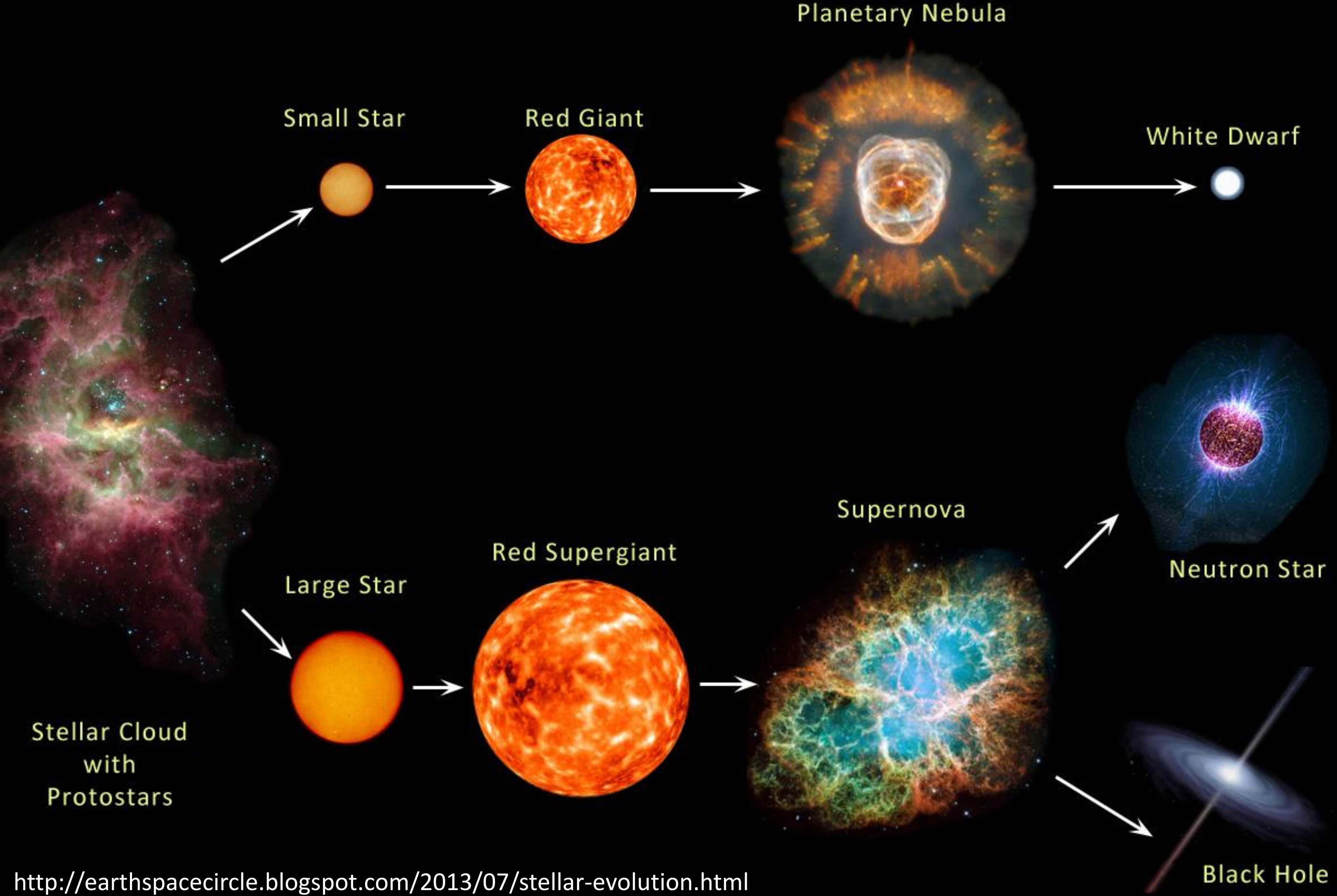

http://earthspacecircle.blogspot.com/2013/07/stellar-evolution.html

Galactic Globular Cluster M55

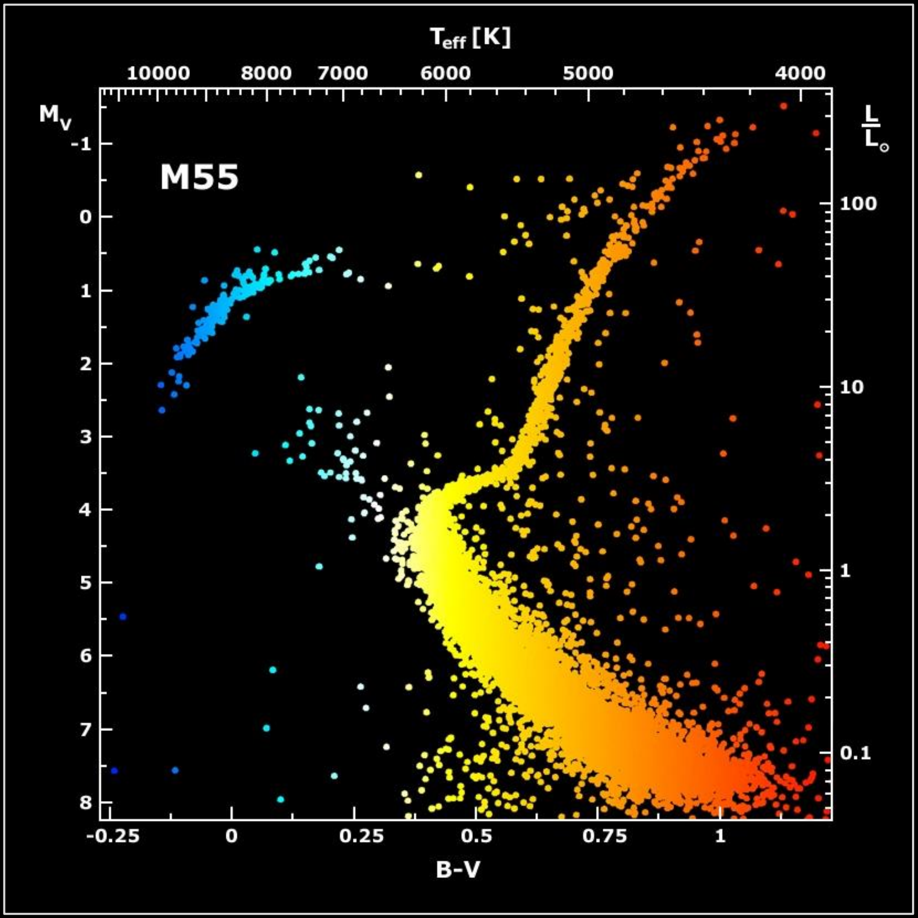

Color-Magnitude Diagram for Globular Clusters

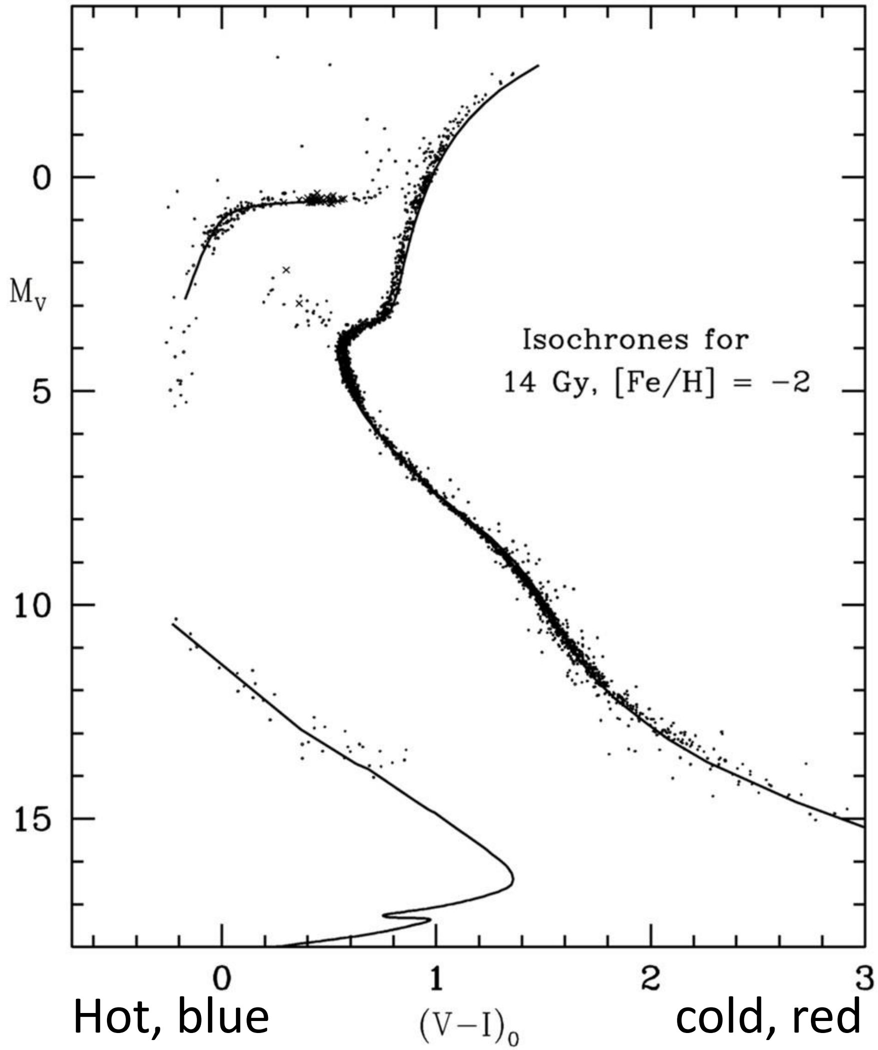

Color-magnitude diagram synthesized from several low-metallicity globular clusters and compared with theoretical isochrones (W.Harris, 2000)

Color-Magnitude Diagram for Globular Clusters

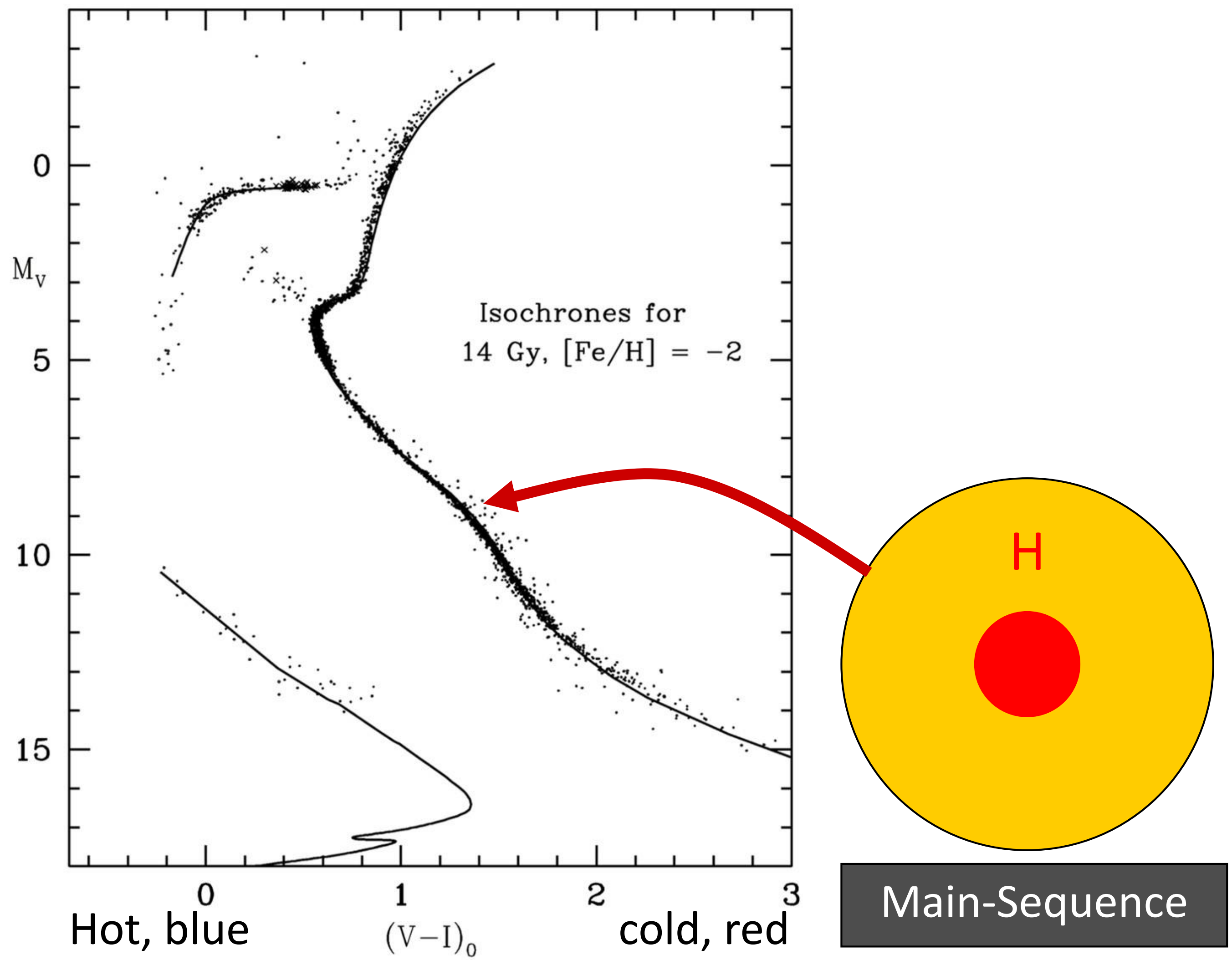

Color-magnitude diagram synthesized from several low-metallicity globular clusters and compared with theoretical isochrones (W.Harris, 2000)

Color-Magnitude Diagram for Globular Clusters

- Stars with M so large that they have burnt out in a Hubble time
- No new star formation in globular clusters

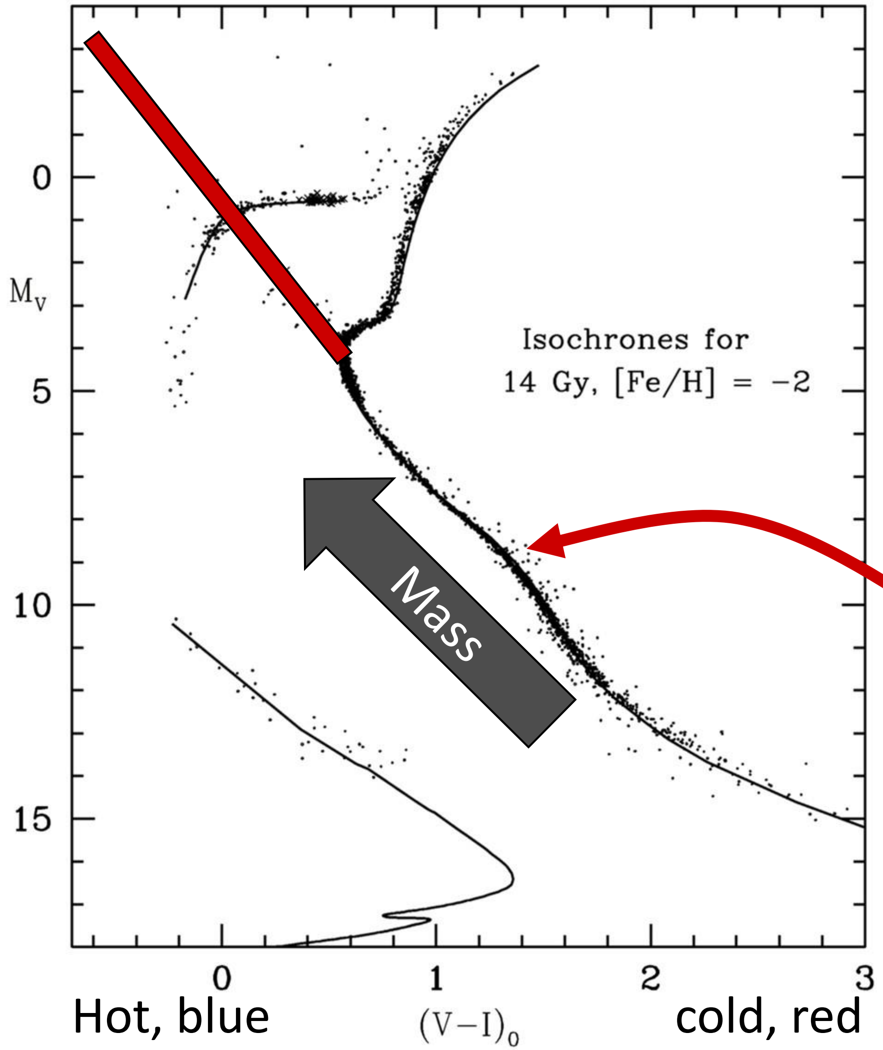

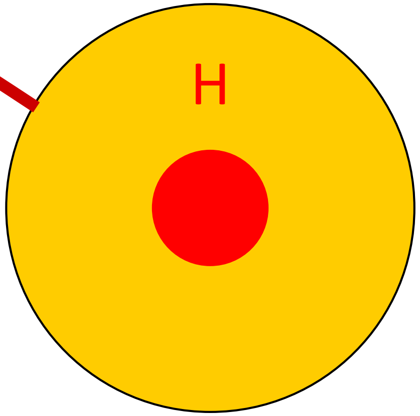

Main-Sequence

Color-magnitude diagram synthesized from several low-metallicity globular clusters and compared with theoretical isochrones (W.Harris, 2000)

Color-Magnitude Diagram for Globular Clusters

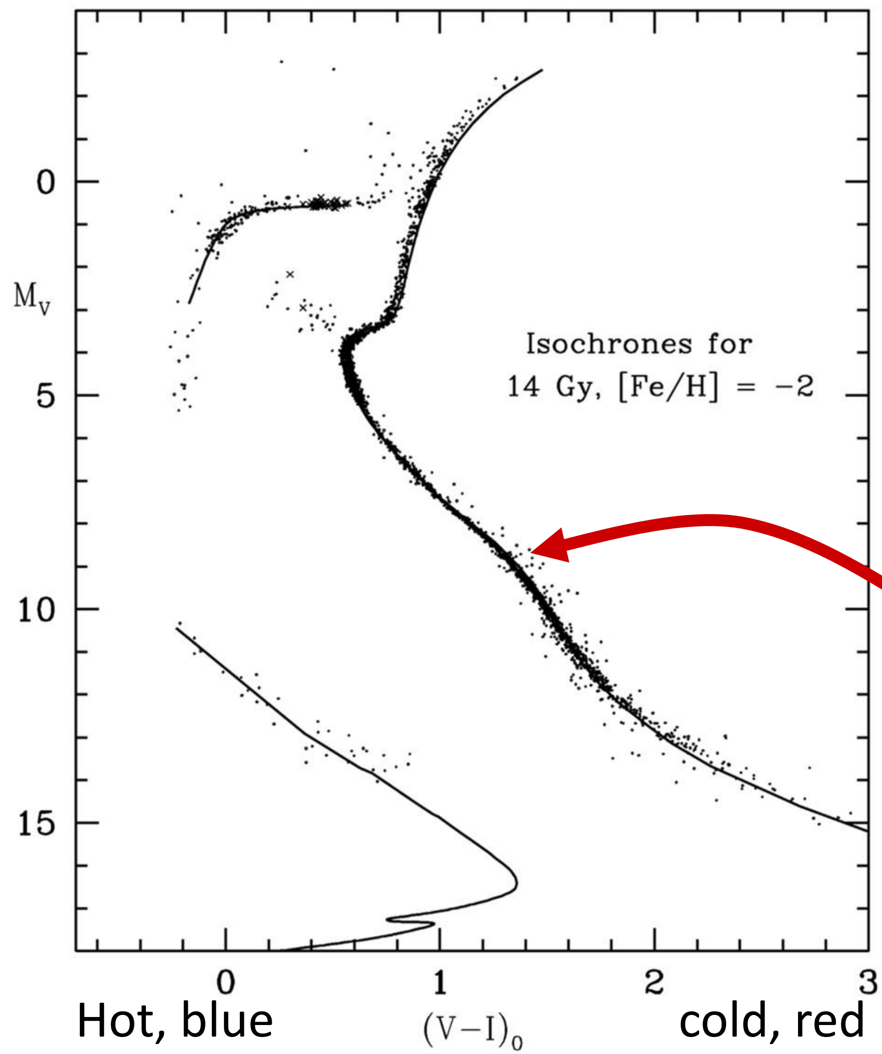

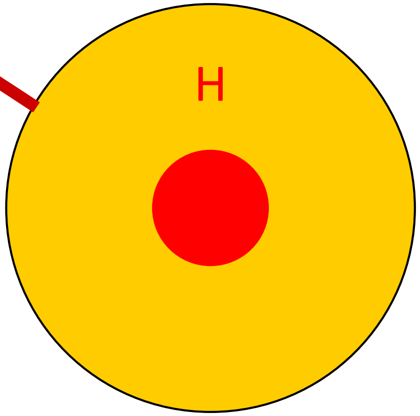

Main-Sequence

Color-magnitude diagram synthesized from several low-metallicity globular clusters and compared with theoretical isochrones (W.Harris, 2000)

Color-Magnitude Diagram for Globular Clusters

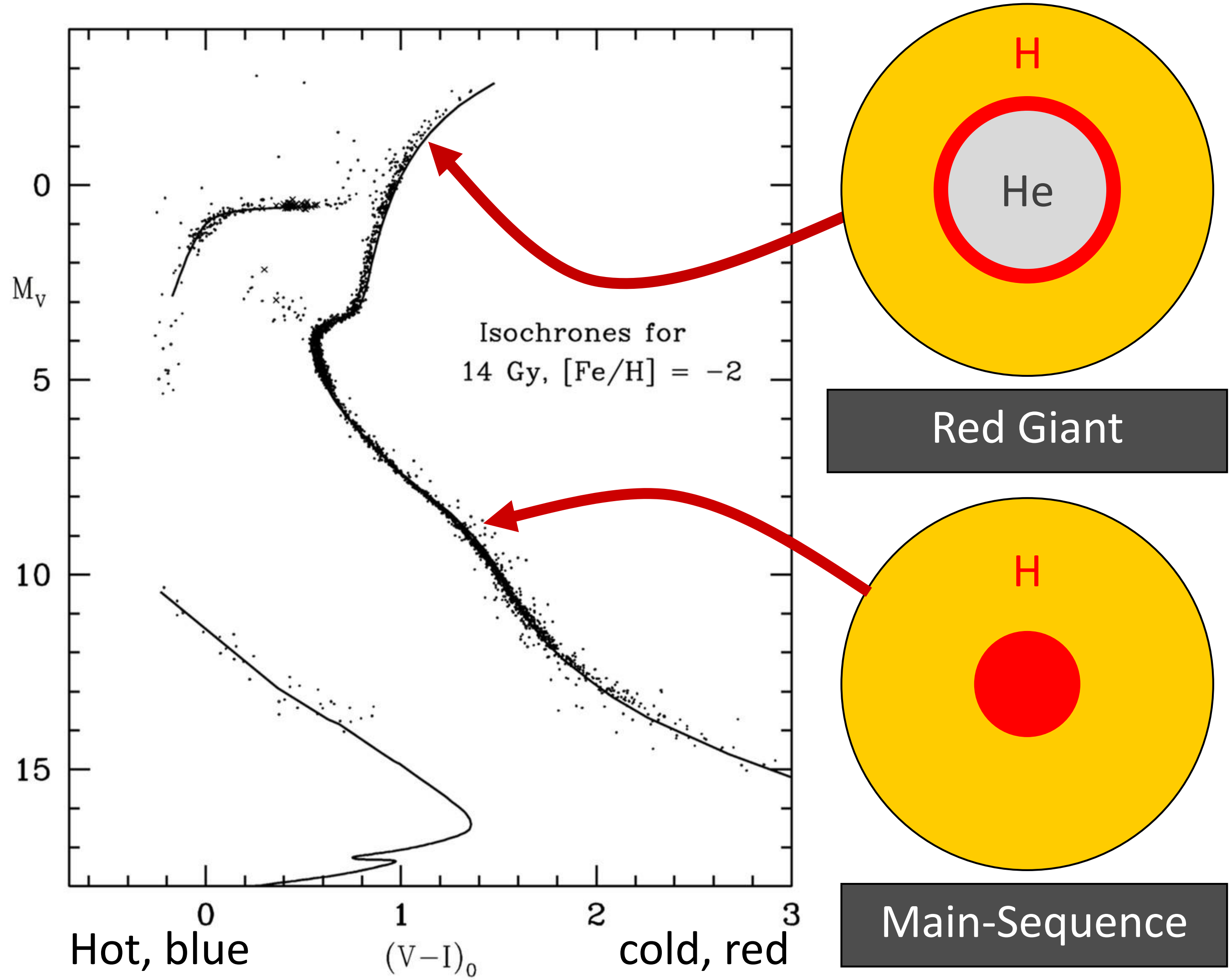

Color-magnitude diagram synthesized from several low-metallicity globular clusters and compared with theoretical isochrones (W.Harris, 2000)

Color-Magnitude Diagram for Globular Clusters

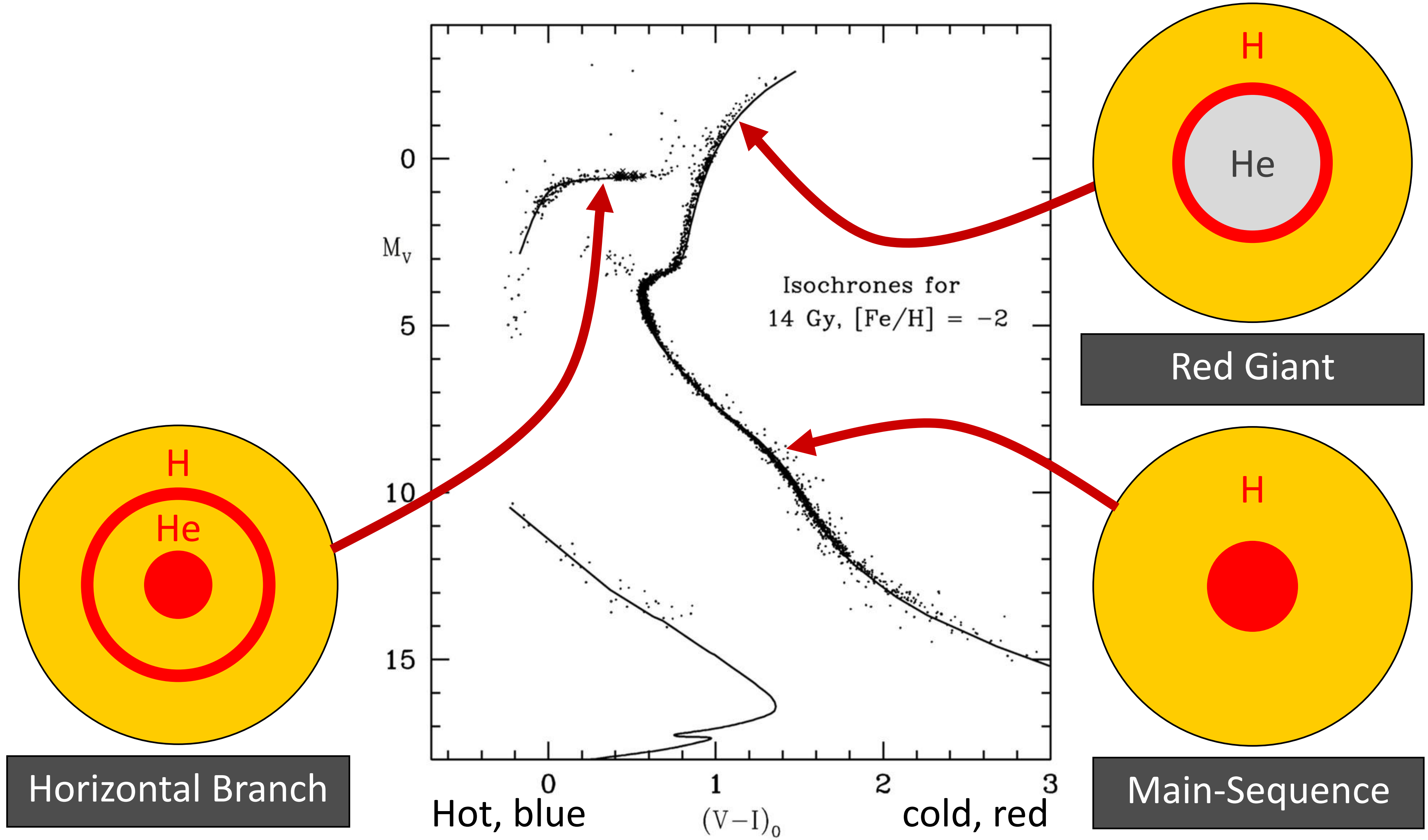

Color-magnitude diagram synthesized from several low-metallicity globular clusters and compared with theoretical isochrones (W.Harris, 2000)

Color-Magnitude Diagram for Globular Clusters

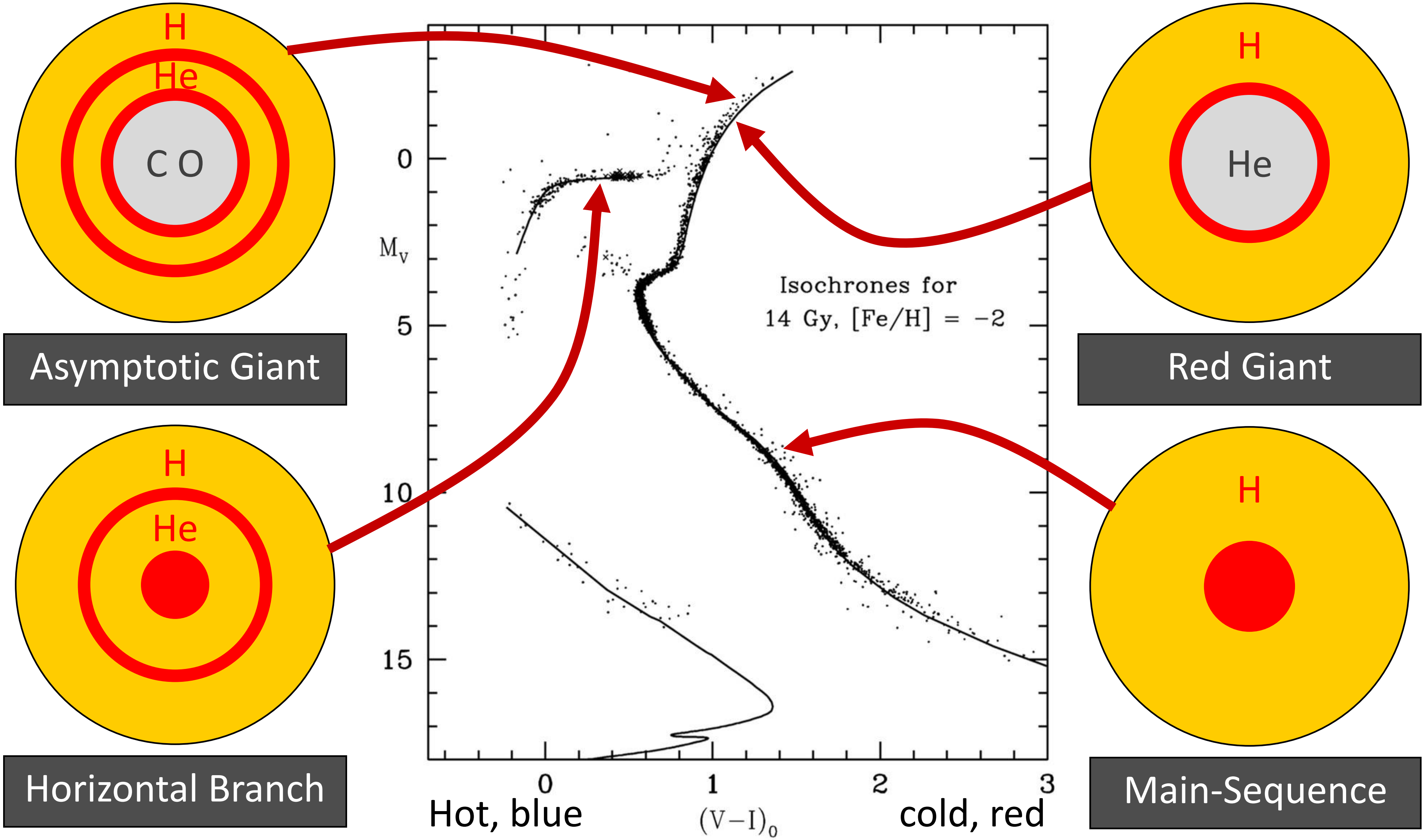

Color-magnitude diagram synthesized from several low-metallicity globular clusters and compared with theoretical isochrones (W.Harris, 2000)

Planetary Nebulae

Hour
Glass
Nebula

Helix Nebula

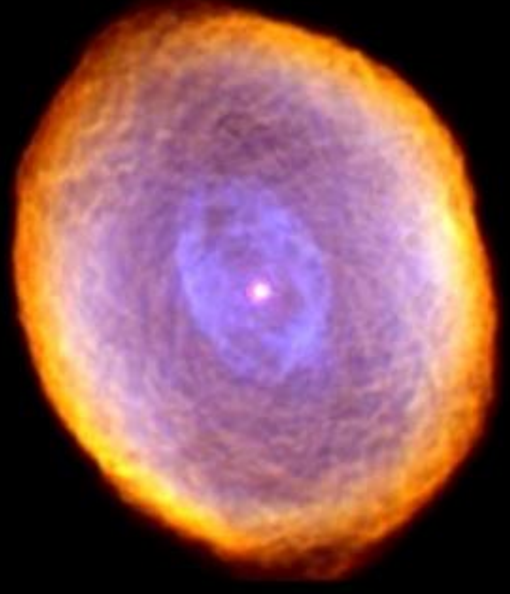

Planetary
Nebula IC 418

Planetary
Nebula NGC 3132

Eskimo
Nebula

Color-Magnitude Diagram for Globular Clusters

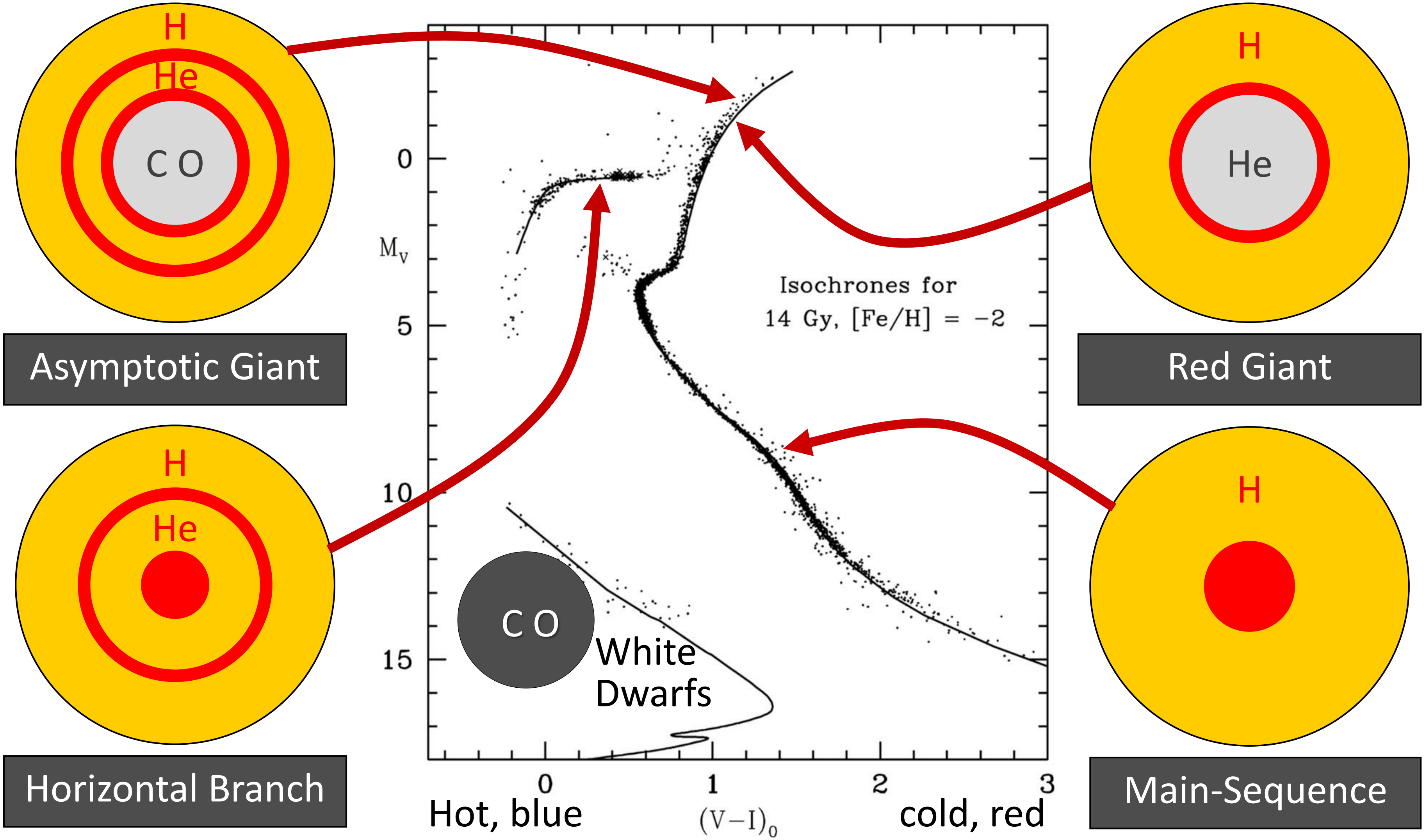

Color-magnitude diagram synthesized from several low-metallicity globular clusters and compared with theoretical isochrones (W.Harris, 2000)

Color-Magnitude Diagram for Globular Clusters

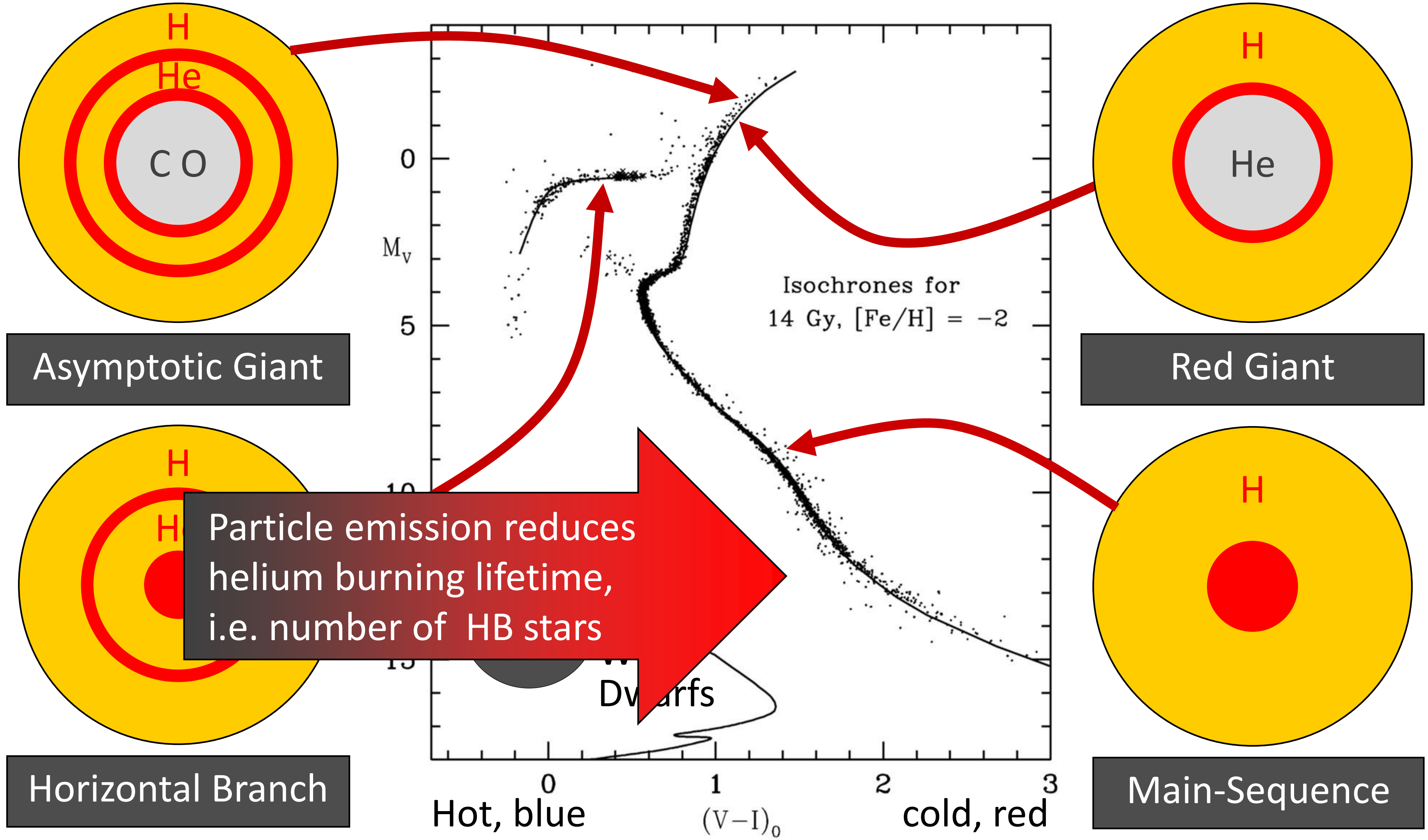

Color-magnitude diagram synthesized from several low-metallicity globular clusters and compared with theoretical isochrones (W.Harris, 2000)

Color-Magnitude Diagram for Globular Clusters

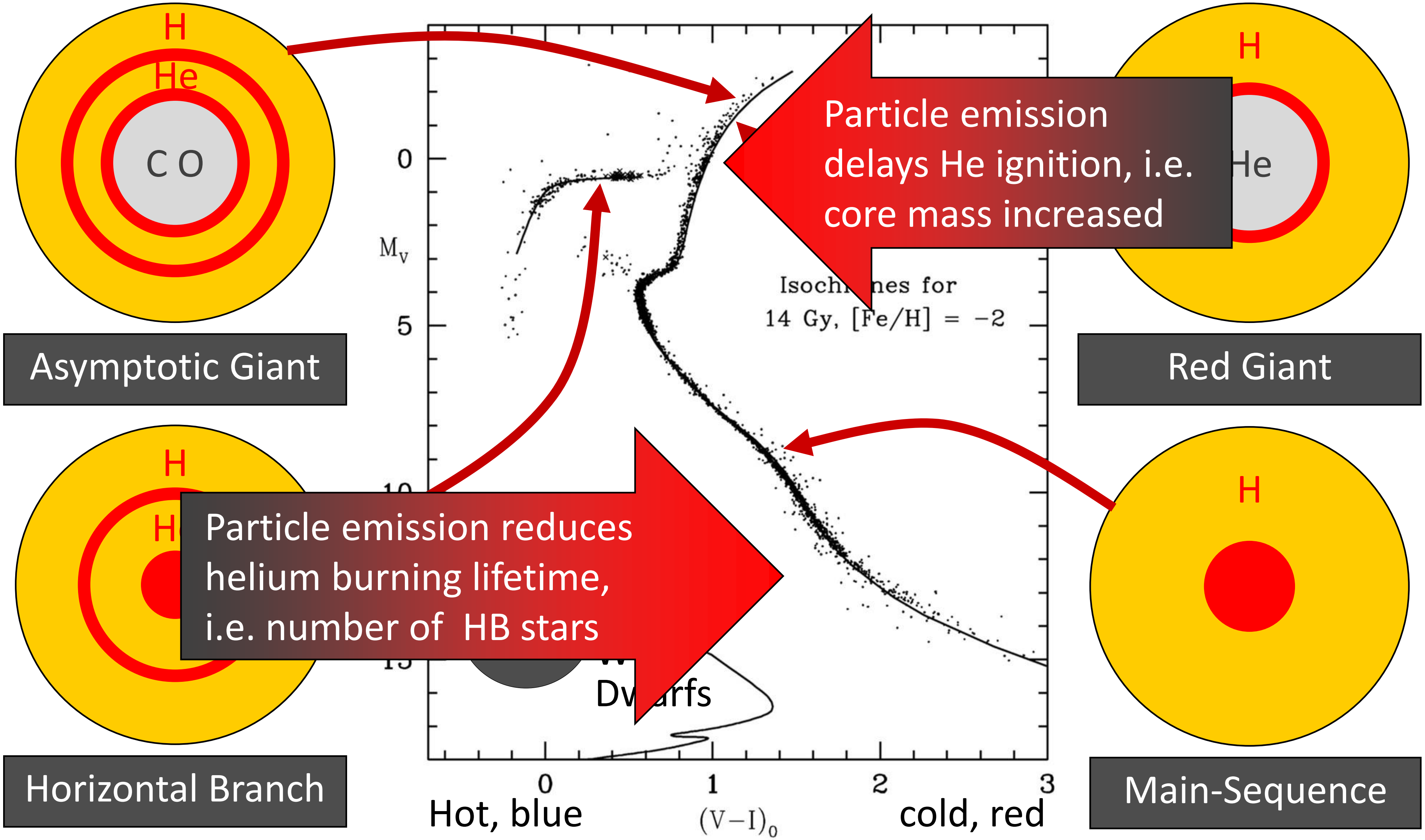

Color-magnitude diagram synthesized from several low-metallicity globular clusters and compared with theoretical isochrones (W.Harris, 2000)

Upper Red Giant Branch of Globular Clusters

Brightest red giant
measures nonstandard energy loss

Beccari et al., arXiv:astro-ph/0610289

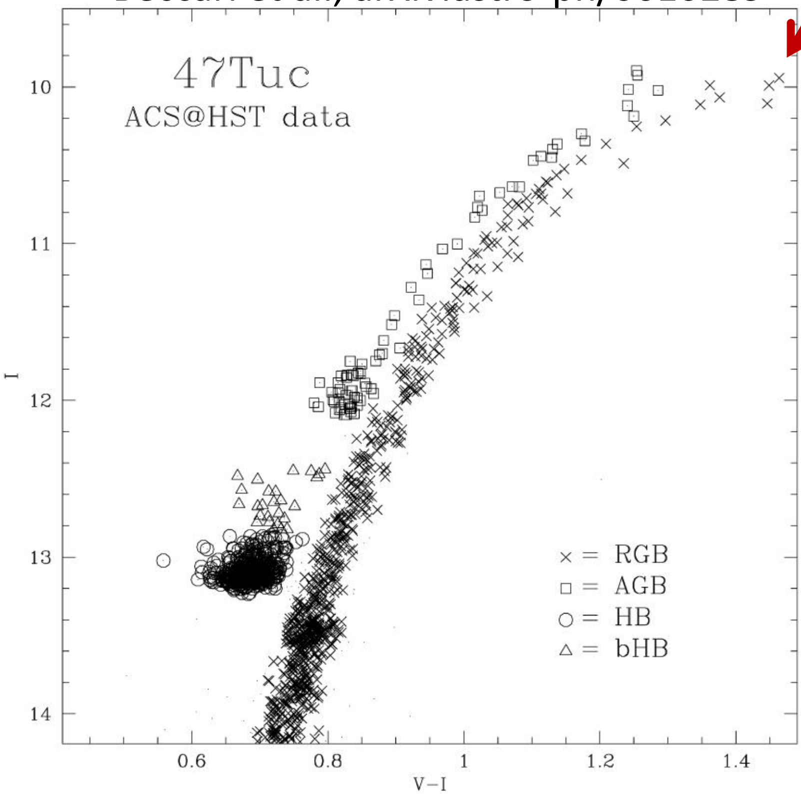

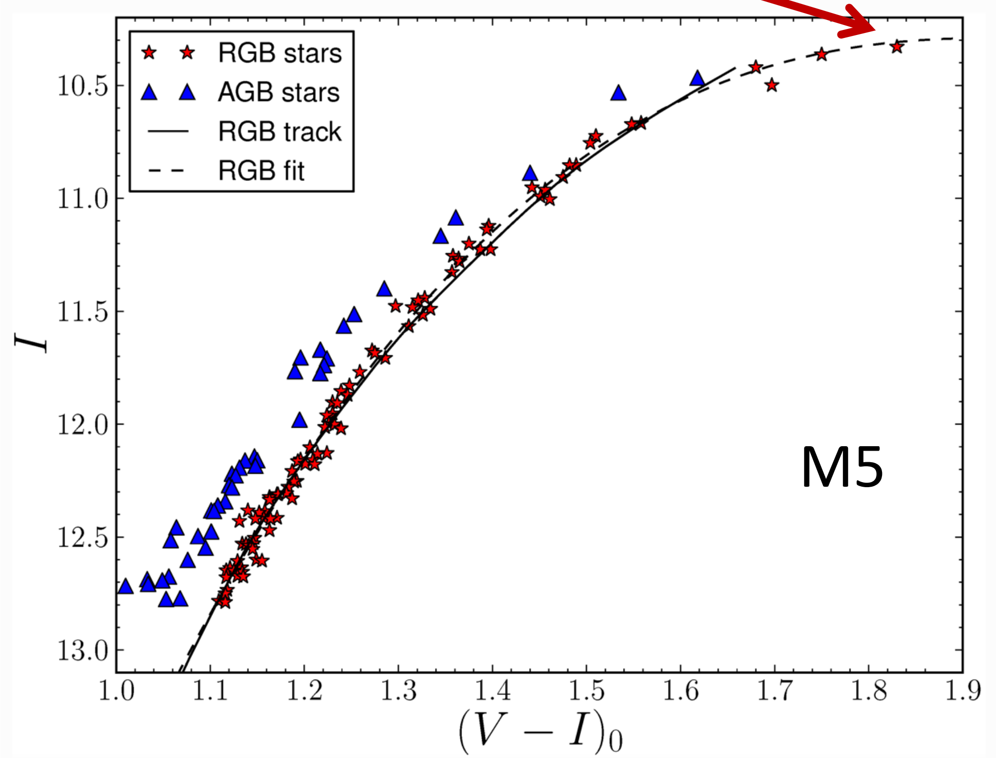

Straniero et al., arXiv:2010.03833

Viaux et al., arXiv:1308.4627

TRGB in 46 Globular Clusters [Cerny+ 2012.09701]

Tip of the Red-Giant Branch in the Galaxy NGC 4258

The Astrophysical Journal, 835:28 (17pp), 2017 January 20 Jang & Lee

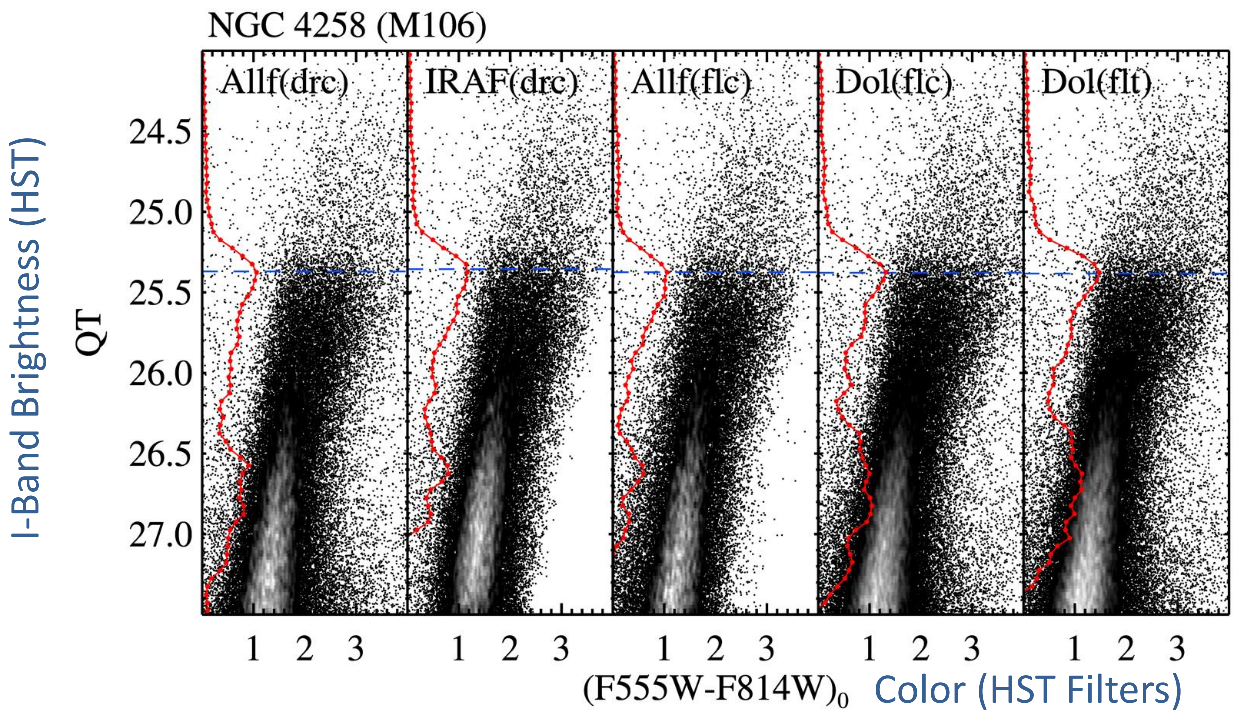

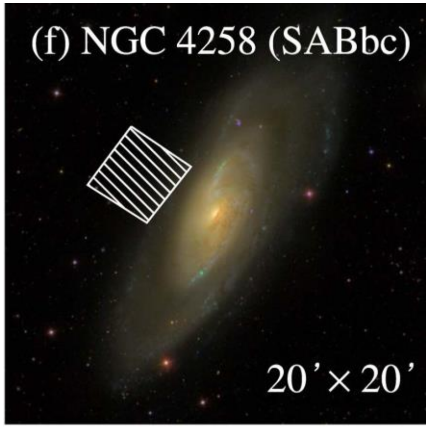

Figure 7. *QT* − (F555W − F814W)$_0$ CMDs of NGC 4258 from five different reduction methods : ALLFRAME on drc, IRAF/DAOPHOT on drc, ALLFRAME on flc, DOLPHOT on flc, and DOLPHOT on flt (from left to right). Edge detection responses are shown by the solid lines. Note that the estimated TRGB magnitudes (dashed lines) agree very well.

NGC 4258 hosts a water megamaser
→ Quasi-geometric distance determination
→ Among the best absolute TRGB calibrations

Determinations of the Hubble Constant

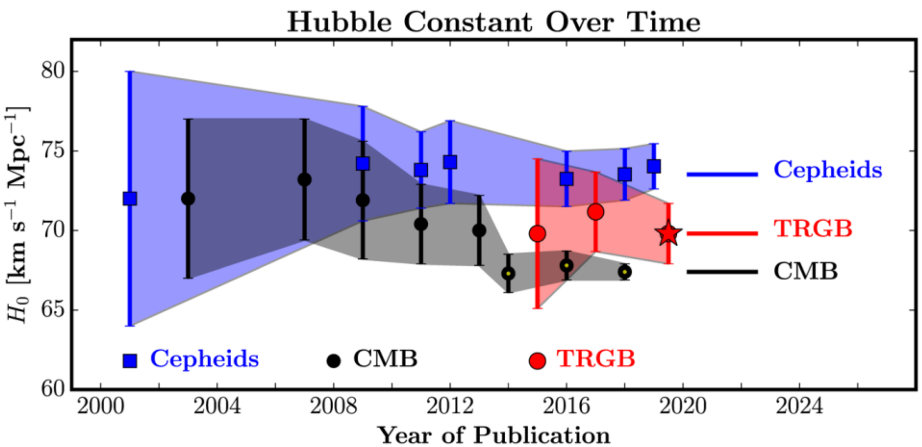

Freedman et al. 2019, ApJ 882:34

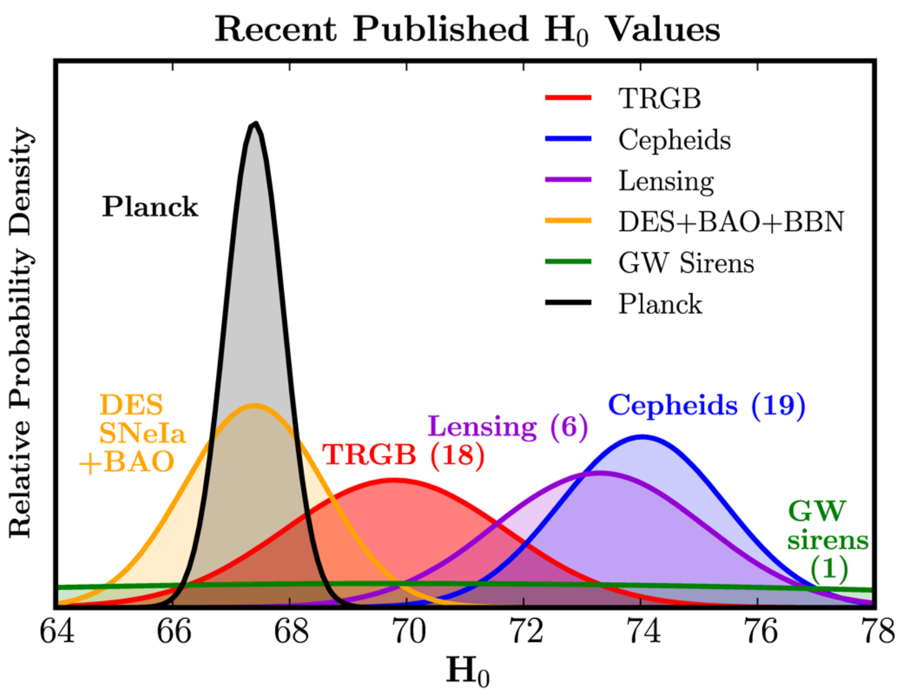

Freedman et al. 2020 ApJ 891:57

Brightness and Core Mass at TRGB

Raffelt & Weiss, Astron. Astrophys. 264 (1992) 536

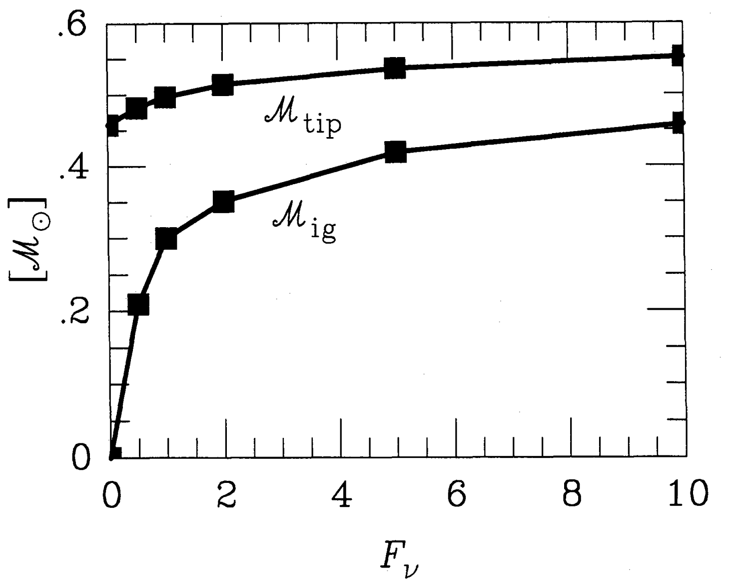

Fig. 2. Core mass at helium flash, $\mathcal{M}_{\rm tip}$, and mass-coordinate of the ignition point, $\mathcal{M}_{\rm ig}$, as a function of F_ν for $\mathcal{M} = 0.80$, $Z = 10^{-4}$, and $Y_0 = 0.22$ (see Table 2).

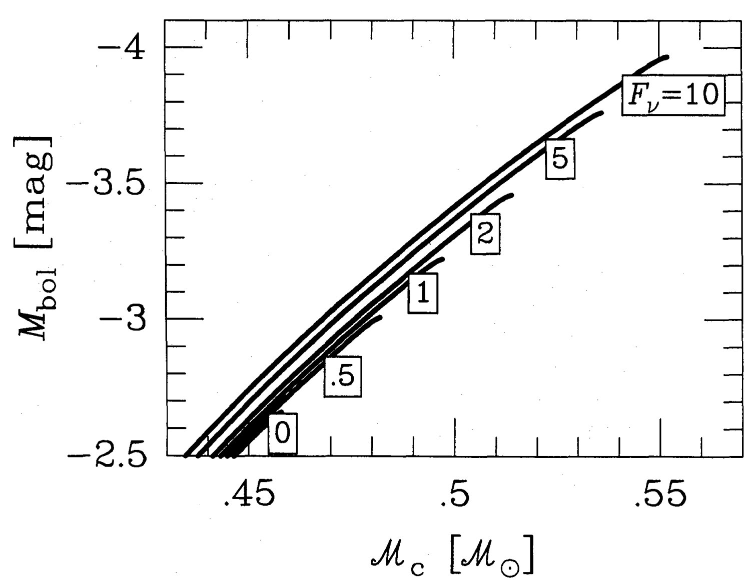

Fig. 3. Absolute surface brightness as a function of core mass for the $Z = 10^{-4}$ runs of Table 2. The curves are marked with the relevant F_ν values.

Parametric study: Vary standard neutrino losses with a fudge factor F_ν ($F_\nu = 1$ standard, $F_\nu = 0$ no losses at all, etc.)

- Helium ignition point (mass coordinate $\mathcal{M}_{ig}$)
- Core mass at ignition $\mathcal{M}_{tip}$
- Bolometric brightness at ignition M_{tip}

Neutrinos from Thermal Processes

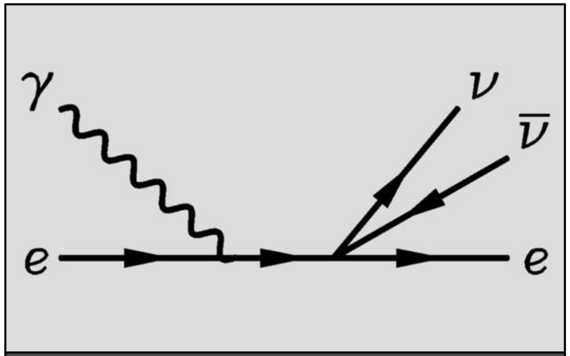

Photo (Compton)

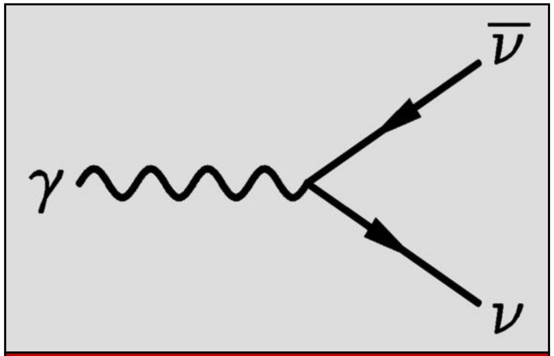

Plasmon decay

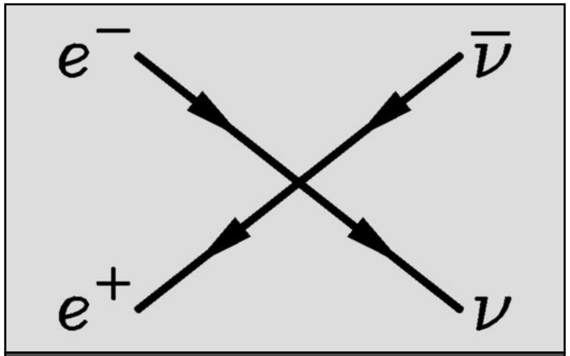

Pair annihilation

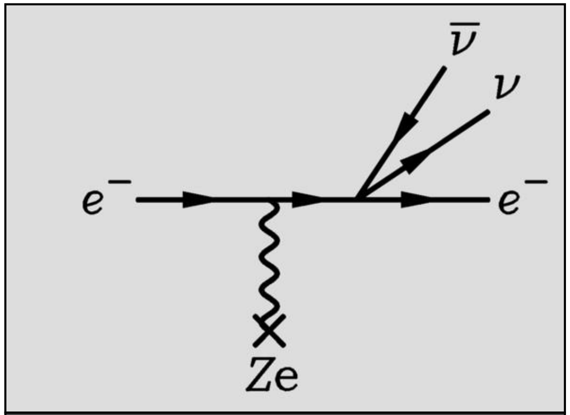

Bremsstrahlung

These processes were first discussed in 1961–63 after V–A theory

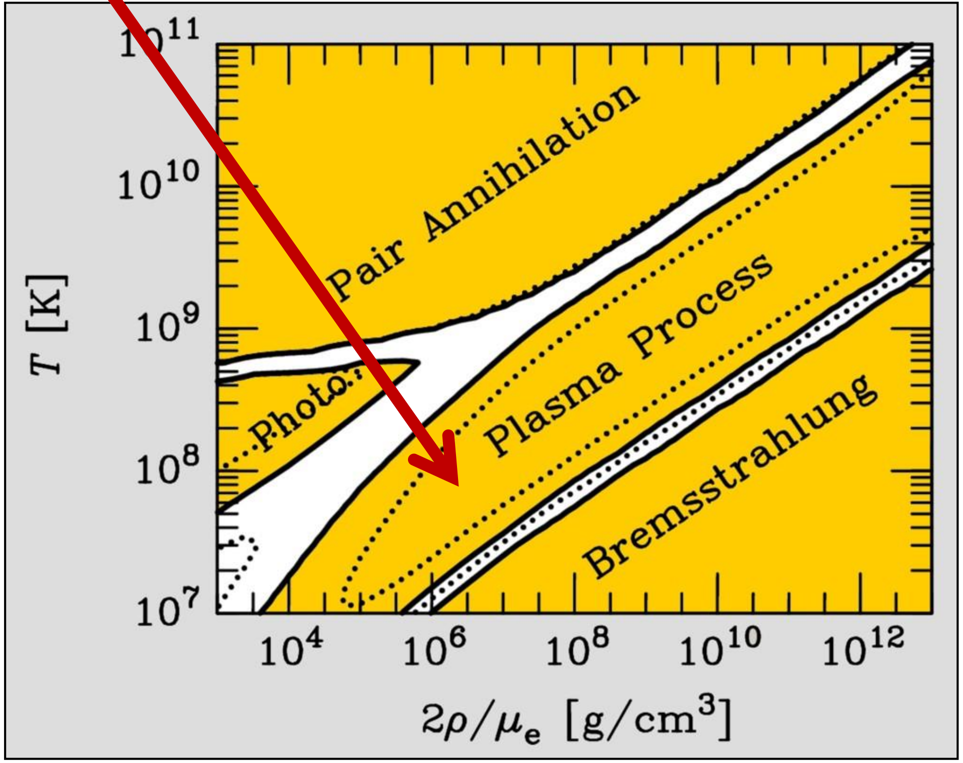

Particle Emission from Red-Giant Core or White Dwarf

Large Neutrino Dipole Moment

- Requires BSM physics
- Direct coupling to EM field
- Enhances plasmon decay

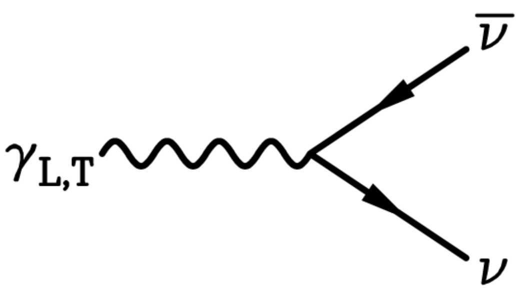

$\mu_\nu < 1.5 \times 10^{-12} \mu_{\mathrm{B}}$ (95% CL)

Axions (or friends) with direct coupling to electrons

- Bremsstrahlung emission by degenerate electrons

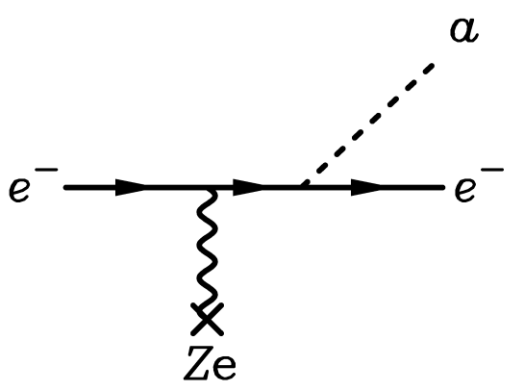

$g_{ae} < 1.6 \times 10^{-13}$ (95% CL)

Axion Bounds from TRGB Calibrations

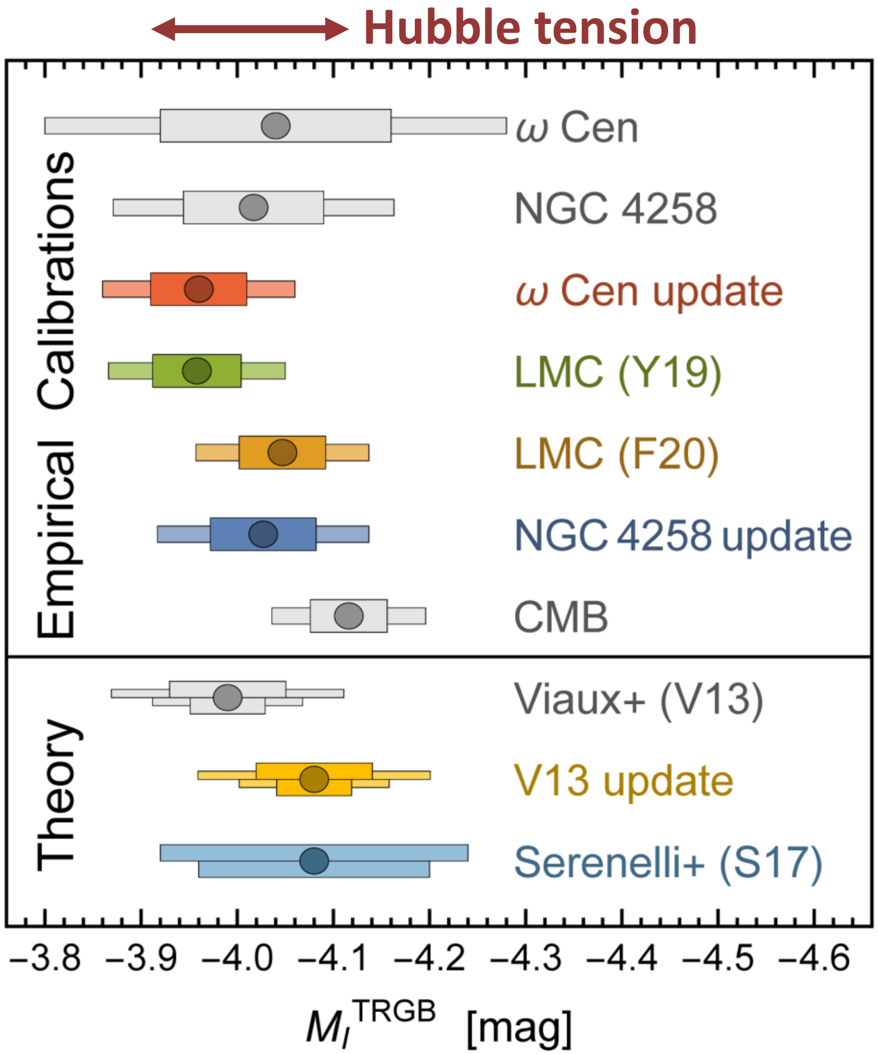

Updated TRGB Calibrations
Capozzi & Raffelt, arXiv:2007.03694

Bounds from "water megamaser" galaxy NGC 4258, compared with stellar evolution theory (95% CL)

$$g_{ae} < 1.6 \times 10^{-13}$$

$$\mu_\nu < 1.5 \times 10^{-12} \mu_{\mathrm{B}}$$

XENON1T interpretation:

$$g_{ae} \sim 30 \times 10^{-13}$$

$$\mu_\nu \sim 20 \times 10^{-12} \mu_{\mathrm{B}}$$

New Distance Determinations in the Galaxy

- Best galactic TRGB calibration with globular cluster ω Centauri
- Depends on distance determination

- Kinematical distance determination using Gaia DR2 data (Baumgardt+ 2019, arXiv:1811.01507, used by Capozzi & Raffelt)
  $d = 5.24 \pm 0.05$ kpc $\mu = 13.597 \pm 0.021$ mag

- TRGB calibration with 46 globular clusters (Cerny+ 2012.09701, 17 Dec 2020), using ω Cen as a distance anchor based on Detached Eclipsing Binaries (DEBs)
  $d = 5.44 \pm 0.27$ kpc $\mu = 13.68 \pm 0.11$ mag

- ω Cen distance based on Gaia EDR3 data (Soltis+ 2012.09196, 16 Dec 2020) to improve TRGB Hubble estimate
  $d = 5.24 \pm 0.11$ kpc $\mu = 13.595 \pm 0.047$ mag

- ω Cen distance based on Gaia EDR3 data (Maíz Apellániz+ 2101.10206 28 Jan 2021)
  $d = 5.25 \pm 0.27$ kpc $\mu = 13.60 \pm 0.11$ mag

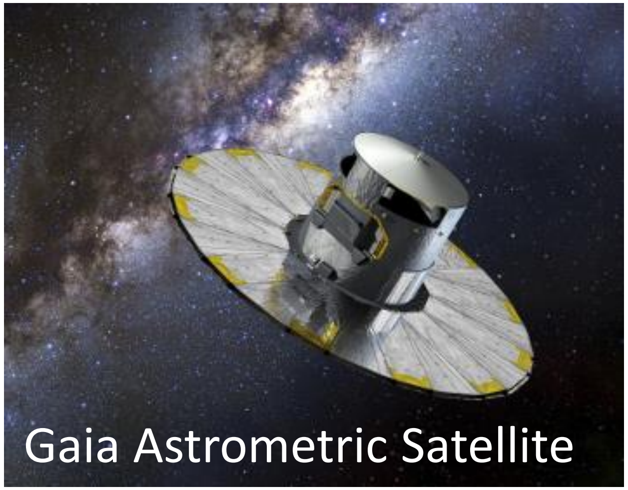

New TRGB Calibration from 22 Globular Clusters

Straniero et al., arXiv:2010.03833 (8 Oct. 2020)

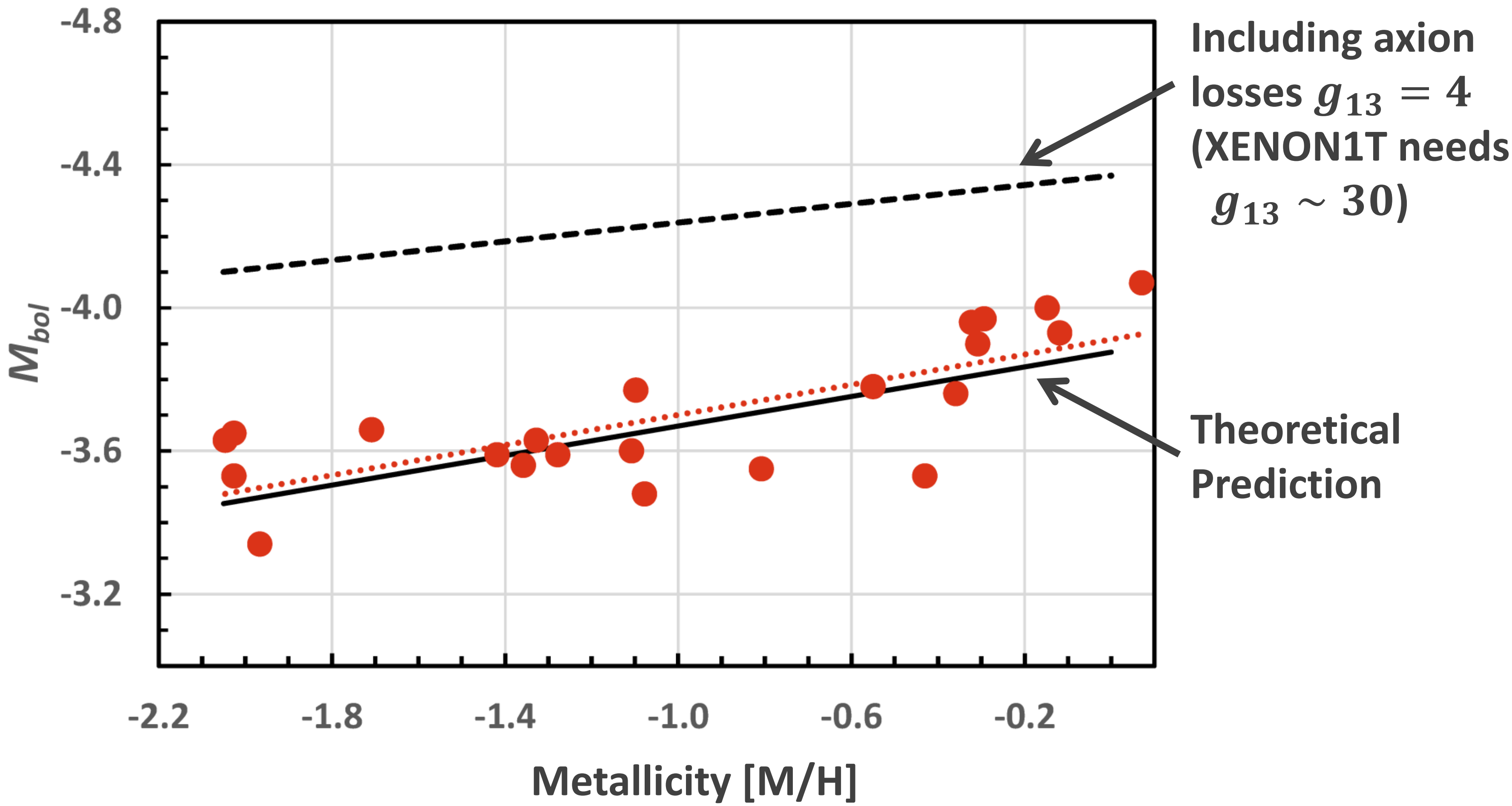

Their final axion limit: $g_{ae} < 1.2 \times 10^{-13}$ (95% CL)

EVOLUTION OF STARS

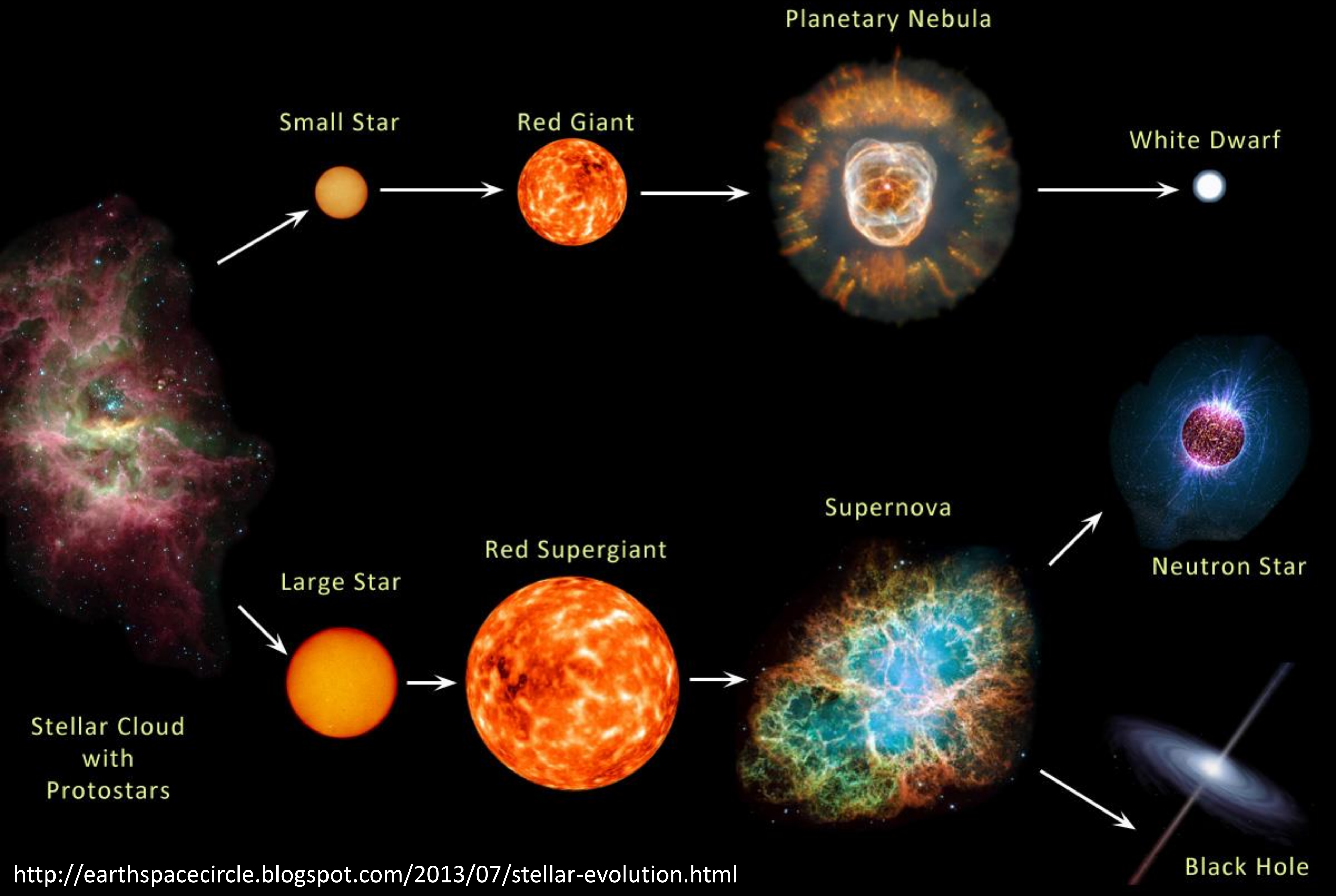

http://earthspacecircle.blogspot.com/2013/07/stellar-evolution.html

Crab Nebula – Remnant of SN 1054

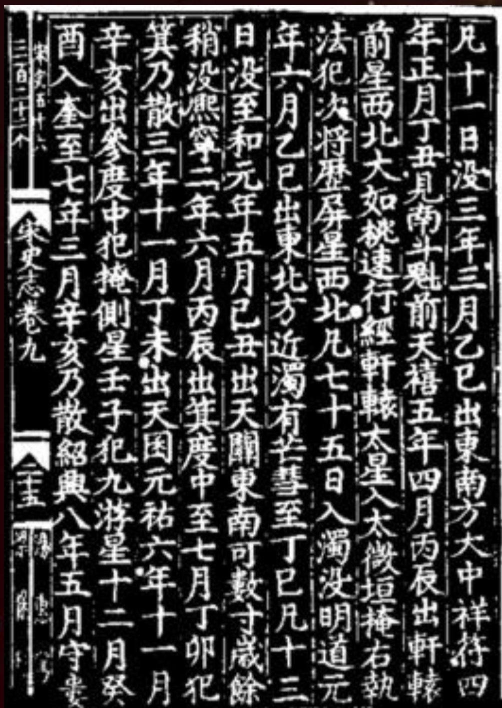

凡十一日沒三年三月乙巳出東南方大中祥符四
年正月丁丑見南斗魁前天禧五年四月丙辰出軒轅
前星西北大如桃速行經軒轅太星入太微垣掩右執
法犯次將歷屏星西北凡七十五日入濁沒明道元
年六月乙巳出東北方近濁有芒彗至丁巳凡十三
日沒至和元年五月己丑出天關東南可數寸歲餘
稍沒熙寧二年六月丙辰出箕度中至七月丁卯犯
箕乃散三年十一月丁未出天囷元祐六年十一月
辛亥出參度中犯掩側星壬子犯九游星十二月癸
酉入奎至七年三月辛亥乃散紹興八年五月守婁

宋史志卷九

Core-Collapse Supernova Explosion

End state of a massive star $M \gtrsim 6–8\ M_\odot$	Collapse of degenerate core	Bounce at $\rho_{\rm nuc}$ Shock wave forms explodes the star	Grav. binding E $\sim 3\times10^{53}$ erg emitted as nus of all flavors

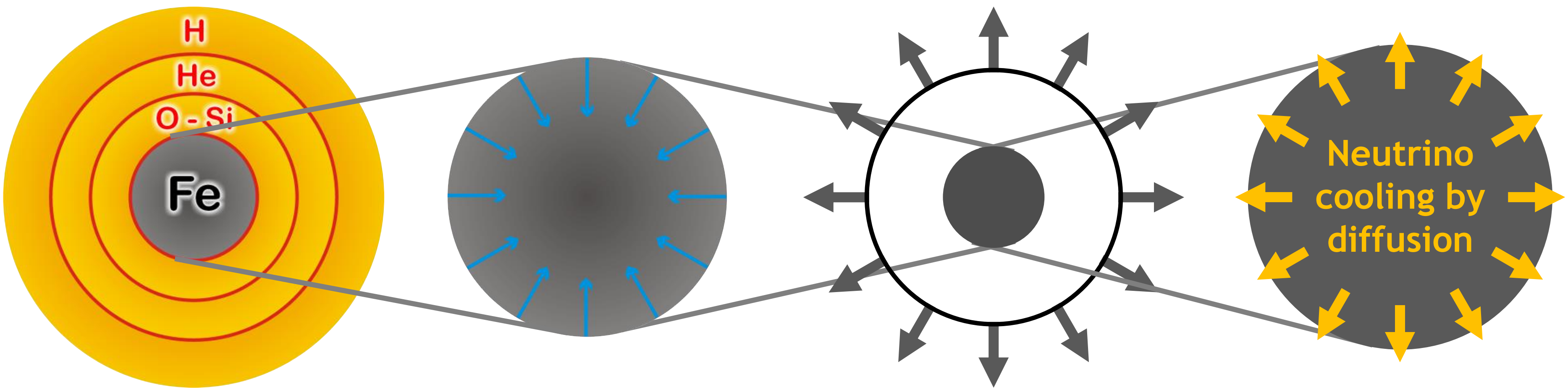

- Huge rate of low-E neutrinos (tens of MeV) over few seconds in large-volume detectors
- A few core-collapse SNe in our galaxy per century
- Once-in-a-lifetime opportunity

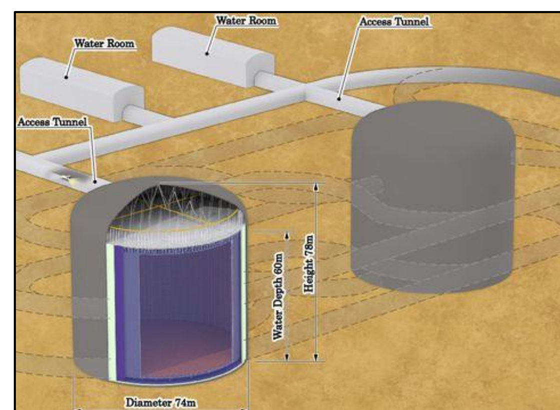

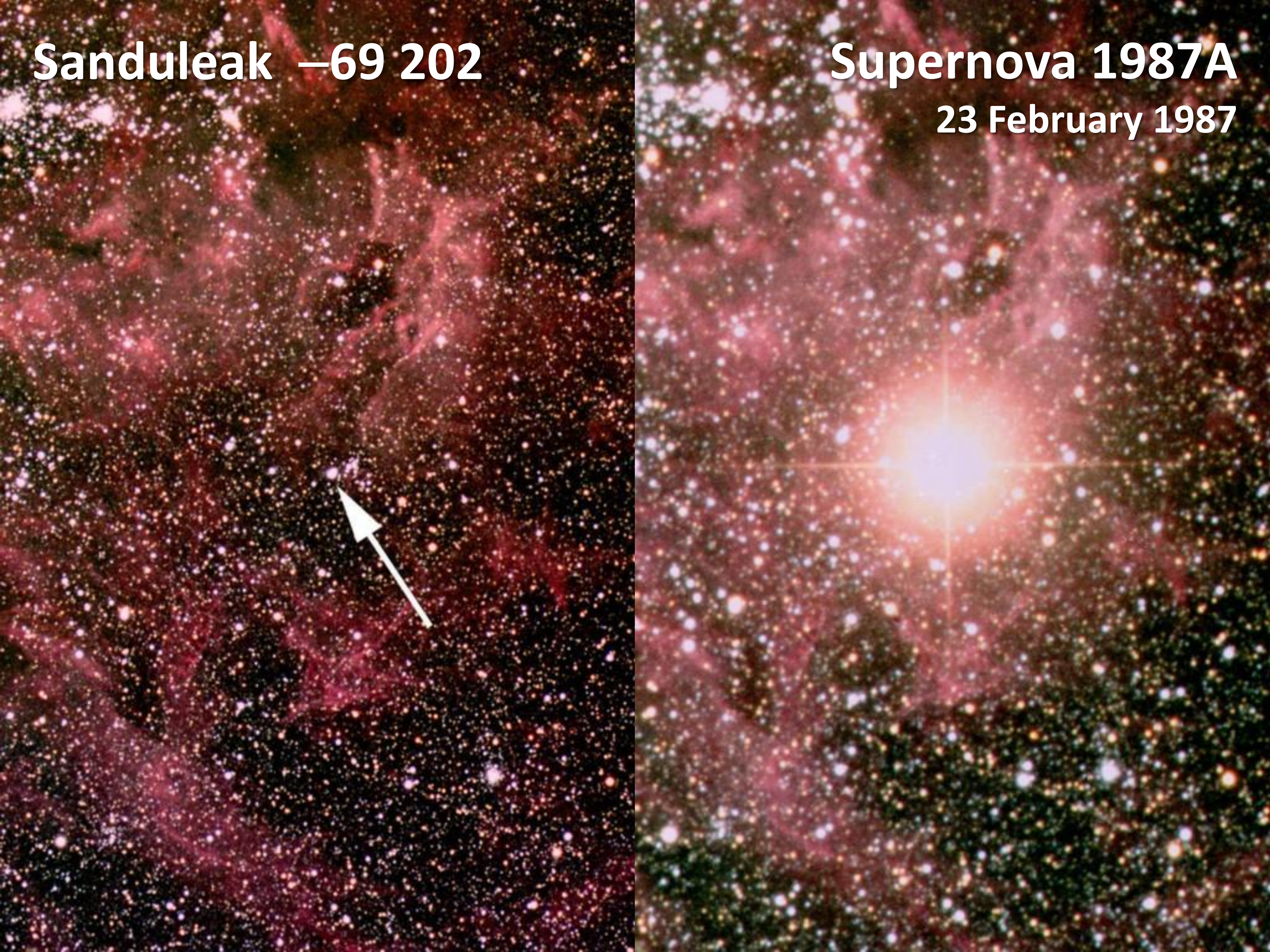
Sanduleak –69 202
Supernova 1987A
23 February 1987

Neutrino Signal of Supernova 1987A

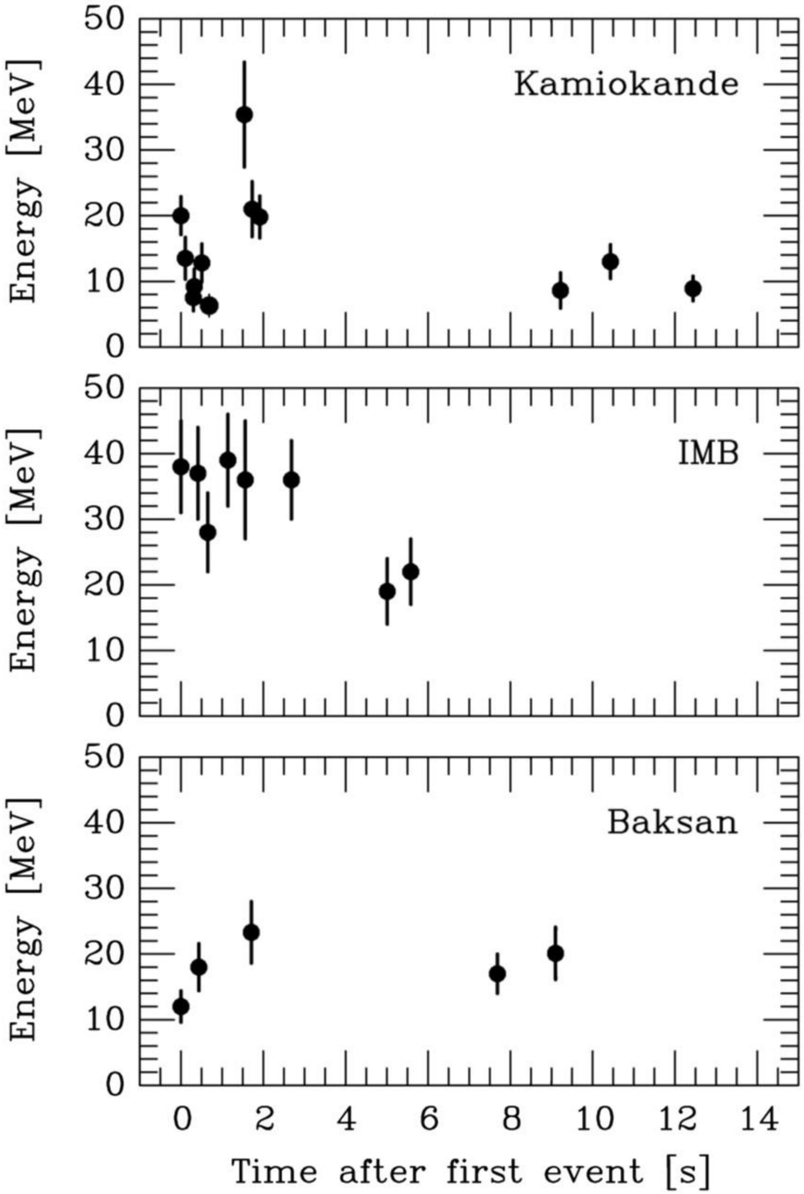

Kamiokande-II (Japan)
Water Cherenkov detector
2140 tons
Clock uncertainty $\pm$1 min

Irvine-Michigan-Brookhaven (US)
Water Cherenkov detector
6800 tons
Clock uncertainty $\pm$50 ms

Baksan Scintillator Telescope
(Soviet Union), 200 tons
Random event cluster $\sim$ 0.7/day
Clock uncertainty $+2/-54$ s

Within clock uncertainties,
all signals are contemporaneous

Supernova 1987A Energy-Loss Argument

SN 1987A neutrino signal

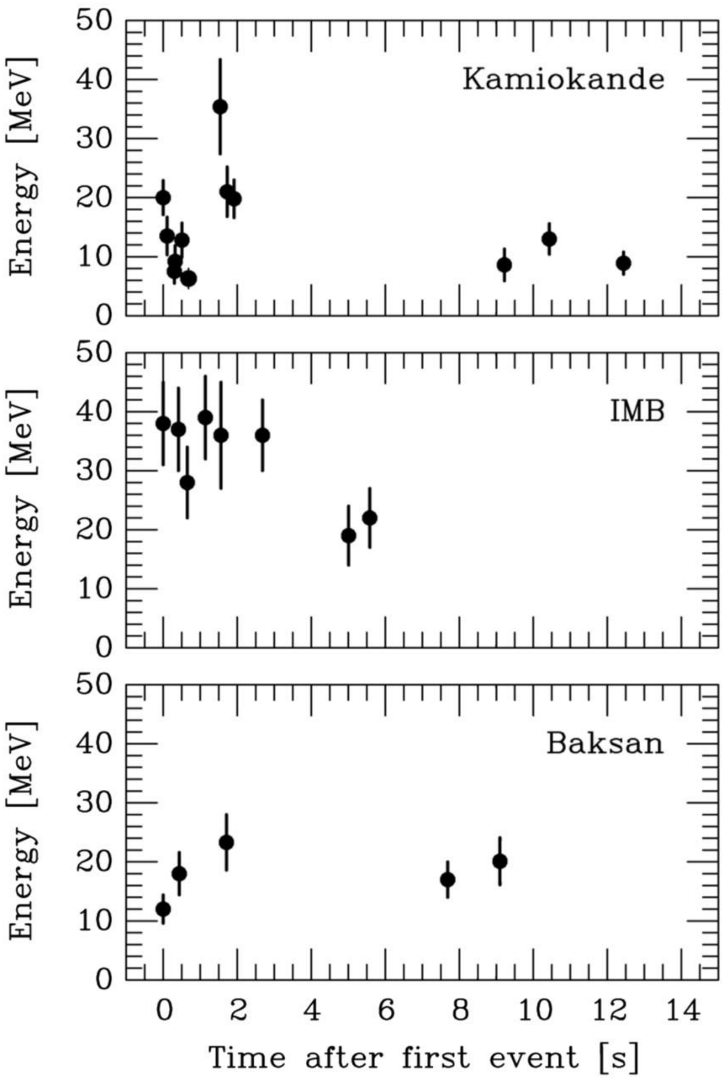

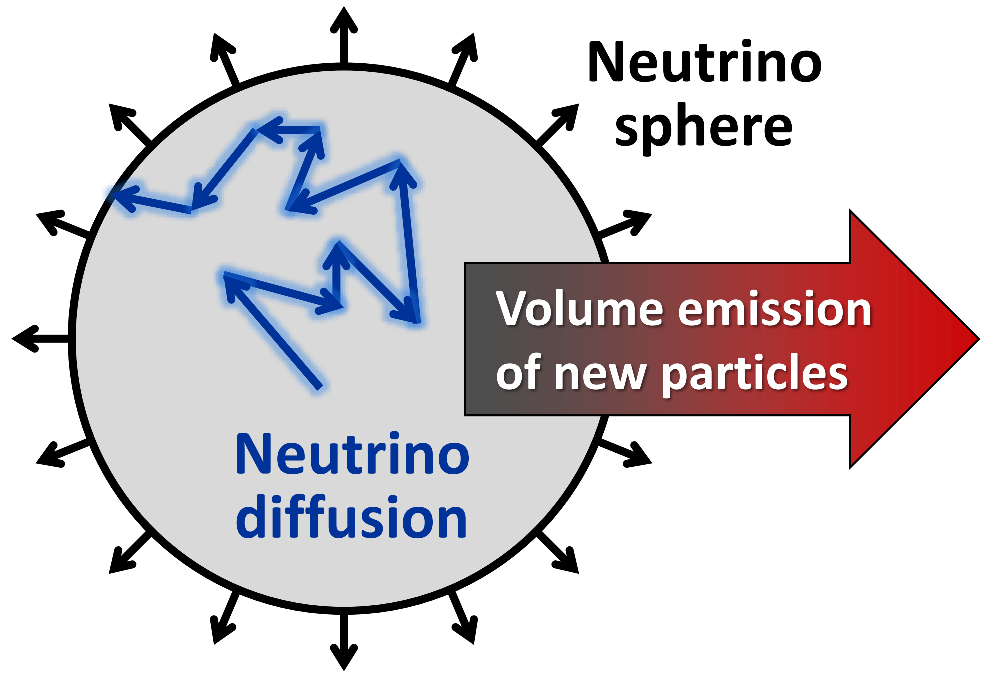

Emission of very weakly interacting particles would "steal" energy from the neutrino burst and shorten it.
(Early neutrino burst powered by accretion, not sensitive to volume energy loss.)

Late-time signal most sensitive observable

Cooling Time Scale

Exponential cooling model: $T = T_0\, e^{-t/4\tau}$, constant radius, $L = L_0\, e^{-t/\tau}$

Fit parameters are T_0, τ, radius, 3 offset times for KII, IMB & BST detectors

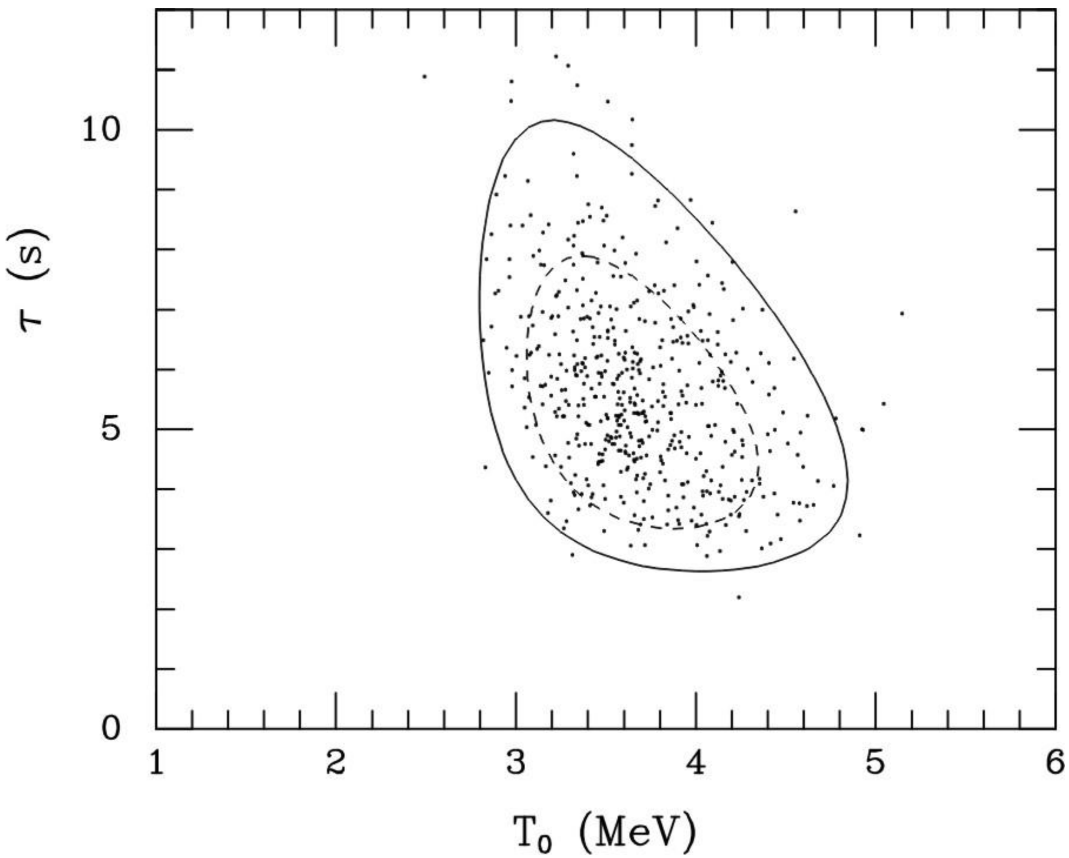

Loredo and Lamb, Bayesian analysis
astro-ph/0107260

SN 1987A Axion Limits from Burst Duration

- Raffelt, Lect. Notes Phys. 741 (2008) 51 [hep-ph/0611350]
  Burst duration calibrated by early numerical studies
  "Generic" emission rates inspired by OPE rates
  $f_a \gtrsim 4 \times 10^8$ GeV and $m_a \lesssim 16$ meV (KSVZ, based on proton coupling)
- Chang, Essig & McDermott, JHEP 1809 (2018) 051 [1803.00993]
  Various correction factors to emission rates, specific SN core models
  $f_a \gtrsim 1 \times 10^8$ GeV and $m_a \lesssim 60$ meV (KSVZ, based on proton coupling)
- Carenza, Fischer, Giannotti, Guo, Martínez-Pinedo & Mirizzi,
  JCAP 10 (2019) 016 & Erratum [1906.11844v3]
  Beyond OPE emission rates, specific SN core models: similar to Chang et al.
  $f_a \gtrsim 4 \times 10^8$ GeV and $m_a \lesssim 15$ meV (KSVZ, based on proton coupling)
- Carenza, Fore, Giannotti, Mirizzi & Reddy [arXiv:2010.02943]
  Including thermal pions $\pi^- + p \to n + a$ (factor 3 larger emission)
  $f_a \gtrsim 5 \times 10^8$ GeV and $m_a \lesssim 11$ meV (KSVZ, based on proton coupling)
- Bar, Blum & D'Amico, Is there a supernova bound on axions? [1907.05020]
  Alternative picture of SN explosion (thermonuclear event)
  Observed signal not PNS cooling. SN1987A neutron star (or pulsar) not yet found.
  (but see "NS 1987A in SN 1987A", Page et al. arXiv:2004.06078)

Supernova Remnant in Cas A (SN 1680?)

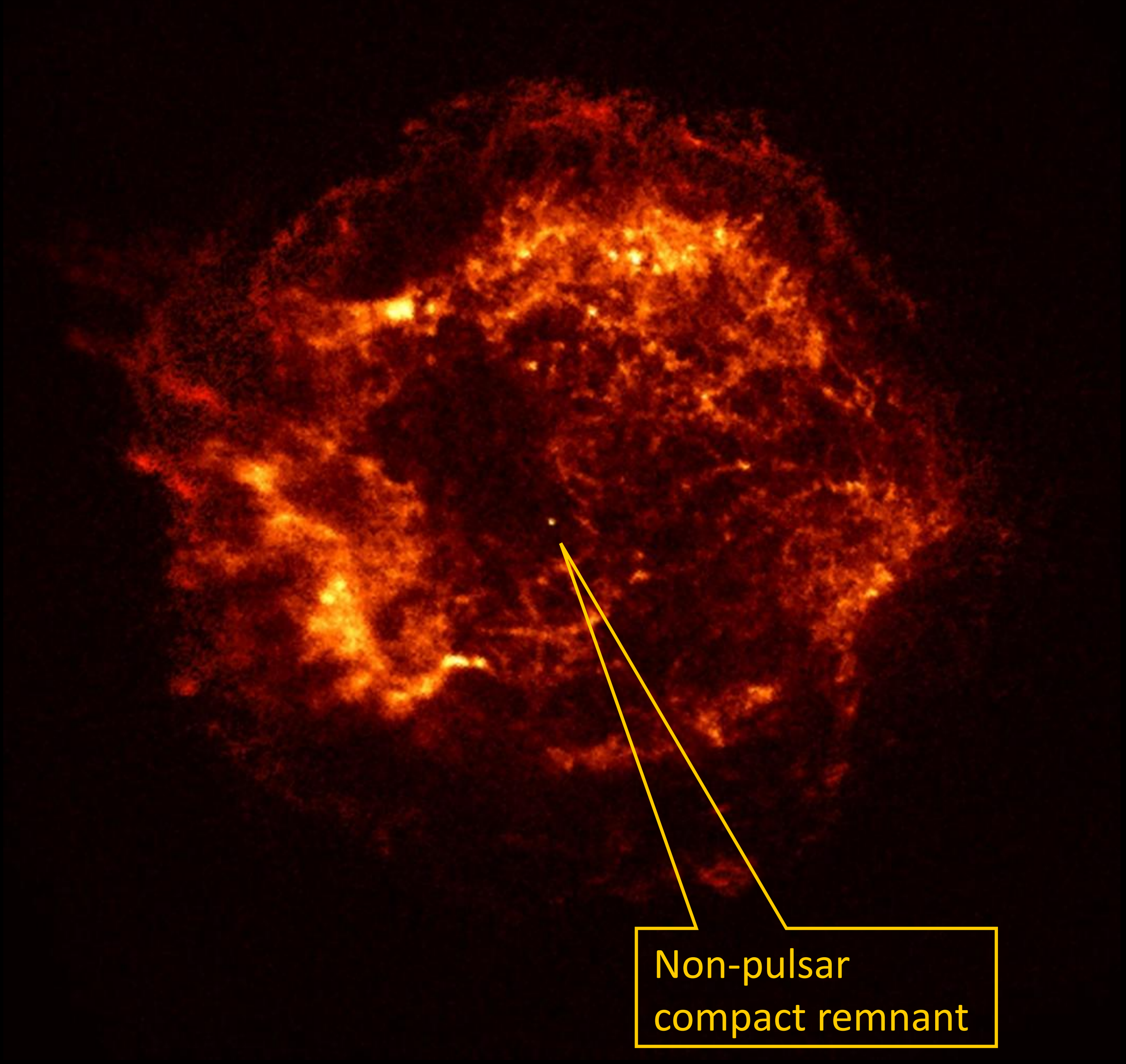

Chandra
x-ray image

Neutron Star Cooling

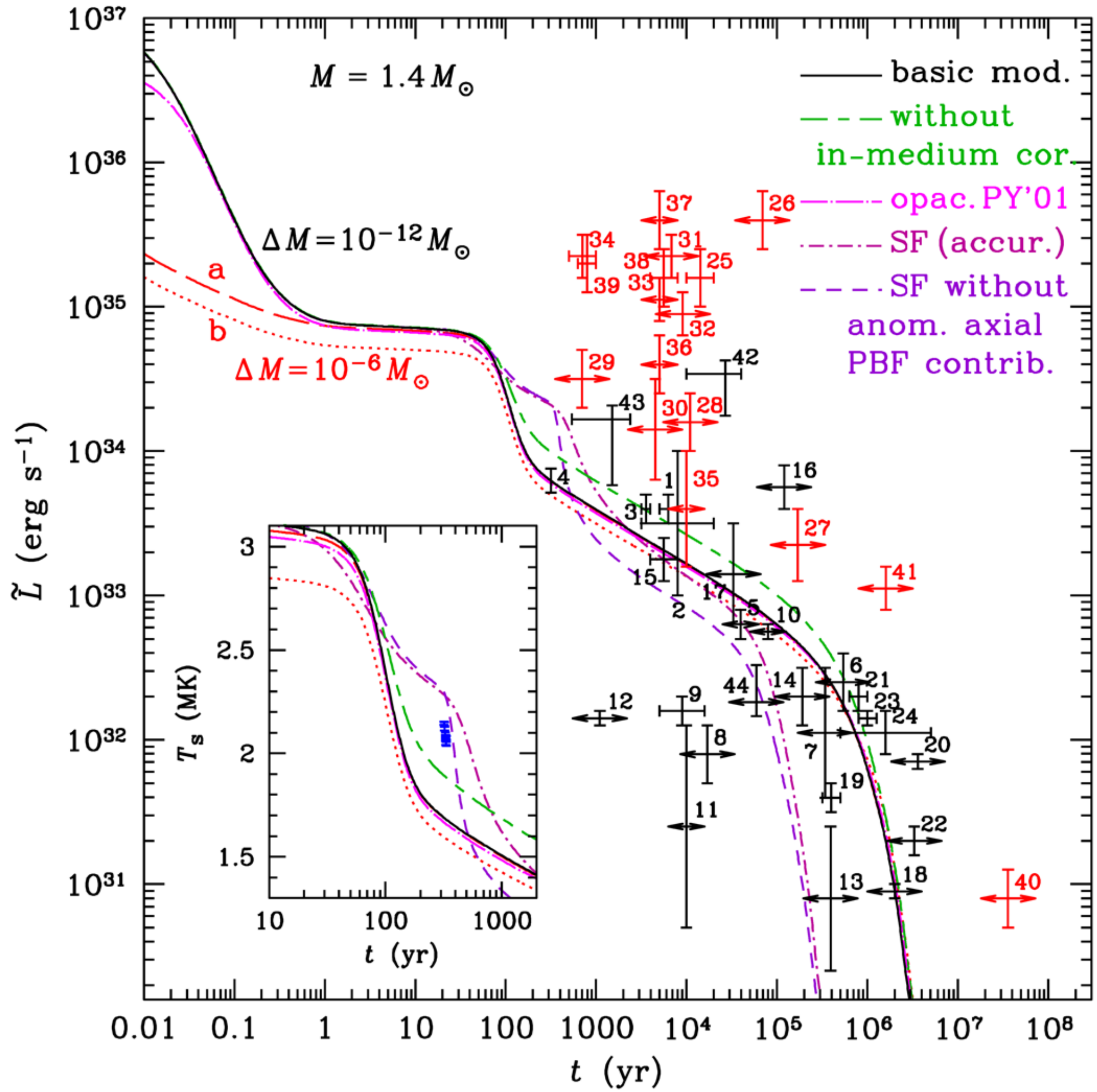

Potekhin & Chabrier: Magnetic neutron star cooling and microphysics [1711.07662]

Axion Limits from Neutron Star Cooling

Selection of pulsars at different age:

- Umeda, Iwamoto, Tsuruta, Qin & Nomoto, astro-ph/9806337
- A. Sedrakian, arXiv:1512.07828 (hadronic axions)
- A. Sedrakian, arXiv:1810.00190 (non-hadronic axions)

Supernova Remnant Cas A (320 years)

- Leinson, arXiv:1405.6873
- Hamaguchi, Nagata, Yanagi & Zheng, arXiv:1806.07151

Supernova Remnant HESS J1731-347 (27 kyears)

- Beznogov, Rrapaj, Page & Reddy, arXiv:1806.07991
  $g_{an}^2 < 0.77 \times 10^{-19}$
- Leinson, arXiv:1909.03941
  $g_{an}^2 < 1.1 \times 10^{-19}$

$$C_n m_a \lesssim 2\ \mathrm{meV}$$

Limits broadly comparable to SN 1987A bounds (m_a tens of meV range)

- Protons superconducting – bremsstrahlung from neutrons
- Neutron-axion coupling can be very small or vanish

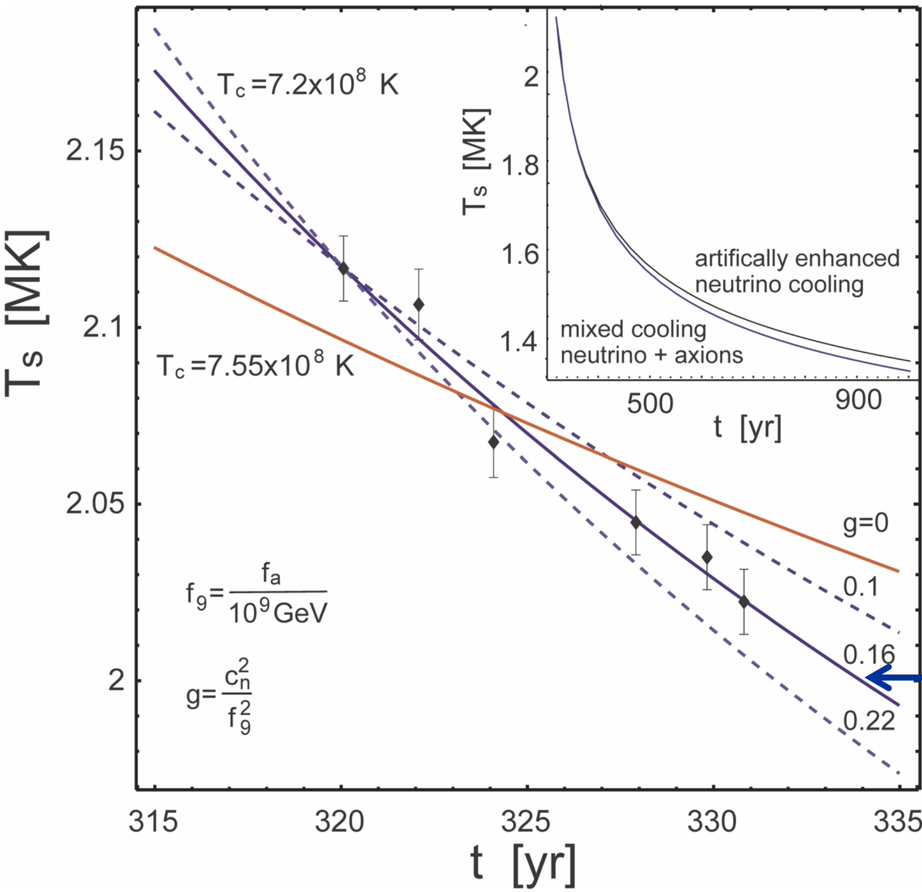

$C_n m_a \sim 2.4$ meV

Chandra x-ray image of non-pulsar compact remnant

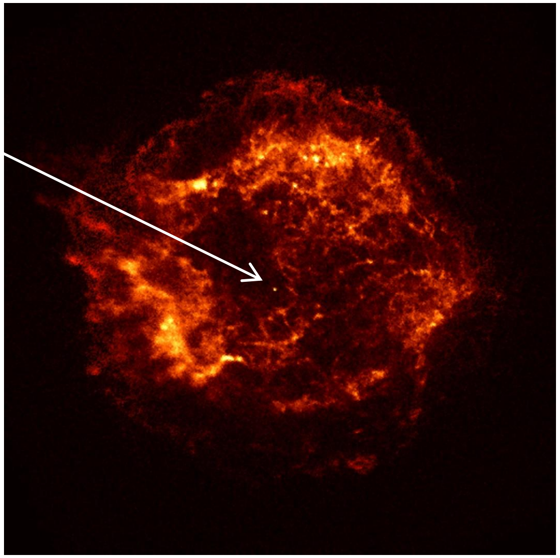

Measured surface temperature over 10 years reveals unusually fast cooling rate

- Neutron Cooper pair breaking and formation (PBF) as neutrino emission process?
- Evidence for extra cooling (by axions)?

Leinson, arXiv:1405.6873

Axion Bounds from Magnetic WDs and NSs

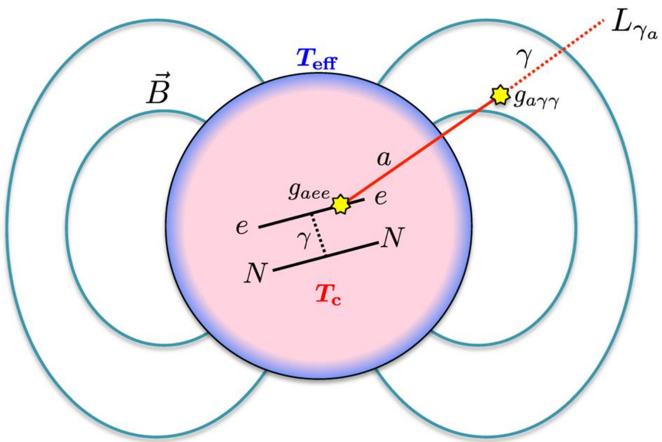

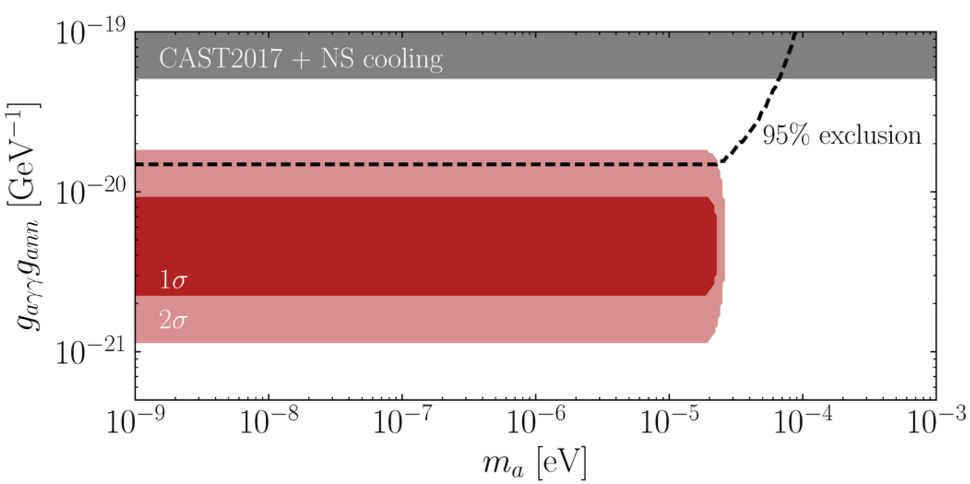

Magnetic White Dwarf

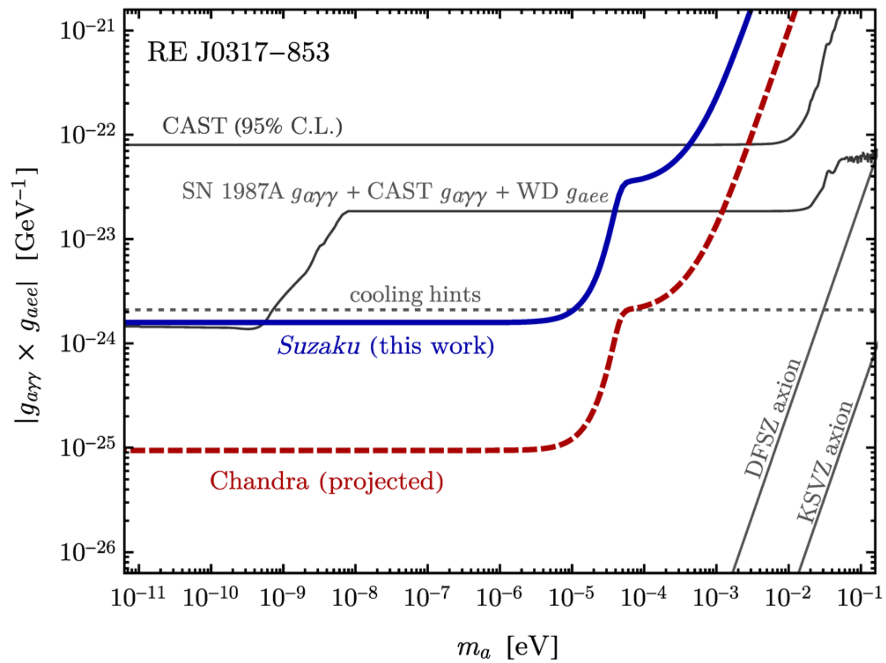

Magnificent Seven Neutron Stars
X-Ray limits and excess

- Buschmann, Co, Dessert & Safdi:
  X-Ray Search for Axions from Nearby Isolated Neutron Stars, arXiv:1910.04164
- Dessert, Long & Safdi: *X-Ray Signatures of Axion Conversion in Magnetic White Dwarf Stars*, PRL 123 (2019) 061104, arXiv:1903.05088

Radio Search for Axion Dark Matter in Pulsars

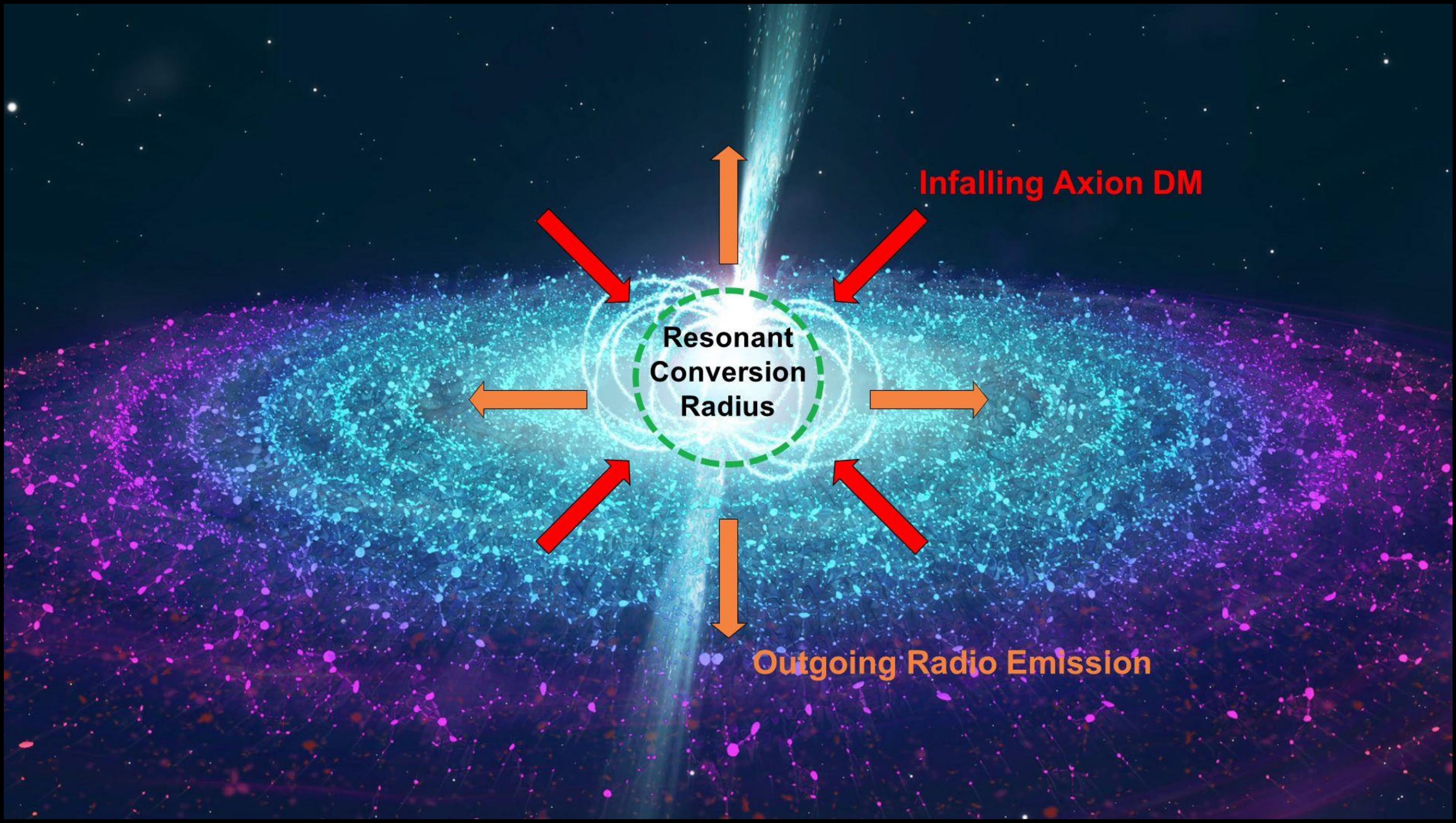

See Josh Foster, 9 Oct 2020, https://indico.cern.ch/event/950670/

Radio Search for Axion Dark Matter in Pulsars

Two viable strategies

1. Observe isolated neutron stars in clean environments
2. Observe high density targets in messy environments

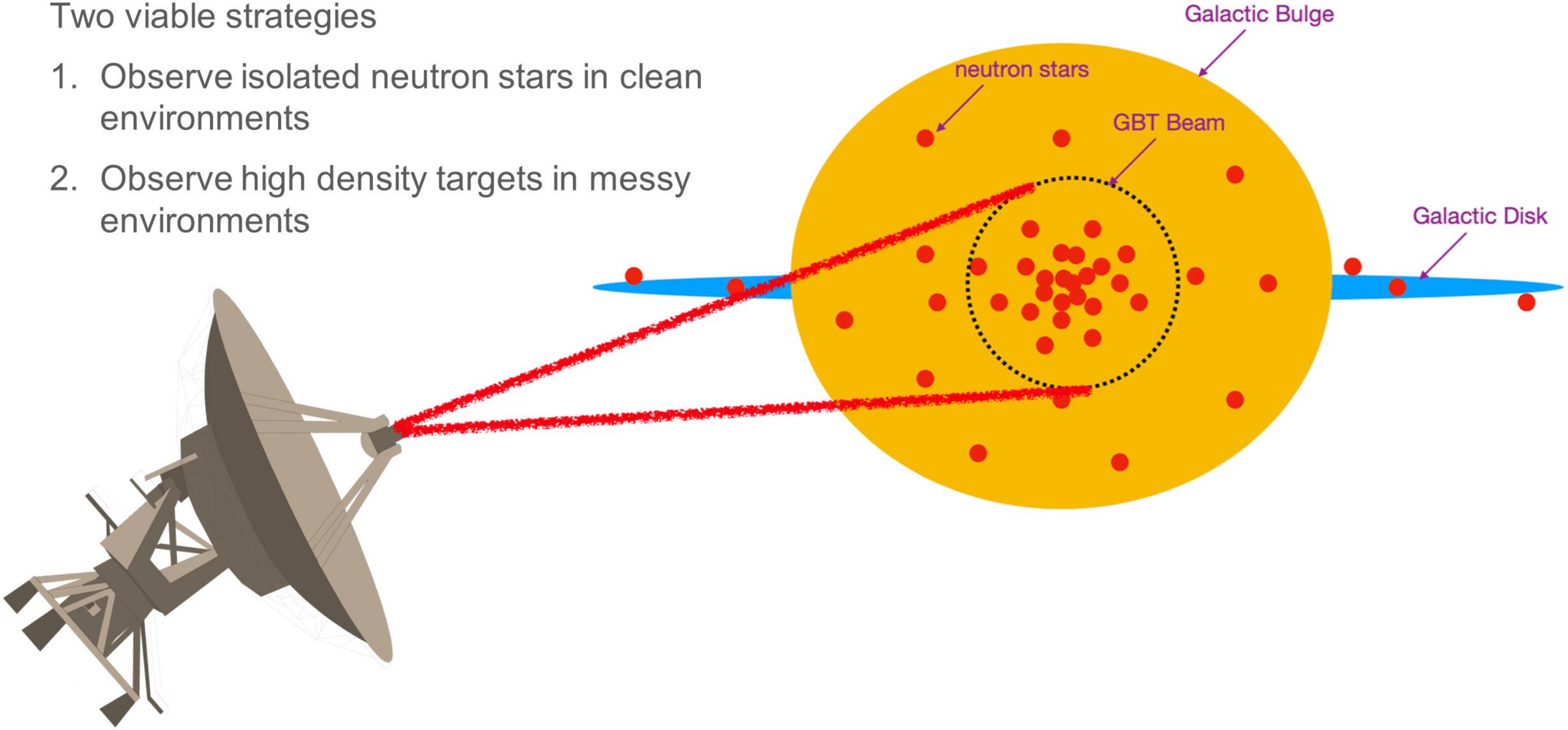

See Josh Foster, 9 Oct 2020, https://indico.cern.ch/event/950670/

Superradiance

Initially slow particle scattering in the ergoregion speeds up by extracting angular momentum and energy from the BH;

Waves similarly increase in amplitude

Particles/waves trapped in orbit around the BH repeat this process continuously

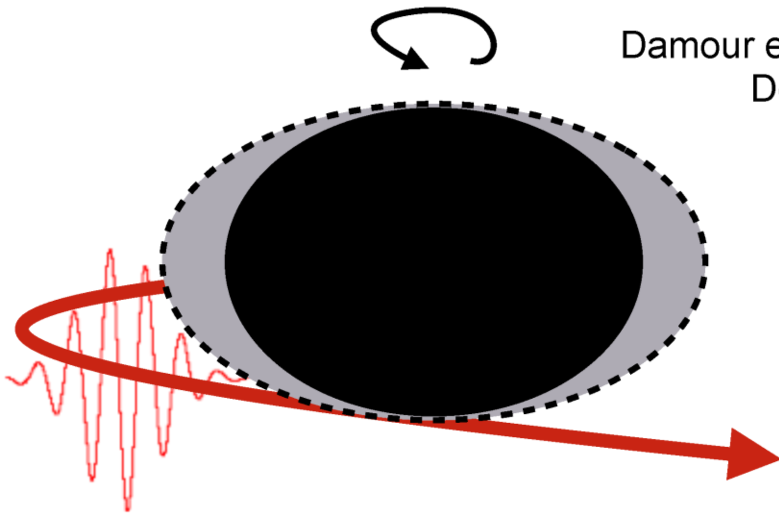

Damour et al; Zouros & Eardley; Detweiler; Gaina

Superradiance condition:

Angular velocity of particle slower than angular velocity of BH horizon

$$\frac{\omega_a}{m} < \Omega_{BH}$$

(m = magnetic quantum number)

Particles in orbits that satisfy the SR condition are amplified:

“Black hole bomb”

Kinematic, not resonant condition

Black Hole Spins

Five currently measured black holes combine to set limit:

$$2 \times 10^{-11} > \mu_a > 6 \times 10^{-13}\ \mathrm{eV}$$
$$3 \times 10^{17} < f_a < 1 \times 10^{19}\ \mathrm{GeV}$$

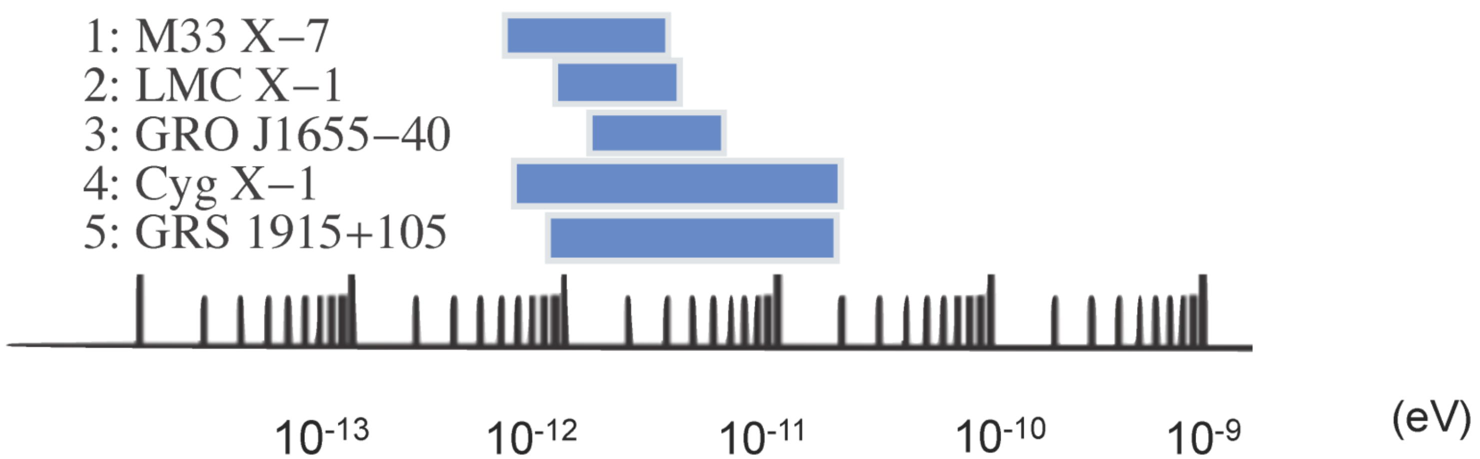

Arvanitaki , Baryakhtar & Huang, arXiv:1411.2263, PRD 91 (2015) 084011

But see Fernandez, Ghalsasi & Profumo, arXiv:1911.07862

Gravitational Wave Signals

- Transitions between levels

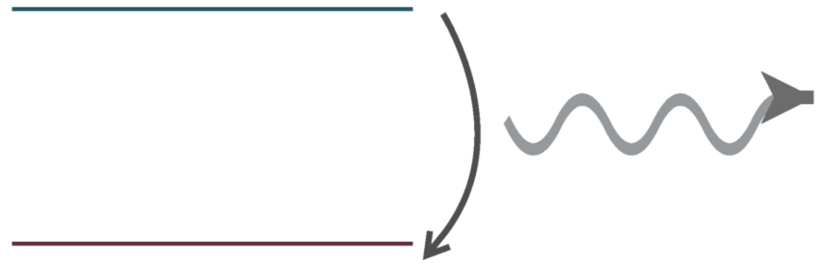

- Annihilations to gravitons

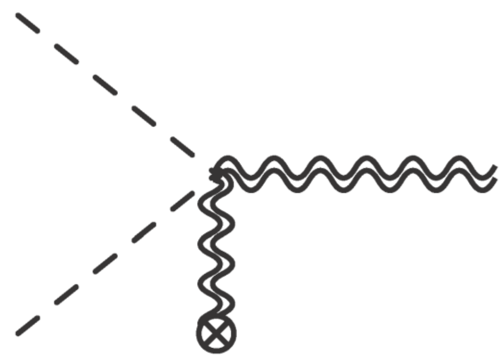

Arvanitaki, Baryakhtar, Dimopoulos, Dubovsky & Lasenby, arXiv:1604.03958

Masha Baryakhtar, Talk at Invisibles 2016, https://indico.cern.ch/event/464402/

Direct Constraints on the Ultralight Boson Mass from Searches of Continuous Gravitational Waves

C. Palomba,[1] S. D'Antonio,[2] P. Astone,[1] S. Frasca,[3,1] G. Intini,[3,1] I. La Rosa,[4] P. Leaci,[3,1] S. Mastrogiovanni,[5] A. L. Miller,[3,1,6] F. Muciaccia,[3] O. J. Piccinni,[3,1] L. Rei,[7] and F. Simula[1]

Superradiance limits from LIGO O2 all-sky search for periodic GWs

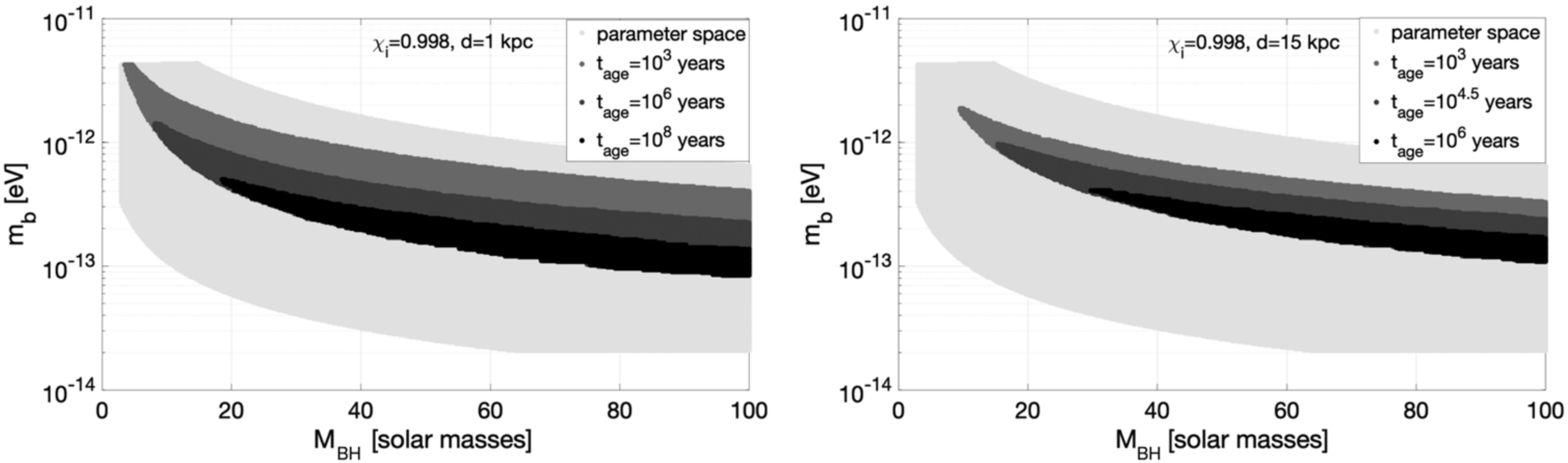

FIG. 2. 95% C.L. exclusion regions in the plane $m_b - M_{\mathrm{BH}}$ assuming a maximum distance $d = 1$ kpc (left plot) and $d = 15$ kpc (right plot), a black hole initial adimensional spin $\chi_i = 0.998$, and three possible values for t_{age}: 10^3, 10^6, 10^8 yr (left plot) and 10^3, $10^{4.5}$, 10^6 yr (right plot). The larger light gray area is the accessible parameter space. As expected, the extension of the excluded region decreases for increasing t_{age} (corresponding to darker color).

See also:
Search for ultralight bosons in Cygnus X-1 with Advanced LIGO, arXiv:1909.11267

Axions and Stars

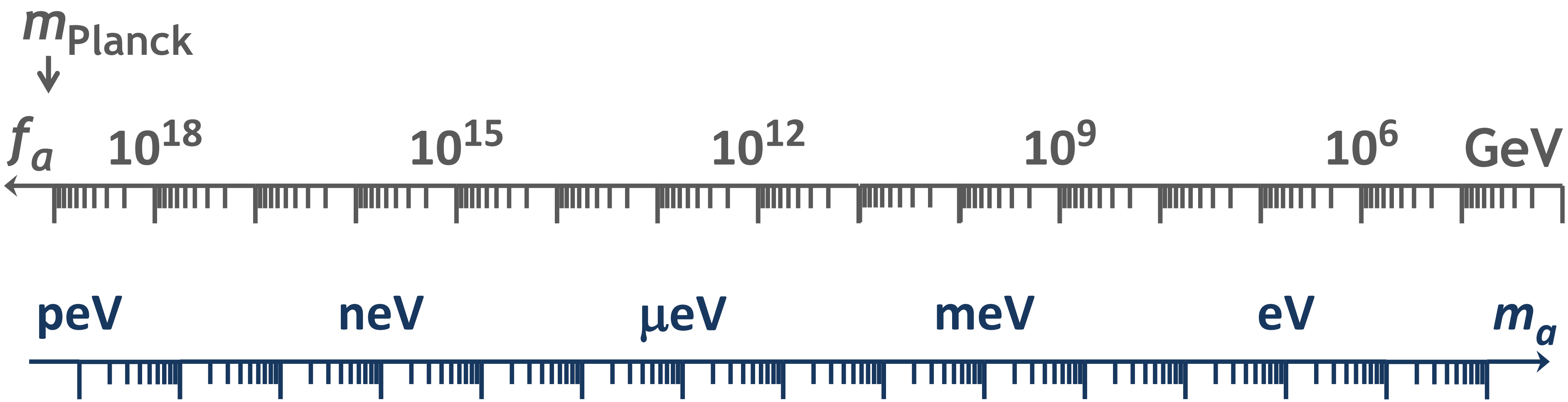

Opportunities for detection

Astrophysical Bounds (Energy loss of stars)

Super Radiance

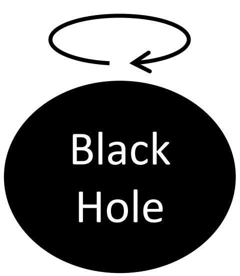

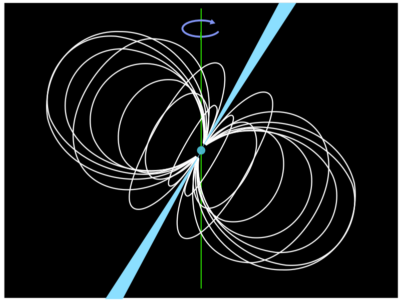

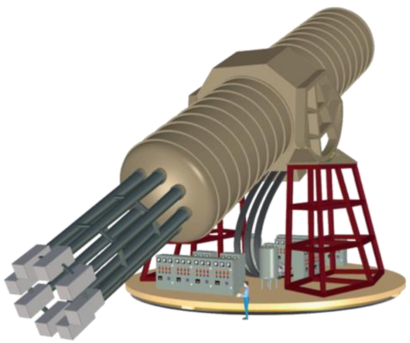

IAXO Solar Axion Telescope

Axion conversion in neutron star magnetospheres